


The author hereby certifies that the use of any copyrighted material in the thesis manuscript entitled:

**“Mechanisms of angiogenesis and lymphangiogenesis in TSC skin tumors”**

is appropriately acknowledged and, beyond brief excerpts, is with the permission of the copyright owner.



Sangeetha Rajesh  
Molecular and Cell biology  
Department of Dermatology  
Uniformed Services University  
09/16/2011

## **Abstract**

Title of Dissertation:	Mechanisms of angiogenesis and lymphangiogenesis in TSC skin tumors
Name, degree, year:	Sangeetha Rajesh
Doctor of Philosophy:	2011
Dissertation directed by:	Dr. Thomas Darling, MD, Ph.D Associate Professor Department of Dermatology Uniformed Services University of the Health Sciences

Tuberous sclerosis complex (TSC) is an inherited tumor syndrome in which tumor formation is associated with loss of function of the TSC1-TSC2 complex and activation of mammalian target of rapamycin complex 1 (mTORC1), a central regulator of cell growth, and proliferation. Patients develop tumors in the brain, eyes, heart, kidneys, lungs and skin. The skin tumors contain large fibroblast-like cells in the dermis and increased vessels, epidermal proliferation and infiltration of mononuclear phagocytes. It is known that angiogenesis and lymphangiogenesis are important in tumor growth and spread in cancer, but the roles of angiogenesis and lymphangiogenesis in the pathogenesis of TSC tumors, and the mechanisms underlying vessel formation, are not well understood. In a novel xenograft model of TSC skin tumors, tumor xenografts showed greater mTORC1 activity, angiogenesis, lymphangiogenesis, mononuclear phagocytes and epidermal proliferation than normal xenografts. The observation that tumor xenografts recapitulated characteristics of TSC skin tumors suggested that they would be useful for studying responses to treatment and identifying mechanisms of angiogenesis and lymphangiogenesis in TSC skin tumors.

To investigate the cellular targets of rapamycin, a specific inhibitor of mTORC1, we treated xenografted mice with rapamycin for 15 weeks. Rapamycin decreased blood vessel density and size in tumor xenografts, and it almost completely abrogated lymphatic vessel formation in tumor or normal grafts. These results suggest that rapamycin exerts strong anti-angiogenic and anti-lymphangiogenic effects in the xenografts.

Angiogenesis and lymphangiogenesis are stimulated by hypoxia, via increased levels of hypoxia inducible factor (HIF-1 $\alpha$ ), and increased production of soluble factors, such as VEGF-A, HGF and VEGF-C. The factors responsible for angiogenesis and lymphangiogenesis in TSC were unknown. We found that TSC tumor cells showed increased expression of HIF-1 $\alpha$ , and maintained mTORC1 activation for at least 24 hours of hypoxia. TSC tumor cells also secreted more HGF and VEGF-C than dermal fibroblasts from the same patient. Rapamycin treatment did not affect the production of HGF and VEGF-C. These data indicate that TSC2-null tumor cells induce angiogenesis and lymphangiogenesis and that rapamycin inhibits these processes in TSC skin tumors.

# **MECHANISMS OF ANGIOGENESIS AND LYMPHANGIOGENESIS IN TSC SKIN TUMORS**

**By**

**Sangeetha Rajesh**

Dissertation submitted to the Faculty of the  
Molecular and Cell Biology Graduate Program  
Uniformed Services University of the Health Sciences  
in partial fulfillment of the requirements for the degree of  
Doctor of Philosophy 2011

## **Dedication**

I dedicate this thesis to my mom and dad, who with their unconditional love and support all through these years have been instrumental in my success and to my loving husband, Tadi for his support, love, encouragement and sacrifices he made during this graduate program.

## ACKNOWLEDGMENTS

This dissertation was possible only because of guidance, help and support from several individuals over the years.

First and foremost, I wish to thank my mentor Dr. Darling for his patient guidance, unwavering support and excellent mentorship. He is an amazing role model and he gave me an opportunity to do exciting research, to think critically and pay attention to details. He has taught me to strike a balance between professional and personal life. I enjoyed tasting all the different cuisines as part of our birthday celebrations and also his Christmas decorations.

I would like to thank Dr. Saibal Dey, chair of my committee for helping me get an admission at USUHS. My sincere thanks to Dr. Dey and other members of my dissertation committee, Dr. Mary Lou Cutler, Dr. Chou-Zen Giam, and Dr. Joel Moss for their insightful and invaluable comments, suggestions and critical feedbacks. Furthermore, I would like to express my thanks to Dr. Joel Moss for his excellent collaboration and helping us with the patient samples. I extend my appreciation to the patients who were very generous in donating their samples. This project would not have been possible without Dr. Moss and the patient's samples.

My lab members Ji-an Wang, Ying Liu, Shaowei Li, and Rajesh Thangapazham have assisted me all these years with training in the use of equipment, lab procedures, data collection and analysis. They along with Peter Klover and Amanda Devine provided a very vibrant working ambience. Thank you all for your support.

I really appreciate the constant support from Dr. Eleanor Metcalf, Dean of graduate education. She is an amazing person, full of energy and is always very friendly and helpful. I am grateful to Janet, Kelly, and Elena at the graduate education office and Ne Tina Finley at the MCB office for their support. I wish to express my thanks and appreciation to all the faculty and staff at USUHS for being great teachers and especially to the director of MCB program, Dr. Mary Lou Cutler. I am thankful to Dr. Leonard Sperling, Chair of Dermatology for his encouragement, support and all the wonderful Christmas celebrations at Guapos. I thank Dr. Cara Olsen for helping me with the statistical analysis.

I would like to acknowledge all my friends for making my life at USUHS more enjoyable and a memorable one. My thanks are due to Reyda, who started off this journey together with me and ever since she has been my good friend.

My family has played a major role in my accomplishment. My Ph.D would have been just a dream if not for my parents. Their constant support and encouragement, their belief in my potential and all their trips to US to take care of my little daughter are commendable. Special thanks to my sister and friend Priya for all her love, care and affection. She and her husband Sp always made each and every occasion of ours very special with their thoughtfulness and always were of great moral support. Thanks Sp. My

in-laws are my second parents and they supported my career path right from the start. They were of great physical and moral support especially during the last few years. My thanks are due to my brother in law and co-sister Kavitha and her family for always having us in their prayers.

Last but most importantly, I am indebted to my husband and best friend Tadi. He is my foundation and has helped me balance between home and school. His thoughtful and timely jokes always made me smile and livened the moment. He has helped me a lot in preparing for my talks and has patiently heard me practice umpteen times. I love and thank you with all my heart.

Finally, thanks to my little angel Ritika for her innocent talks, lovely smiles, hugs and kisses and letting me work peacefully the last few months. Love u pattu kutti.

## Abbreviations

Akt	v-akt murine thymoma viral oncogenes homolog	Foxc2	Forkhead transcription factor 2
AML	Angiomyolipoma	GFP	Green fluorescent protein
AMPK	AMP-activated protein kinase	HGFA	Hepatocyte growth factor activator
AP23573	Deforolimus	HGF	Hepatocyte growth factor
BVEC	Blood vessel endothelial cell	HIF	Hypoxia inducible factor
CCI779	Tacrolimus	HLA	Human leukocyte antigen
CD31	Cluster of differentiation 31	HRE	Hypoxia response element
CD68	Cluster of differentiation 68	HSP47	Heat-shock protein of 47 kDa
c-Met	Met protooncogene	IGF	Insulin-like growth factor
COX-2	Cyclooxygenase-2	IL-1 $\beta$	Interleukin 1- $\beta$
COX IV	Cytochrome c oxidase	IRS1	Insulin receptor substrate 1
D2-40	Monoclonal antibody against podoplanin	LAM	Lymphangioliomyomatosis
DC	Dendritic cell	LEC	Lymphatic endothelial cell
DAPI	4',6-diamidino-2-phenylindole	LOH	Loss of heterozygosity
DMEM	Dulbecco's Modified Eagle's Medium	LYVE-1	lymphatic vessel endothelial hyaluronan receptor 1
DNA	Deoxyribonucleic acid	MAPK	mitogen-activated protein kinase
4EBP1	initiation factor 4E binding protein 1	MCP-1	Monocyte chemotactic protein-1
EGF	Epidermal growth factor	MEF	Mouse embryonic fibroblast
FKBP12	FK506 Binding Protein 12	MMP	Matrix metalloproteinase
FISH	Fluorescence <i>in situ</i> hybridization	mTOR	Mammalian target of rapamycin
FITC	Fluorescein isothiocyanate	mTORC1	Mammalian target of rapamycin complex 1



mTORC2	Mammalian target of rapamycin complex 2	shRNA	Short hairpin RNA
PCR	Polymerase chain reaction	siRNA	Small interfering RNA
PI3K	Phosphoinositide Kinase-3	TAM	Tumor associated macrophage
PKD	Polycystic kidney disease	TGF- $\beta$	Transforming growth factor- $\beta$
pS6	Phospho ribosomal protein S6	TNF- $\alpha$	Tumor necrosis factor- $\alpha$
RAD001	Everolimus	TSC	Tuberous sclerosis complex
REDD1	Regulated in development and DNA damage responses	VEGF-C	Vascular endothelial growth factor-C
Rheb	Ras-homologue enriched in brain	VEGF-D	Vascular endothelial growth factor-D
RNA	Ribonucleic acid	VEGFR3	Vascular endothelial growth factor receptor 3
RT-PCR	Reverse transcription polymerase chain reaction	VHD	VEGF homology domain
S6	Ribosomal protein S6		

## Table of figures

### **CHAPTER 1: INTRODUCTION**

Figure 1: Schematic representation of the structural-functional domains of hamartin (A) and tuberin (B)	7
Figure 2: mTOR signaling pathway	10
Figure 3: Structure of rapamycin	15
Figure 4: <i>In vitro</i> effects of rapamycin in TSC	16
Figure 5: Cutaneous findings in TSC	18
Figure 6: Receptor binding specificities of VEGF family members	22
Figure 7: Hypoxic regulation of the hypoxia-inducible factor-1 $\alpha$ (HIF-1 $\alpha$ )	26

### **CHAPTER 3: RESULTS**

Table 1: Diagnostic Criteria of TSC at the Time of Enrollment for 20 Adult Women	46
Table 2: Locations and number of skin samples obtained from patients with tuberous sclerosis complex	47
Figure 1: Histological and immunohistological differences between TSC skin tumors and normal-appearing skin	49
Figure 2: Histological appearance of normal, TSC normal and TSC tumor cells	50
Figure 3: Characterization of TSC skin tumor cells	51
Figure 4: Genetic analysis of TSC2-null fibroblast-like cells	52
Figure 5: Xenograft model of TSC skin hamartomas	54
Figure 6: TSC angiofibroma (AF) cells induce human hair follicle formation in xenografts	55
Figure 7: Double FISH analysis on xenograft samples	56
Figure 8a: Tumor grafts replicate features of TSC skin tumors	60

Figure 8b: Effects of rapamycin on tumor and normal xenografts	61
Figure 9: HIF-1 $\alpha$ expression in normal fibroblasts, TSC fibroblasts and TSC2-null tumor fibroblasts	63
Figure 10: D2-40 positive vessels in TSC skin tumors and patient normal- appearing skin	66
Figure 11: Effect of rapamycin on lymphangiogenesis in TSC skin tumors	67
Figure 12: Pathological analysis of the grafted tissue	69
Figure 13: Lymphatic vessels in xenografted mice treated with or without rapamycin	71
Figure 14: HGF expression in TSC skin tumors	74
Figure 15: VEGF-C expression in TSC skin tumors	75
Figure 16: Expression levels of VEGF-A in TSC skin tumors	75
Figure 17: Effect of TSC2 knockdown on TSC2 and phosphorylation of ribosomal protein S6 in neonatal fibroblasts	77
Figure 18: Effect of TSC2 knockdown on HGF production	78
Figure 19: Effect of TSC2 knockdown on VEGF-C production	79
Figure 20: Effect of rapamycin on HGF production	81
Figure 21: Effect of rapamycin on VEGF-C production	82
<b><u>CHAPTER 4: DISCUSSION</u></b>	
Figure 22: Model for angiogenesis and lymphangiogenesis in TSC skin tumors	96

## **Table of contents**

APPROVAL SHEET	i
COPYRIGHT STATEMENT	ii
ABSTRACT	iii
TITLE PAGE	v
DEDICATION	vi
ACKNOWLEDGEMENTS	vii
ABBREVIATIONS	ix
TABLE OF FIGURES	xi
TABLE OF CONTENTS	xiii
<b>CHAPTER 1: INTRODUCTION</b>	
<b>OVERVIEW</b>	1
<b>TUBEROUS SCLEROSIS COMPLEX</b>	4
TSC molecular genetics	6
Functions of TSC genes	9
mTOR signaling	12
• mTORC1 signaling	12
• mTORC2 signaling	14
Rapamycin as a therapeutic agent	14
TSC skin tumors	17
<b>ANGIOGENESIS</b>	20
Vascular endothelial growth factor	21
Angiogenesis in TSC	23
Hypoxia	24
• Hypoxia inducible factor (HIF-1 $\alpha$ )	24

• Role of hypoxia in angiogenesis	26
<b>LYMPHANGIOGENESIS</b>	27
Lymphatic vascular system	27
Embryology of the lymphatic system	29
Lymphangiogenesis	32
• Vascular endothelial growth factors	32
• Hepatocyte growth factor	34
• Other important lymphangiogenic factors	35
Lymphangiogenesis in TSC associated tumors	36
<b>CHAPTER 2: METHODS</b>	
Tumor sample and cell culture	37
Cytoplasm and nuclear fraction	37
Western blot analysis	38
<i>TSC2</i> sequence analysis	39
Loss of heterozygosity analysis	39
Creation of <i>in vitro</i> composites for xenografts	39
Mouse grafting	40
Animal treatment	40
Immunohistochemistry and quantification	41
Fluorescence <i>in situ</i> hybridization	41
Y-chromosome fluorescence <i>in situ</i> hybridization	42
Gene array analysis	42
SearchLight protein array	42
ELISA	43
RT-PCR	43
ShRNA lentiviral transduction	44
Statistics	44

## CHAPTER 3: RESULTS

TSC patients and samples	45
<b>PART1: ANGIOGENESIS IN TSC SKIN TUMORS</b>	45
TSC skin tumors are highly vascular with constitutive mTOR activation and are enriched with mononuclear phagocytes	47
Fibroblast-like cells from TSC skin tumors are null for TSC2 with constitutive mTOR activation	50
Fibroblast-like cells from TSC skin tumors are 2-hit cells	51
Skin equivalents grafted onto nude mice to develop a xenograft mouse model of TSC skin tumors	53
Delineation of human and mouse cells in the xenografts	54
Tumor grafts recapitulate hamartoma features of a human tumor including hyperphosphorylation of S6, increased proliferation of epidermis, recruitment of mononuclear phagocytes and increased angiogenesis	57
Rapamycin reverses hamartoma features induced by TSC2-null cells	58
TSC tumor cells show greater basal and hypoxia-stimulated levels of HIF-1 $\alpha$ than normal fibroblasts	62
<b>PART2: LYMPHANGIOGENESIS IN TSC SKIN TUMORS</b>	65
TSC skin tumors show greater lymphangiogenesis than normal skin	65
Periungual fibromas from patients on rapamycin treatment trend towards decreased lymphatic vessels	66
Lymphatics invade grafts containing human cells	68
Rapamycin dramatically decreases lymphangiogenesis in the normal and tumor grafts	70
<b>PART3A: ANGIOGENIC AND LYMPHANGIOGENIC FACTORS IN TSC SKIN TUMORS</b>	72
TSC skin tumor cells secrete increased amounts of HGF and VEGF-C	72
Vegf-A in TSC skin tumors	73
<b>PART3B: REGULATION OF LYMPHANGIOGENIC FACTOR EXPRESSION IN TSC SKIN TUMORS</b>	76
TSC2 knockdown increases HGF secretion in neonatal fibroblasts	76
mTORC1-independent regulation of HGF and VEGF-C in TSC skin tumors	80

## **CHAPTER 4: DISCUSSION**

TSC skin tumors are highly vascular	84
Biallelic TSC2 mutations are observed in fibroblast-like cells and not vessels	85
TSC2-null fibroblast-like cells are the inciting cells for TSC skin tumor development	86
Cells contributing to angiogenesis and lymphangiogenesis in TSC skin tumors	87
• Mononuclear phagocytes	87
• Epidermal cells	88
Rapamycin as a therapeutic agent for TSC skin tumors	89
Angiogenic and lymphangiogenic factors in TSC skin tumors	91
HIF-1 $\alpha$ might contribute to tumor growth in TSC skin tumors	92
Regulation of the lymphangiogenic factors HGF and VEGF-C	94
A model for angiogenesis and lymphangiogenesis in TSC skin tumors	95
Targeting angiogenesis and lymphangiogenesis in TSC skin tumors	97

<b>CHAPTER 5: REFERENCES</b>	99
------------------------------	----

<b>COPYRIGHT PERMISSIONS</b>	130
------------------------------	-----

## Chapter 1: Introduction

### Overview

Angiogenesis and lymphangiogenesis, the formation of blood or lymphatic vessels from preexisting vessels, are two related processes involved in normal growth and development. Sustained activation of either of these processes is associated with multiple diseases, particularly cancer. Tumor cells produce factors that stimulate growth of blood and lymphatic vessels. New blood vessels formed in the tumor and its surroundings supply the tumor with nutrients and oxygen for its survival and growth. Lymphatic vessels provide avenues for spread of tumor cells to regional lymph nodes and ultimately to different parts of the body. Therefore angiogenesis and lymphangiogenesis are integral parts of tumor growth and metastasis that lead to patient suffering and death.

Tuberous sclerosis complex (TSC) is an inherited tumor syndrome that results in the formation of tumors that are highly angiogenic and lymphangiogenic. Little is known about the cellular and molecular mechanisms responsible for angiogenesis and lymphangiogenesis in TSC. Identifying these mechanisms is expected to provide insights into growth of these tumors, and lead to new therapies.

TSC patients develop benign tumors in multiple organs such as brain, kidney, heart, lung and skin. It is caused by mutations in one of the two genes, *TSC1* or *TSC2*, which activate a signaling pathway through mammalian target of rapamycin (mTOR), stimulating cell growth, proliferation and survival. Our laboratory studies the highly vascular TSC skin tumors that are observed in a majority of TSC patients. They are a major concern to patients because they are disfiguring, prone to bleed and can be painful.



TSC skin tumors are treated using surgical approaches, exposing the patient to the risk of anesthesia, pain during the post-operative period, and leaving permanent scars.

The recent discovery that TSC tumors exhibit mTOR activation led to clinical trials using mTOR inhibitors such as rapamycin. Rapamycin appeared to be a promising drug, since it was already approved by the Food and Drug Administration for other indications, and it has been used to treat a variety of cancers with increased mTOR activation. Clinical trials with rapamycin and its analogs in patients with TSC showed partial regression of several types of tumors. Tumors regrew when the drug was discontinued. Therefore, the use of mTOR inhibitors to treat TSC tumors represents a major breakthrough in the medical treatment of TSC, and yet it is inadequate to eradicate the tumors. In order to improve treatment, it is necessary to understand the *in vivo* responses of tumor cells, as well as its effects on angiogenesis and lymphangiogenesis.

An obstacle to studying TSC skin tumors is the fact that animal models of TSC do not develop the characteristic skin lesions. Therefore, our laboratory sought to develop a xenograft model for TSC skin tumors. Human cells were cultured from skin tumor biopsies obtained from TSC patients and grafted to mice. This model was used to study the mechanisms of TSC skin tumor development, the roles of angiogenesis and lymphangiogenesis in these lesions, and to test the efficacy of potential drugs like rapamycin.

The overall objectives of this thesis are a) to study angiogenesis and lymphangiogenesis in TSC skin tumors and to test the effect of rapamycin on these processes b) to identify factors released by skin tumor cells that induce angiogenesis and lymphangiogenesis, and c) to determine how these factors regulate these processes. These

studies will impact the understanding of angiogenesis and lymphangiogenesis in TSC tumors and other tumors with mTOR activation. They have the potential to identify new therapeutic targets for TSC and possibly other cancers.

## **Tuberous Sclerosis Complex**

Désiré-Magloire Bourneville (1840-1909) coined the term “tuberous sclerosis of the cerebral convolutions” for the white nodular tumors embedded in the corpus striatum of a patient with seizures and mental subnormality<sup>1</sup>. The term “tuberous sclerosis complex (TSC)” refers to all the lesions found in multiple organs that are associated with this disease. These TSC tumors are characterized by three types of lesions as proposed by Moolten, including “hamartias” wherein the basic lesions do not grow more rapidly than normal cells, “hamartomas” where the lesions grow into benign tumors and “hamartoblastomas,” which are malignant tumors that are derived from the hamartomas<sup>2</sup>.

TSC is an autosomal dominant disorder that can affect nearly any organ and is characterized by widespread development of usually benign tumors, which rarely develop into malignant tumors. Typical organs of involvement include brain, kidney, heart, skin, eye and lung<sup>3</sup>. The incidence of TSC is about 1 in 6000 to 10,000 individuals<sup>4,5</sup>.

TSC manifests at different developmental stages during the life of the patient, has no known effect on age of the parents or birth order on severity of the disease and the clinical features are variable. Seizures are observed in 80-90% of affected individuals, beginning in early childhood or less commonly at any point in an individual’s life and are attributed to the presence of brain hamartomas. The nervous system is affected by cortical tubers, subependymal nodules, subependymal giant cell astrocytomas (SEGAs) and retinal hamartomas<sup>6,7</sup>. A majority of patients experience mild to severe learning and intellectual disabilities, epilepsy, autism spectrum disorders, anxiety and mood disorders. This significantly impairs the life of the individual with TSC and also their families.

About 80% of TSC patients develop renal angiomyolipomas (AMLs) and renal cysts, usually in adolescence. The AMLs have abnormal blood vessels that can bleed spontaneously<sup>8</sup>. Rarely patients develop large renal cysts and renal cell carcinoma.

Pulmonary lymphangiomyomatosis (LAM) in patients with TSC occurs almost exclusively in adult women. LAM is characterized by proliferation of alveolar smooth muscle cells, which results in airway obstruction that can lead to respiratory failure and death<sup>9</sup>.

About 90% of patients with TSC develop skin lesions<sup>10</sup> making skin and brain the two most commonly affected organ systems. The skin lesions include hypomelanotic macules and several types of benign skin tumors that can be disfiguring, painful, or bleed spontaneously. Skin lesions are discussed in more detail at the end of the introduction.

Heart rhabdomyomas can be detected as early as infancy but these tumors regress during the first years of life<sup>11</sup>. Rhabdomyomas are rarely a cause of intrauterine or neonatal death. The highest source of morbidity and mortality are due to brain and renal lesions<sup>12</sup>

Making a diagnosis of TSC is challenging when the child is young, especially below 2 years, as many of the diagnostic features become apparent only later in childhood or adulthood. Criteria for diagnosis were published in 1998; the features were divided into major and minor categories. A definitive TS diagnosis is established when a patient presents with two of the major criteria or one major and two minor criteria<sup>13</sup>. Major criteria for TSC include dermatological and neurological manifestations, renal angiomyolipomas, pulmonary lymphangiomyomatosis and cardiac rhabdomyomas. Early

detection of TSC is vital as prompt evaluation and treatment may prevent serious clinical consequences.

### **TSC molecular genetics**

TSC is inherited in an autosomal dominant manner. The disease is highly penetrant and disease severity is variable between affected individuals. About two-thirds of patients with TSC sustain sporadic mutations and have no family history of the disease. Linkage studies in TSC families found that TSC is caused by loss-of-function mutations in one of two tumor suppressor genes, *TSC1* located on human chromosome 9q34 or *TSC2* located on chromosome 16p13<sup>14, 15</sup>. Human *TSC1* gene consists of 21 coding exons and encodes a 130kDa protein named hamartin or TSC1 that is evolutionarily conserved. “It has a potential transmembrane domain, a coiled coil domain and functional domains which include tuberin-binding, Rho-activating, ERM-binding and neurofilament interacting domains”<sup>16</sup> (Figure 1A). The human *TSC2* gene consists of 42 exons and encodes for a 200kDa protein, tuberin or TSC2, a ubiquitously expressed protein that is immediately adjacent to the polycystic kidney disease (PKD1) gene. TSC2 has a leucine zipper domain, two coiled-coil domains, a transcriptional activating domain, GAP homology domain and calmodulin binding domain. It also possesses various potential phosphorylation sites<sup>16</sup> (Figure 1B).

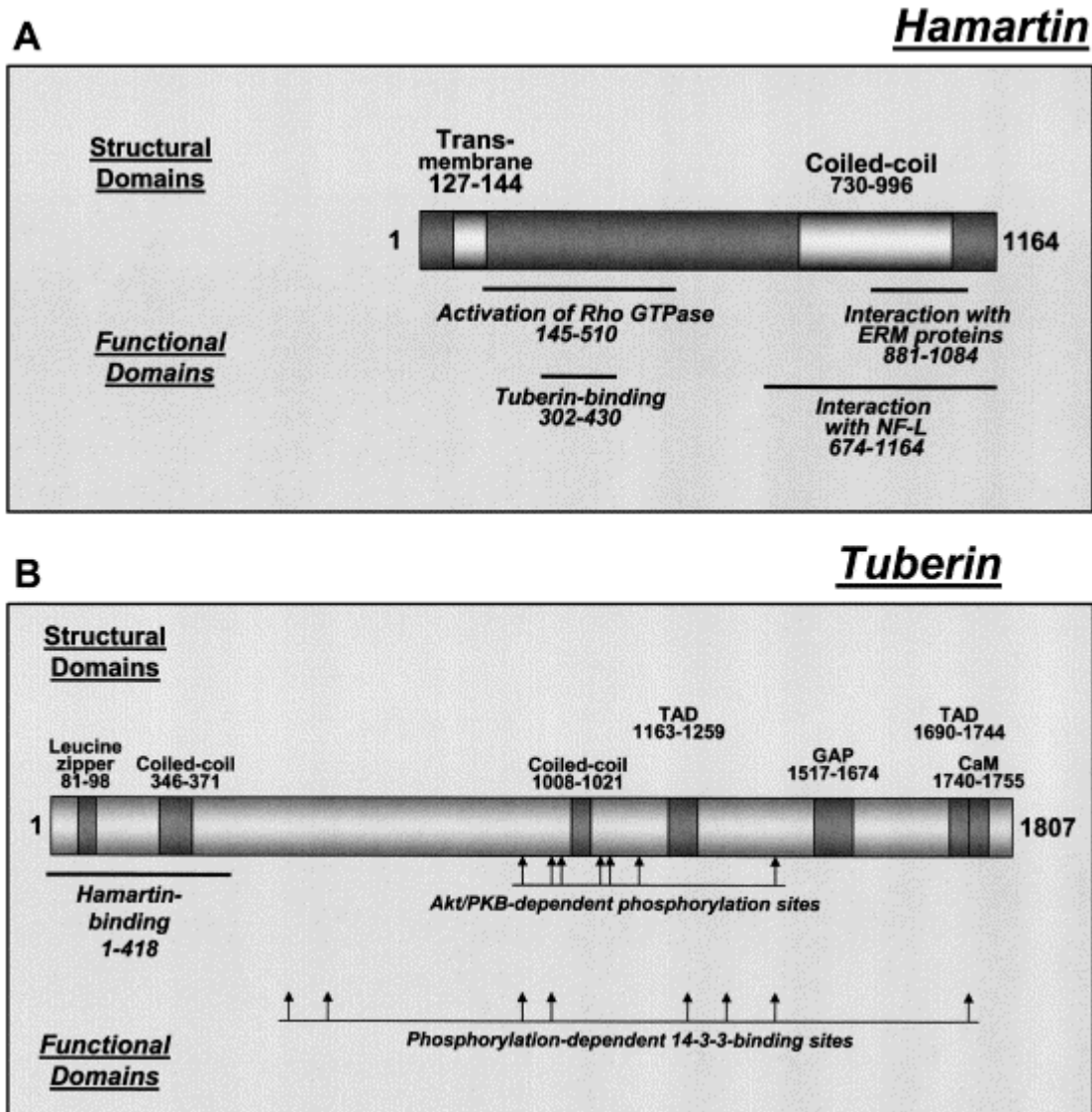


**Figure 1. Schematic representation of the structural-functional domains of hamartin (A) and tuberin (B).** Reprinted from *Cellular Signalling*, 15(8), Vera P. Krymskaya, 729-39, Copyright (2003), with permission from Elsevier.

(A) Hamartin has potential transmembrane and coiled-coil domains. Among functional regions are the tuberin-binding, ERM-binding, neurofilament-L-binding, and Rho-activating domains. (B) Tuberin includes leucine zipper, two coiled-coiled, two transcription-activating domains (TAD), GAP homology, and calmodulin (CaM)-binding domains. Hamartin-binding motif is localized near the N-terminal. Multiple Akt/PKB-dependent phosphorylation sites are indicated with arrows. Phosphorylation sites modulating 14-3-3 association are also indicated with arrows.

About 80% of the disease causing mutations occur *de novo* in either *TSC1* or *TSC2*. The mutation spectrum consists of missense, nonsense, frameshift, deletions/insertions and splice junction domains. *TSC2* mutations are often missense or nonsense and *TSC1* mutations are commonly nonsense or frameshift mutations. Unlike familial cases of TSC, where the frequency of mutation is equal for *TSC1* and *TSC2*, in sporadic cases *TSC1* mutations account for only about 10-15% of patients while *TSC2* mutations are found in about 70% of TSC patients<sup>17</sup>. There is an increased frequency of germline and somatic mutations in *TSC2* compared to *TSC1*.

The clinical features of *TSC1*- and *TSC2*-linked disease are similar, but patients with *TSC2* mutations tend to be more severely affected than those with *TSC1* mutations. They often have more severe cognitive impairment, and more cortical tubers, retinal hamartomas and angiofibromas<sup>18, 19</sup>. In about 15-20% of patients, no mutations can be identified<sup>20</sup>. These patients tend to have a milder clinical phenotype than in patients with identified *TSC1* or *TSC2* mutations. This mild phenotype may be explained in some cases by a somatic mosaicism reported in some patients with *TSC1* or *TSC2* mutations<sup>21</sup>.

TSC tumors follow Knudson's two-hit hypothesis where an inherited (germline) mutation in one allele of a tumor suppressor gene predisposes an individual for tumor formation and a second mutation (somatic) on the wild-type allele of the gene initiates tumor formation<sup>22</sup>. The second hit is usually a deletion of the chromosomal regional surrounding the gene, resulting in loss-of-heterozygosity (LOH). LOH is observed commonly in tumors resected in TSC patients with kidney angiomyolipomas and LAM. LOH is observed less frequently in cardiac rhabdomyomas and SEGAs and is extremely rare in cortical tubers<sup>23-26</sup>.

## Functions of TSC genes

The TSC proteins form a physical and functional complex that is coexpressed in cells of multiple organs<sup>27</sup>. The interaction is regulated by tuberin phosphorylation<sup>28</sup> and is important for the stability of each protein. Studies have shown that the two proteins are diffusely cytoplasmic although TSC2 has been found to be localized to the Golgi apparatus<sup>29</sup> and nucleus<sup>30</sup> while TSC1 localizes to the centrosome<sup>31</sup>.

The normal cellular functions of TSC proteins were uncovered by genetic studies in the fruit fly, *Drosophila melanogaster*. Mutant cells with the drosophila homologues *dTSC1* and *dTSC2* showed that the mutations caused an identical phenotype characterized by an increase in cell and organ size, suggesting a role of TSC proteins in regulating cell size<sup>32</sup>. The TSC proteins are involved in controlling growth signals through the PI3K-Akt pathway. Biochemical and genetic experiments found that the TSC1-TSC2 heterodimer acts downstream of Akt and TSC2 is phosphorylated by Akt/ protein kinase B (PKB) at two residues, S939 and T1462<sup>33-35</sup>. This phosphorylation of tuberin leads to dissociation of the TSC complex and is an important step for insulin and other growth factors to activate downstream effectors of cell growth. A key downstream component that is catalytically activated in response to PI3K signaling is the mammalian target of rapamycin (mTOR). Studies in yeast, insects and mammals have shown that the TSC complex acts upstream and inhibits mTOR<sup>36, 37</sup> (Figure 2). mTOR is a serine threonine kinase that has central roles in controlling cell growth and proliferation through phosphorylation of p70S6k and 4EBP1. Phosphorylation of p70S6k leads to increased ribosomal biogenesis and phosphorylation of 4EBP1 inhibits the translational repressor and permits mRNA translation<sup>38</sup>. Loss of tuberin or hamartin as seen in TSC tumors leads



to activation of mTOR, resulting in phosphorylation of ribosomal S6K and 4EBP1. Activation of mTOR is frequently demonstrated by increased phosphorylation of a substrate of S6K, ribosomal protein S6.

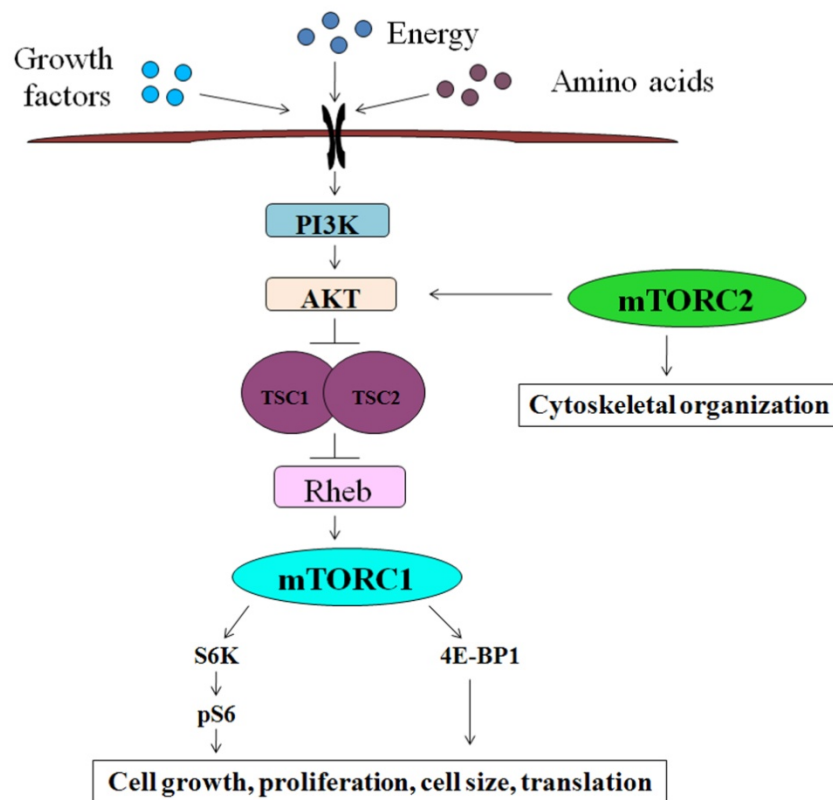


**Figure 2. mTOR signaling pathway.**

The mTOR pathway integrates signals from various sources, including nutrients, growth factors and energy status of a cell. mTOR exists in two distinct complexes, mTORC1 and mTORC2. mTORC1 is rapamycin sensitive, phosphorylates ribosomal S6K and 4EBP1 and determines cell size. mTORC2, is rapamycin insensitive, phosphorylates Akt, and determines cell shape by regulating the actin cytoskeleton. Insulin and growth factors activate mTOR through PI3K and Akt. Akt activation inhibits the TSC1/TSC2 complex, resulting in mTORC1 activation. TSC proteins are upstream regulators of mTOR, which act as a GTPase activating protein for Rheb, a positive mTOR regulator. Loss of TSC1/TSC2 results in constitutive activation of mTORC1, which exerts a negative feedback on Akt activity. On the contrary, mTORC2 activates Akt suggesting a regulation of the pathway through both positive and negative controls.

The TSC proteins receive signals from several signaling cascades in addition to the PI3K pathway. An energy-sensing pathway is activated through AMP-activated protein kinase (AMPK), which is a primary energy sensor. Under energy-deprived conditions, the tumor suppressor LKB1 is activated and phosphorylates the activation loop of AMPK. The activated AMPK in turn phosphorylates TSC2 at sites (S1270 and S1388) that are distinct from those phosphorylated by Akt, enhancing the activity of the TSC complex<sup>39</sup>. This blocks mTOR activation and protects the cells from energy deprivation-induced apoptosis.

TSC proteins are also involved in the mitogen-activated protein kinase (MAPK) pathway activated by oncogenic Ras or mitogens. Phosphorylation of TSC2 by the MAPK-activated kinase RSK1 at S1798 inactivates the complex increases mTOR signaling to S6K, resulting in cell growth and proliferation<sup>40</sup>. A similar abrogation of tumor suppressor function of TSC2 is observed when TSC2 is phosphorylated by Erk at S664 resulting in increased mTOR signaling and cell survival<sup>41</sup>.

These proteins are intertwined in a cellular signaling network but also have distinct functions<sup>42</sup> that trigger different cellular responses. TSC1-knockout studies in mice showed similar tumor development and embryonic lethality but not identical to TSC2 knockout mice<sup>43</sup>. TSC pathology reflects abnormalities in cell size, number, morphology and location, which implies a role for the TSC genes in regulating different cellular responses such as proliferation, growth, differentiation and migration<sup>44</sup>.

### **mTOR signaling**

mTOR was discovered in the early 1990s<sup>45</sup>. It is a serine threonine kinase that regulates various physiological processes including cell growth, proliferation, motility, survival and protein synthesis, metabolism and cytoskeletal organization by integrating signals from nutrient availability, stress factors, hormonal factors and energy status. It is a 289-kDa protein with several structurally conserved domains. The amino-terminal region possesses tandem HEAT repeats (Huntington, elongation factor 3, Protein phosphatase A and TOR). The carboxy terminal domain contains the FAT domain followed by the FRB domain, a kinase domain and the FATC (FAT c-terminus) domain<sup>46</sup>. TOR proteins are found in two functionally distinct multiprotein complexes, mTORC1 and mTORC2, that coexist in cells from yeast to humans<sup>47</sup>.

### **mTORC1 signaling**

mTORC1 is composed of mTOR (also known as FRAP1), Raptor (regulatory associated protein of mTOR) and mLST8 (lethal with SEC13 protein 8). The two well-characterized downstream targets of mTORC1 are ribosomal S6 kinases S6K1 and 4E-BP1 (eukaryotic translation initiation factor 4E-binding protein 1). Phosphorylation of S6K on Thr389 by mTORC1 can in turn initiate protein synthesis by phosphorylation and activation of its downstream targets, ribosomal S6 and eIF4B, promoting mRNA translation. 4E-BP1 can be phosphorylated at four different sites by mTORC1 (Thr37, Thr47, Ser65 and Thr70). 4E-BP1 binds and prevents the translation initiation factor eIF4E from binding to 5'-capped mRNAs and their recruitment to the ribosomal initiation complex. Phosphorylation of 4EBP1 triggers the release of eIF4E at the 5'-cap of mRNAs, initiating cap-dependent translation of translational factors and ribosomal

proteins<sup>48</sup>. Therefore, phosphorylation of mTORC1 downstream targets promotes cell growth by constitutive activation of S6K1 and ribosomal S protein phosphorylation which are crucial components required for cell growth and proliferation<sup>38, 49-51</sup>.

mTORC1 acts as a nutrient/energy/redox sensor that responds to various growth factors, mitogens, energy, nutrients and cellular stress and directly controls protein synthesis<sup>38</sup>. mTOR and raptor have a strong interaction at the N-terminus, with a weaker interaction at the C-terminus. The interaction between mTOR and raptor regulates the activity of mTORC1<sup>52</sup>. Under nutrient-stimulated signaling, the mTOR-raptor interaction is weakened, allowing signaling to the downstream effector S6K1, maintenance of cell size, and mTOR protein expression. Once the nutrients are deprived or stimulatory signals withdrawn, the interaction between mTOR and raptor is stabilized and mTOR kinase activity is inhibited.

The TSC1-TSC2 complex has been shown to inhibit phosphorylation of both S6K and 4EBP1, and inactivating mutations of the TSC gene leads to activation of these mTORC1 targets. Studies in *Drosophila* identified a small G-protein Rheb (Ras homolog enriched in brain) that is ubiquitously expressed and promotes cell growth in a mTOR- and S6K- dependent manner<sup>53, 54</sup>. This GTPase acts downstream of the TSC complex and is a functional link between the TSC complex and mTOR<sup>39, 55</sup>. TSC2 in complex with TSC1 acts as a GTPase-activating protein for Rheb, increasing GDP bound on Rheb, thereby inactivating Rheb. Rheb is active in its GTP-bound form and inactive in the GDP-bound form. Conversely, accumulation of GTP-bound Rheb results in activation of mTOR suggesting that the TSC complex regulates mTOR activation by suppressing

Rheb<sup>56</sup>. Rheb exists as two homologues namely Rheb1 or Rheb 2 (Rheb like-1) in a number of organisms with an overlapping function of activating mTORC1 signaling<sup>57</sup>.

### **mTORC2 signaling**

mTOR Complex 2 (mTORC2) is composed of mTOR, rictor (rapamycin-insensitive companion of mTOR), mLST8, and SIN1 (stress-activated protein kinase interacting protein 1)<sup>58</sup>. It is involved in regulating the actin cytoskeleton by phosphorylation of F-actin stress fibers, paxillin, Rho A, Rac1, Cdc42 and PKC $\alpha$ . mTORC2 responds to growth factors, insulin, serum and nutrients but its regulation is not clear. One of the downstream targets of mTORC2 is the cell survival protein Akt. mTORC2 phosphorylates Akt on ser 473 in its C-terminal hydrophobic motif<sup>59</sup> and results in its activation. Loss of TSC1 or TSC2 attenuates the kinase activity of mTORC1 resulting in attenuated phosphorylation levels of Akt in several cell lines. Also, blocking with mTORC1 inhibitors did not reverse the kinase activity of mTORC2, suggesting an involvement of the TSC complex in mTORC2 regulation. Further studies showed that regulation by the TSC complex is through a direct physical association with mTORC2<sup>60</sup>. Thus, downregulation of Akt in TSC2 deficient cells can be accounted for by mTORC1 negative feedback and direct effects on mTORC2.

### **Rapamycin as a therapeutic agent**

Rapamycin is a drug, first investigated as an anti-fungal agent, isolated from the bacteria *Streptomyces hygroscopicus* from an Easter Island (Rapa Nui) soil sample in 1975<sup>61</sup>. The chemical structure (Figure 3) is similar to cyclosporine A and FK506 but it is not a calcineurin inhibitor. Rapamycin potently inhibits yeast cell growth and it has been shown to arrest several cell types in G1 including B and T lymphocytes. It has powerful

anti-microbial, anti-proliferative and immunosuppressant properties<sup>62</sup>. The oral bioavailability of rapamycin is 15% and a maximum blood concentration is reached after 0.5-2.3hrs.

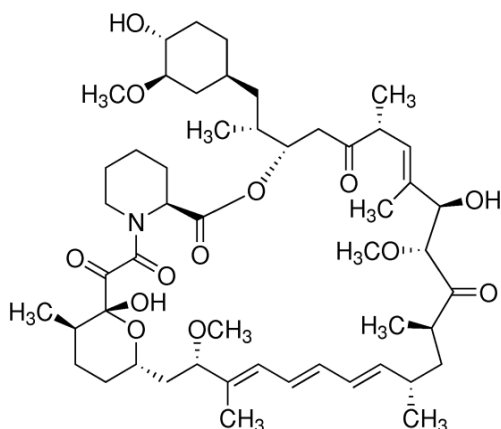


**Figure 3: Structure of rapamycin.** *Reprinted from [www.dominiosweb.org/drugs/rapamycin](http://www.dominiosweb.org/drugs/rapamycin) with copyright permission.*

Rapamycin binds to its intracellular cytoplasmic 12-kDa receptor FKBP12 (FK506-binding protein 12), that is ubiquitously expressed. The rapamycin-FKBP12 complex then interacts with the FRB (FKBP\_rapamycin binding) domain of TOR, a segment amino terminal to the catalytic kinase domain<sup>63-65</sup>, and inhibits TORC1 signaling. Rapamycin inhibits the interaction between raptor and mTOR and reduces the recruitment of the downstream targets of mTOR by raptor, thereby inhibiting mTOR without affecting its catalytic activity<sup>66</sup>.

*In vitro* studies in our laboratory showed that rapamycin treatment blocked mTORC1 activation in TSC2-null cells as measured by inhibition of S6K and S6<sup>67</sup> (Figure 4a). The viability of TSC2-null cells was reduced to a greater extent than that of normal appearing fibroblasts (subsequently referred to as TSC normal fibroblasts)

obtained from the same patient (Figure 4b). Rapamycin treatment therefore results in reduced growth, cell cycle progression and proliferation.

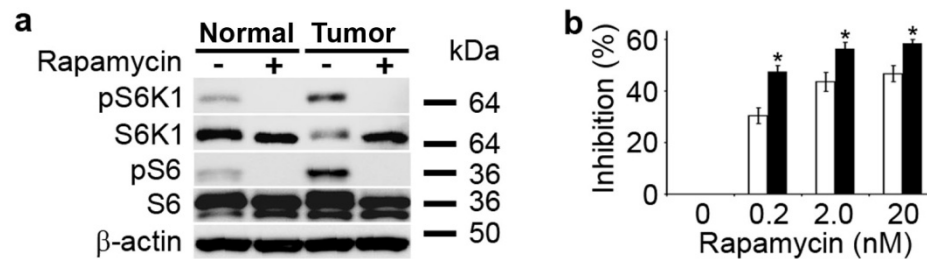


**Figure 3: *In vitro* effects of rapamycin in TSC.** Reprinted from Li et al, *Nature Communications*. 2011; 2:235 with copyright permission from Nature Publishing Group  
a) Western blot analysis of protein lysates from serum-starved cells shows that rapamycin blocked phosphorylation of S6K and S6 in fibroblast-like cells from a forehead plaque. b) Rapamycin at 0.2, 2 and 20nm inhibited proliferation of TSC2-null cells to a greater level than that of TSC normal fibroblasts as measured by MTT assay.

The interaction between mTOR and rictor is not affected by rapamycin. Acute exposure to rapamycin did not affect the rapamycin-insensitive complex mTORC2 or Akt phosphorylation as the FKBP12-rapamycin complex did not bind to mTORC2<sup>59</sup>. However prolonged exposure to rapamycin in some cell lines inhibited mTORC2 and Akt phosphorylation<sup>59</sup>.

Rapamycin exerts anti-tumor effects in cancer cell lines in culture by promoting apoptosis of cancer cells<sup>68</sup> and restricting tumor vascularization by inhibiting vascular proliferation<sup>69</sup>. A number of rapamycin analogs have been developed and are used clinically, including CCI779 (tacrolimus), RAD001 (everolimus) and AP23573 (deforolimus). These have the same mechanism of action as rapamycin and inhibit mTOR by binding to FKBP12<sup>70</sup> but differ in their pharmacokinetic profiles,

bioavailability and side effects. Rapamycin is also used in arterial stents to inhibit restenosis that occurs after coronary angioplasty<sup>71</sup>.

Preclinical studies with rapamycin or CCI779 in TSC rodent models show apoptosis, decreased proliferation with significant reductions in kidney, subcutaneous and pancreatic tumors<sup>72-74</sup>. In humans, rapamycin induces partial regression of renal AMLs and brain SEGAs<sup>75-77</sup>. Hofbauer GF et al, demonstrated that treatment of TSC patients with rapamycin dramatically improved facial angiofibromas<sup>78</sup>. Rapamycin treatment was found to be effective in LAM patients by stabilizing lung function<sup>79</sup>.

### **TSC skin tumors**

Our laboratory focuses on TSC skin tumors because they are common and a major concern to patients and are also readily accessible for biopsy. Skin lesions constitute four major and one minor feature in TSC diagnosis<sup>80</sup>. The lesions include hypomelanotic macules, forehead plaques, facial angiofibromas, ungual fibromas and shagreen patches<sup>81</sup> (Figure 5). These lesions range from being subtle to disfiguring.





**Figure 5. Cutaneous findings in TSC.** TSC skin lesions include hypomelanotic macules, shagreen patch, angiofibromas, forehead plaque, and ungual fibroma. TSC skin tumors are frequently pink to red, a clinical indication of increased vascularity.

Hypomelanotic macules, also referred to as ash leaf spots, may appear during birth or early infancy and persist throughout life. They are most commonly found distributed on the trunk, limbs and buttocks and are diagnosed in fair-skinned individuals using the UV light of a Wood lamp. Hypomelanotic macules are among the most common early manifestations of TSC, since they are observed in 90% of children below 2 years<sup>82</sup>. One or two hypomelanotic macules may appear in healthy individuals as well, so there must be three or more hypomelanotic macules to fulfill a diagnostic criterion for TSC. The hypopigmentation is related to a decrease in number, size and melanization of the melanosomes<sup>83</sup>. A second type of hypomelanotic macules, called “confetti-like lesions”, are also observed in TSC patients<sup>10, 82</sup>. These are smaller spots that constitute a minor feature for diagnosis.

Shagreen patches are irregular sections of thickened bumpy skin of varying size with a surface appearance of an orange peel generally found on the lower back. Histologically,

they are connective tissue hamartomas that are composed of collagen, vessels, adipose tissue and cutaneous appendages<sup>84</sup>. These skin-colored, pink or brown lesions are a rarity in infancy, but occur in almost 50% of the patients and increases in size and number with age. They are sometimes mistaken for normal skin under microscopic examination<sup>85</sup>.

Facial angiofibromas were inaccurately termed as “adenoma sebaceum” and first linked to TSC by Vogt in 1908. These were considered pathognomonic for TSC and affect about 75-90% of patients<sup>10, 82</sup>. Angiofibromas are small red to reddish brown spots with a smooth, glistening surface. They are symmetrically and bilaterally distributed in the central face, especially on the cheeks, nose and chin in a “butterfly” distribution. They can also occur on the forehead or eyelids, but typically spare the upper lip. Angiofibromas develop at about 3-5 years of age and grow progressively into adulthood. Histological sections show large, stellate fibroblasts in the dermis with increased number of dilated capillaries. The sebaceous glands are often atrophic and collagen fibers are found around the follicles and vessels<sup>86, 87</sup>. Angiofibromas cause psychological distress as they can bleed spontaneously or under trauma and are a major cosmetic concern. The current treatment modalities include cryosurgery, chemical peeling, excision, curettage, dermabrasion and laser therapy<sup>88</sup>.

Forehead plaques are skin-colored, erythematous, rubbery to firm, raised plaques with variable size and shape seen unilaterally on the forehead but also on the scalp, cheeks and anywhere on the face. They gradually develop with age and can be detected as early as infancy. They are seen in 20-40% of TSC patients<sup>82</sup>. They occur as single or multiple lesions. Histologically, they are similar to facial angiofibromas<sup>85</sup>. Surgical removal of the plaques is the best treatment, along with CO<sub>2</sub> laser treatment for larger

plaques. Facial angiofibromas and forehead plaques are considered as one major feature in the TSC diagnostic criteria<sup>13</sup>.

Ungual fibromas, also termed Koenan's tumors, are skin- or pink-colored fibrous growths that emerge in the teen years or later. They are rare in children and affect up to 88% of TSC adults<sup>10, 82</sup>. Ungual fibromas are seen around the nail beds of fingernails or toenails, and are more infrequent in the toes than fingers<sup>10</sup>. Nodules arising from below the proximal nail fold are termed periungual and those under the nail plate as subungual fibromas. These fibromas disfigure the nail, tend to bleed when traumatized and are painful. Histologically, they resemble angiofibromas but with extensive hyperkeratosis<sup>89</sup>. Solitary lesions can also occur following trauma in the general population, so the TSC diagnostic criteria require the presence of non-traumatic ungual fibromas<sup>13</sup>. The treatment options currently available are surgical excision or laser ablation<sup>88</sup>.

Overall, the surgical treatments of TSC skin tumors are efficient but expose the patient to anesthesia risks and cause permanent scarring and pigmentary changes<sup>90</sup>. There is also an issue of recurrence requiring frequent treatments with painful postoperative periods. The ideal treatment would be quick, painless, permanent, and leave no scarring. This treatment does not currently exist.

### **Angiogenesis**

Blood vessels supply oxygen and nutrients to tissues to maintain homeostasis and function. Blood vessels are formed in two processes: 1) vasculogenesis, the formation of primitive capillaries by differentiation of precursor cells called angioblasts or 2) angiogenesis, the sprouting of endothelial cells from preexisting blood vessels through enlargement or division. Angiogenesis is a multistep complex vital process that

is normally involved in growth and development, wound healing and in granulation tissue<sup>91</sup>. However, it also serves as a major process by which tumors transform into a malignant state<sup>92</sup>.

A number of key molecules have been identified that participate in inducing angiogenesis, including vascular endothelial growth factor (VEGF), platelet-derived growth factor (PDGF), angiopoietins, hepatocyte growth factor (HGF) and fibroblast growth factor (FGF). One of the well-characterized family of growth factors that are primary players in vasculogenesis and angiogenesis is the VEGF family<sup>93</sup>.

### **Vascular endothelial growth factor**

The VEGF family of proteins includes VEGF-A, -B, -C, -D and placental growth factor (PlGF). These ligands bind to one of the three type III tyrosine kinase receptors namely Flt-1/VEGFR-1, Flk-1/VEGFR-2, and Flt-4/VEGFR-3 and 2 co-receptors neuropilin-1 and 2. VEGFR-1 binds VEGF-A and -B, VEGFR-2 binds VEGF-A, -B, -C, -D and VEGFR-3 binds VEGF-C and VEGF-D (Figure 6). VEGF-A is a disulphide 46-kDa dimeric glycoprotein that occurs in four different isoforms VEGF-A 121, 165, 189 and 201 by alternate splicing<sup>94</sup>. VEGF-A is produced by different cell types and binds to its receptors VEGFR-1 and VEGFR-2, which are expressed on endothelial cells. Binding causes receptor dimerization, phosphorylation of the tyrosine residues and activation of a signaling cascade that mediates different angiogenesis processes like endothelial cell proliferation, invasion, migration and survival<sup>95, 96</sup>. VEGFR-2 is thought to be the primary receptor for inducing angiogenesis<sup>97</sup>. VEGFR-1 also binds VEGF-B and PlGF and plays a more important role during embryonic angiogenesis than tumor angiogenesis<sup>95</sup>.

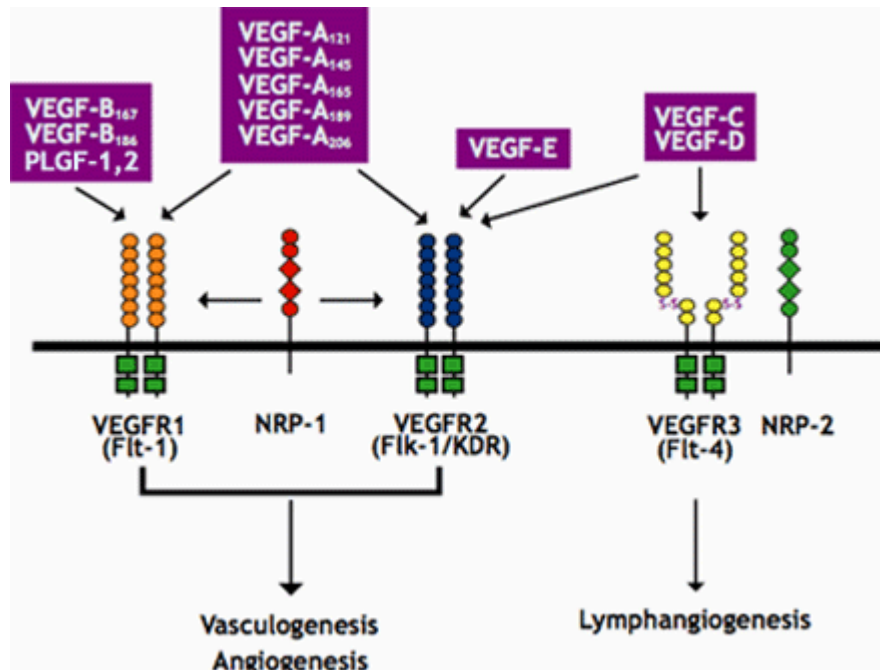


**Figure 6. Receptor binding specificities of VEGF family members.** *Reprinted from Hicklin DJ, Ellis LM, Journal of Clinical Oncology, 23(5), 2005:1011-27 with copyright permission.*

VEGF receptors are shown spanning the plasma membrane. VEGFR-1, VEGFR-2, and VEGFR-3 are structurally homologous and consist of seven immunoglobulin homology domains in the extracellular region and a tyrosine kinase domain in the intracellular portion that is interrupted by a tyrosine kinase insert domain. A soluble form of VEGFR-1 exists but is not shown. The extracellular domain of VEGFR-3 is proteolytically cleaved in the fifth immunoglobulin-like domain and the fragments remain associated by disulfide bonds (S-S). Neuropilin 1 consists of a short intracellular domain and an extracellular domain containing two complement C1r/s homology domains, two domains with homology to coagulation factors V and VIII, and a single MAM domain.

Neuropilin-2, which also binds VEGF, is not shown here. The VEGF family members (represented as dimers) that interact with each receptor are indicated at the top of the figure and are represented in the diagram as dimers bound to the receptors. The biological consequence of signaling through VEGFR-1 is not fully understood whereas activation of VEGFR-2 and VEGFR-3 signals predominately for angiogenesis and lymphangiogenesis, respectively. Nonetheless, it is apparent that VEGFR-2 is also present on lymphatic endothelium and that VEGFR-3 can be expressed on the endothelium of tumor blood vessels.

Targeted disruption of VEGF-A or its receptors in mice caused defective vascular development and embryonic lethality<sup>98, 99</sup>. Overexpression studies in chick embryos led to hypervascularization of the limb bud<sup>100</sup> confirming the indispensability of the VEGF-A system in angiogenesis. VEGF-A and its receptors are expressed at high levels in many tumors including renal cell carcinomas and gliomas<sup>101, 102</sup> and correlates with poor survival. Nude mice injected with human tumor cell lines, including rhabdomyosarcoma, glioblastoma multiforme or leiomyosarcoma, showed decreased tumor growth when treated with an anti-human VEGF-A monoclonal antibody<sup>103</sup>. The importance of the VEGFR-2 was established using dominant-negative mutant of the Flk-1/VEGF receptor, which inhibited glioblastoma growth *in vivo*<sup>104</sup>.

### **Angiogenesis in TSC**

Paraffin sections obtained from TSC patients with angiomyolipomas, SEGA brain neoplasms, facial angiofibroma and ungual fibromas showed strong staining for CD-31, demonstrating a high degree of neovascularization. These tumors tend to be highly angiogenic by secreting VEGF-A<sup>105</sup>. High levels of expression of angiogenic factors including bFGF, VEGF and angiogenin are observed in TSC-linked angiofibromas. Conditioned media from TSC2 null rat embryonic fibroblasts stimulated endothelial cell proliferation, suggesting a link between loss of TSC2 and angiogenesis<sup>106</sup>.

## **Hypoxia**

### **Hypoxia inducible factor**

Rapidly growing tumors experience regions of hypoxia. Hypoxia is associated with acquisition of a metastatic phenotype characterized by uncontrolled tumor growth, angiogenesis and resistance to therapy. One of the transcription factors activated during hypoxia to stimulate angiogenesis is hypoxia-inducible factor (HIF)<sup>107</sup>, a heterodimeric protein composed of HIF-1 $\alpha$  and HIF-1 $\beta$  subunits. These two subunits are members of the basic helix–loop–helix (bHLH) and PER-ARNT-SIM (PAS) domain family of transcription factors that bind DNA. The N-terminal region has bHLH and two PAS domains that mediate protein-protein interactions. The c-terminal of HIF-1 $\alpha$  contains two transactivation domains (N-TAD and C-TAD) that mediate interaction with coactivators CBP (CREB binding proteins) and p300. The N-TAD domain contains an oxygen-dependent degradation domain (ODD) and C-TAD whose transcriptional activity is repressed by the inhibitory domain (ID) in normoxia<sup>108</sup> (Figure 7).

HIF-1 $\beta$  is constitutively expressed while the  $\alpha$  subunit is regulated by cellular oxygen levels. Under normal cellular conditions, HIF-1 $\alpha$  undergoes post translational enzymatic hydroxylation at two prolyl residues by prolyl and asparaginyl hydroxylases. This mediates interaction with von Hippel-Lindau tumor suppressor E3 ligase that rapidly ubiquitinates it thereby subjecting it to proteasomal degradation. Under limited oxygen availability, the hydroxylases that utilize oxygen as substrate are inhibited. The  $\alpha$  subunit is stabilized and forms an active complex with the  $\beta$  subunit<sup>109</sup>. The HIF-1 complex then translocates to the nucleus and stimulates transcription of its target genes by binding to the hypoxia response elements (HRE) in the promoter of the respective genes that contain

the sequence 5' ACGTGC 3'. Under hypoxic conditions, HIF- $\alpha$  accumulates instantly but has a very short half life. When cultured cells are subjected to cellular oxygen, HIF is degraded rapidly (<5mins)<sup>110</sup>.

HIF-1 $\alpha$  is a master regulator of gene expression that triggers expression of genes to promote cellular adaptation to reduced oxygen levels. The genes that are upregulated are involved in increasing glucose uptake and glycolysis (GLUT1, lactate dehydrogenase A), increasing oxygen transport to hypoxic tissues by promoting red blood cell maturation (e.g., Epo, transferrin) or inducing angiogenesis/vasomotor control (including VEGF, endothelin-1), and promoting cell proliferation and survival (insulin-like growth factor [IGF] 2 and IGF-binding proteins 1, 2, and 3)<sup>111</sup>. HIF is also essential during embryonic development as deficiency of either subunit has been associated with defective blood vasculature, resulting in embryonic lethality<sup>112, 113</sup>.



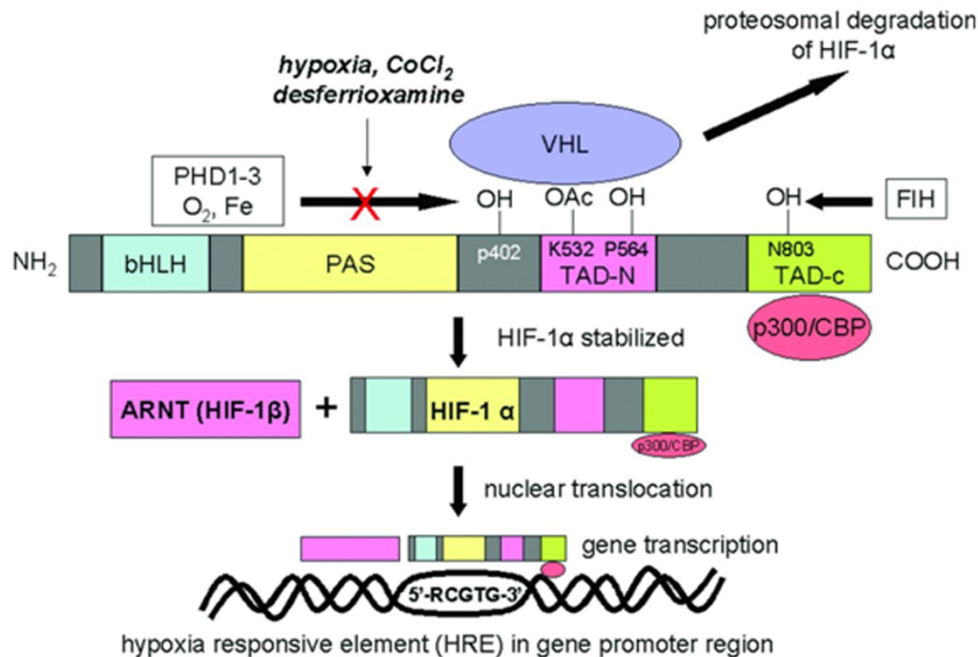


**Figure 7. Hypoxic regulation of the hypoxia-inducible factor-1 $\alpha$  (HIF-1 $\alpha$ ).** Reprinted from Hitchon and El-Gabalawy, *Arthritis Research and Therapy*, 2004;6(6):265-78 with copyright permission from BioMed Central.

Levels of HIF-1 $\alpha$  are regulated primarily through inhibition of degradation. Under normoxic conditions, HIF-1 $\alpha$  undergoes rapid proteosomal degradation once it forms a complex with von Hippel–Landau tumor suppressor factor (VHL) and E3 ligase complex. This requires the hydroxylation of critical proline residues by a family of HIF-1 $\alpha$ -specific prolyl hydroxylases (PHD-1,2,3), which requires O<sub>2</sub> and several cofactors, including iron. Under hypoxic conditions, or when iron is chelated or competitively inhibited, proline hydroxylation does not occur, thus stabilizing HIF-1 $\alpha$  and allowing it to interact with the constitutively expressed HIF-1 $\beta$ . The HIF-1 complex then translocates to the nucleus and activates genes with hypoxia-responsive elements in their promoters. bHLH, basic helix-loop-helix; CBP, cAMP response element binding protein; FIH, factor inhibiting HIF-1 $\alpha$ ; PAS, PER-ARNT-SIM; TAD, transactivation domain.

### Role of hypoxia in angiogenesis

In addition to its role in maintaining homeostasis during hypoxia, HIF-1 $\alpha$  is also associated with diseases including ischemic cardiovascular disease<sup>114</sup> and cancer<sup>115, 116</sup>.

HIF-1 $\alpha$  is one of the main regulators of tumor angiogenesis and progression. HIF-1 $\alpha$  upregulates expression of the angiogenic genes namely VEGF-A, angiopoietins, FGF,

matrix metalloproteinases, and plasminogen activator receptors that are shown to facilitate cell migration or endothelial tube formation in cells cultured under hypoxic conditions<sup>117, 118</sup>. VEGF-A is one of the main angiogenic factors upregulated by HIF-1 $\alpha$ <sup>119, 120</sup>.

HIF-1 $\alpha$  levels are highly elevated in a number of cancers, including breast, lung, colon, glioblastoma and its expression correlates with tumor progression and aggressive behaviour<sup>116, 121</sup>. Homozygous deletion of HIF-1 $\alpha$  in mice showed a marked regression of vessels within the cephalic mesenchyme and embryonic lethality at E9.25<sup>122</sup>. Mouse hepatoma cells that are functionally defective for HIF-1 $\beta$  injected subcutaneously formed tumors. The tumors showed a drastic reduction in vascularization and the tumors grow slowly. The mutant cells also showed almost a complete loss of expression of VEGF-A<sup>123</sup>.

## **Lymphangiogenesis**

### **Lymphatic vascular system**

The lymphatic vascular system was first described by the Italian Gaspero Aselli in 1627. There are two theories proposed for the mechanism leading to formation of lymphatic vasculature namely 1) sprouting from pre-existing blood capillaries or veins<sup>124</sup> and 2) *de novo* differentiation of blood or lymphatic endothelium from angioblasts or lymphangioblasts in the mesenchyme and connections with veins forming later during development<sup>125</sup>. The lymphatic system is composed of a hierarchical network of thin-walled, low-pressure open-ended vessels that are unidirectional including peripheral capillaries, collecting vessels, lymph nodes, larger trunks and the thoracic duct<sup>126</sup>. Lymphatic vessels generally accompany blood vessels but are not always parallel to the

blood supply. They are found in the skin and other tissues except the central nervous system, bone marrow and avascular structures including epidermis, hair, nails, cartilage and cornea. The lymphatic endothelium is distinct functionally and structurally from the blood vessel counterparts<sup>126</sup>. It has fewer tight junctions and lacks a continuous basement membrane, associated pericytes and smooth muscle cells<sup>127, 128</sup>. They have wider lumens that are irregularly shaped and so appear collapsed in tissue sections. The lymphatic endothelial cells (LEC) are seen overlapping the peripheral capillary walls and are anchored to the extracellular matrix by elastic fibers (anchoring filaments) and collagen<sup>129</sup>. These filaments facilitate uptake of soluble tissue components during increased interstitial fluid pressure by widening the capillary lumens and opening cell junctions. In contrast, the collecting lymphatic vessels possess valves that prevent lymph backflow and allow propulsion of lymph through the vessels and are surrounded by sparse smooth muscle cells. These collecting vessels pass through the lymph nodes that function as filters and reservoirs where the T and B lymphocytes are activated. A rather quiescent system under physiological conditions is important for normal maintenance of fluid balance in tissues. It acts as a conduit for return of interstitial protein-rich fluids and macromolecules into the blood stream as well as clearance of the excess fluids, thereby maintaining tissue homeostasis. It directs antigen presenting cells and other immune cells from the peripheral tissues to the draining lymph nodes<sup>130</sup>. The foreign particles are then taken up by these antigen-presenting cells, which then initiate specific immune responses. In the intestine, lacteal lymphatic vessels are present in the intestinal villi. These aid in the absorption of dietary fats from the gut. Impairment in the lymphatic functions leads to

a number of disease processes such as cancer metastasis, lymphedema and various inflammatory disorders<sup>131</sup>.

### **Embryology of the lymphatic system**

Though the lymphatic vascular system was discovered in the seventeenth century, major advances have been made only in the last ten years with the identification of the growth factors and molecular markers specific for the lymphatic vessels. The most common markers identified are Prox1, LYVE-1, podoplanin and VEGFR-3. The development of the lymphatic vessels starts once the blood vascular system is established. The developments starts about embryonic weeks 6-7 in humans and days 9.5-10.5 in mice when a subset of venous endothelial cells get committed to lymphatic endothelial lineage and starts sprouting from the major veins in jugular and perimesonephric area to form the primordial lymphatic vascular structures called the lymph sacs<sup>132</sup>. The peripheral lymphatic system then develops by sprouting of lymphatic vessels from the lymph sacs and merging of the separate lymphatic capillary networks, followed by remodeling and maturation.

One of the earliest events in the development of the lymphatic system is the expression of the homeobox transcription factor Prox1(prospero-related homeobox1) on the endothelial cells at E9.5 in the jugular vein after which these cells migrate in a polarized manner to form the lymph sacs<sup>133</sup>. Prox1-/- knockout embryos do not develop a lymphatic vascular system and die at embryonic day 11.5. Prox-/- deficient endothelial cells initially bud and sprout from the cardinal vein in an unpolarized manner but do not migrate and fail to express any lymphatic markers. They instead appear to have a blood vascular endothelial phenotype. Over-expression of Prox1 upregulates lymphatic-

endothelial cell specific genes and suppresses expression of blood vascular specific genes<sup>134, 135</sup>. Therefore, Prox1 acts as a master switch for commitment of vascular progenitor cells to lymphatic endothelial cell.

Polarized expression of Prox-1 results in upregulation of lymphatic-specific genes such as vascular endothelial growth factor receptor 3 (VEGFR-3) and LYVE-1<sup>136</sup>. LYVE-1 is cell surface lymphatic vessel hyaluronan receptor-1 that is expressed on venous endothelium from E9 in mice. This receptor is highly specific for hyaluronic acid in epithelial, mesenchymal and lymphoid cells and functions in transport of hyaluronan from tissue to the lymph<sup>137</sup>. Hyaluronan plays an important role in maintaining tissue integrity and facilitates cell migration during wound healing, embryogenesis and inflammation. LYVE-1 is a first marker of lymphatic endothelial commitment expressed in subset of endothelial cells in the central veins. Its expression is almost simultaneous with Prox1 but remains highly expressed in the lymphatic capillaries and its expression is reduced in the collecting vessels. The expression levels of LYVE-1 are unpredictable and knockdown experiments in mice showed that LYVE-1<sup>-/-</sup> had a normal phenotype, with no changes in lymphatic structure and function, suggesting a dispensable role in lymphatic development<sup>138</sup>.

Podoplanin is an integral mucin-type plasma membrane glycoprotein highly expressed in podocytes, keratinocytes, cells of choroid plexus, alveolar lung cells and in the endothelium of lymphatic capillaries but not in the blood endothelium<sup>139</sup>. Mice deficient in podoplanin die at birth due to respiratory failure and have lymphedema, and defects in lymphatic vessel patterning but not in blood vessel pattern formation<sup>140</sup>. *In vitro* studies have indicated the involvement of podoplanin in promoting cell adhesion,

and cell motility by promoting rearrangement of the actin cytoskeleton and tube formation. Podoplanin serves as a key player in regulating multiple aspects of lymphatic vessel formation.

Vascular endothelial growth factor receptor 3 (VEGFR-3) is one of the major regulators in LECs. It is activated by its ligands VEGF-C and VEGF-D. The receptor is expressed in all the endothelial cells at a very early stage as VEGFR-3 deletion causes embryonic death at E9.5 and mice show defects in vessel remodeling before the emergence of the lymphatic vessels<sup>141</sup>. However, once the endothelial cells are committed to the lymphatic origin, VEGFR-3 is expressed in the angioblasts of head mesenchyme and the cardinal vein and in the later stages becomes restricted to the LEC<sup>142</sup> as well as activated macrophages and dendritic cells<sup>143</sup>. Makinen et al were able to isolate and culture stable lineages of blood and lymphatic endothelial cells from primary human dermal microvascular endothelium using antibodies against VEGFR-3<sup>144</sup>. Further studies with VEGF-C and its mutant form VEGF 156S, which specifically binds VEGFR-3 but not VEGFR-2, showed that signaling via VEGFR-3 is sufficient and essential for cell migration, growth and survival of the LECs. Also, inhibition of VEGFR-3 signaling results in apoptosis of LEC and regression of pre-existing lymphatic vessels during embryogenesis. Transgenic mice created by overexpressing a soluble form of the VEGFR-3 extracellular domain or VEGF-D in the epidermal keratinocytes as a transgene under the control of a keratin 14 promoter showed selective hyperplasia of the lymphatics but not the blood vasculature in the transgenic skin<sup>144, 145</sup>. Stimulation of VEGFR-3 signaling pathway seems to be the primary receptor to induce lymphangiogenesis *in vivo*.

A more extensive range of lymphatic markers related to different stages of lymphatic endothelial cell (LEC) differentiation and function are currently known. However, all the markers are not expressed by the lymphatic vessels. Some are not essential for lymphatic development, like the LYVE-1, while many others are indispensable for embryonic development of lymphatic vasculature.

### **Lymphangiogenesis**

Lymphangiogenesis is the process of formation of lymphatic vessels from pre-existing vessels. Tube-like structures are formed by association of endothelial cells that proliferate and migrate towards a stimulus. The stimulation of lymphatic vessel growth is a complex process that is triggered by overproduction of lymphangiogenic factors and downregulation of lymphangiogenic inhibitors. The factors are either secreted by the tumor cells, stromal cells or inflammatory cells. A number of factors have been identified as stimulators of lymphangiogenesis *in vitro* and *in vivo* namely members of the VEGF namely VEGF-C, VEGF-D and VEGF, HGF, PDGF, FGF and insulin-like growth factor (IGF) families.

### **Vascular endothelial growth factors**

VEGF-C and VEGF-D are the most potent lymphatic factors that bind to the VEGFR-3 and induce lymphangiogenesis by stimulating proliferation, migration and survival of LECs<sup>144, 145</sup>. VEGF-C and -D are structurally different from VEGF-A because of the amino and C-terminal COOH extensions but retain the central conserved VEGF homology domain (VHD) and are alternatively spliced in both human and mouse<sup>146</sup>. They are secreted as full-length proteins with amino and carboxy terminal regions flanking the VHD<sup>147</sup>. They then undergo proteolytic cleavage from the VHD by plasmin

and other proteases after secretion<sup>148</sup>. This generates mature VEGF-C and -D that bind the receptors VEGFR-2 and VEGFR-3 with higher affinity than the full-length form and can induce angiogenesis under certain conditions in addition to lymphangiogenesis<sup>149</sup>. VEGF-C<sup>-/-</sup> mice commit to the lymphatic lineage but do not sprout into lymphatic vessels resulting in prenatal death. VEGF-C heterozygous mice show severe lymphatic hypoplasia. Further, vegf-c deletion in *Xenopus* tadpoles and zebrafish results in initial differentiation in the embryonic veins but without migration to form the lymph sacs<sup>150, 151</sup>. This highlights the importance of VEGF-C for sprouting of the first lymphatic vessels from embryonic veins. However mutant mice deficient for VEGF-D were healthy and fertile with no visible lymphatic abnormalities. They just had reduced levels of lymphatics in the bronchioles, suggesting a dispensable role for VEGF-D during embryogenesis<sup>152</sup>. Overexpression of VEGF-C in MBA-MD-435 breast cancer cells implanted in nude mice resulted in tumors with enlarged lymphatics and also facilitated metastasis of the tumors to regional lymph nodes and lung<sup>153</sup>. A similar phenotype with increased lymphangiogenesis and metastasis was observed in VEGF-D overexpressing epithelioid tumors<sup>154</sup>.

VEGF-A, a strong angiogenic factor is also known to induce lymphangiogenesis. Overexpression of VEGF-A in immunodeficient mice, resulted in formation of abnormal giant lymphatics with incompetent valves<sup>155</sup> but very little sprouting. Satoshi et al showed that mice overexpressing VEGF-A under carcinogenic induction upregulated proliferation of VEGFR-2 expressing tumor associated lymphatic vessels<sup>156</sup>.



## **Hepatocyte growth factor**

Hepatocyte growth factor (HGF), also known as scatter factor, was first discovered as a mitogen of rat hepatocytes<sup>157, 158</sup>. It is a heparin-binding and dermatan sulfate-binding pleiotropic glycoprotein secreted by various cells of the mesenchymal origin. It is primarily involved in morphogenesis of epithelial tissues and the development of different organ structures<sup>159</sup>. The cellular targets of this multipotent cytokine include hepatocytes and other epithelial cells, melanocytes, endothelial and haematopoietic cells<sup>160</sup>. It is synthesized as a single inactive pro-HGF and requires proteolytic cleavage by extracellular serine proteases such as urokinase plasminogen activator and tissue-type plasminogen activator to form the mature HGF<sup>161, 162</sup>. In 1991, c-Met was identified to be the tyrosine kinase receptor for HGF by Bottaro et al<sup>163</sup>. HGF binding to the proto-oncogenic c-Met receptor induces receptor dimerization, and transphosphorylation of the c-terminal tyrosine residues, generating a multidocking site, which activates a tyrosine kinase signaling cascade that regulates mitogenic, morphogenic and motogenic activities in a wide variety of cells<sup>164</sup>. Some of the cellular responses elicited by HGF and c-Met binding include proliferation of hepatocytes, renal tubule cells and endothelial cells. HGF has been identified as a potential angiogenic factor by affecting endothelial cell motility, proliferation, protease production, invasion, and organization into capillary-like tubes, regulating cell adhesion between cells and matrix and potential morphogenesis. HGF has been shown to stimulate angiogenesis by inducing the expression of VEGF, a key angiogenic factor<sup>165</sup>. Recent studies explore the involvement of HGF in lymphatic vasculature. Clinical studies have also shown a correlation between HGF and/or its receptor and nodal spread and lymphatic invasion in cancer<sup>166-168</sup>. *In vitro* studies have

demonstrated that HGF directly promotes proliferation, migration and tube formation of lymphatic endothelial cells as well. Kentaro Kajiya et al showed that HGF receptor levels are significantly higher in LECs than blood vascular endothelial cells (BVECs).<sup>169</sup>. *In vivo* HGF stimulates lymphatic vessel formation when overexpressed in transgenic mice and that blockade of the c-Met receptor impairs lymphatic vessel function. In a chronic skin inflammation mouse model, activated lymphatic endothelium showed strong expression of HGF-receptor c-Met but quiescent lymphatic vessels of the normal skin did not<sup>170</sup>. HGF and c-Met collectively contribute to promoting lymphangiogenesis and could be potential therapeutic targets for blockade of lymphatic cancer spread.

#### **Other important lymphangiogenic factors**

Some of the soluble factors identified to induce lymphangiogenesis include FGF2, PDGF and IGF. FGF2 is an angiogenic molecule that stimulates angiogenesis *in vitro* and *in vivo*<sup>171</sup>. Recent *in vitro* studies have shown involvement of FGF2 in lymphangiogenesis. It promotes proliferation, migration and tube formation of LECs<sup>172</sup>. The platelet derived growth factors (PDGFs) are a family of growth factors that play a significant role in angiogenesis<sup>173</sup>. Its members, PDGF-AA and PDGF-BB, can also stimulate lymphangiogenesis. They are highly expressed in human tumors that have higher incidence of metastasis<sup>174, 175</sup>. The insulin growth factor family consists of two ligands IGF-1 and IGF-2. Its two transmembrane receptors IGF-1R and IGF-2R have been shown to be expressed on endothelial cells both blood and lymphatic endothelium<sup>176</sup>. The two ligands are highly angiogenic and IGF-1 can also upregulate VEGF expression<sup>177, 178</sup>. Studies by Meit Bjorndahl et al show that IGF-1 and 2 also induce lymphangiogenesis<sup>179</sup>.

### **Lymphangiogenesis in TSC associated tumors**

The existence of lymphangiogenesis in TSC tumors was first reported in lymphangioleiomyomatosis (LAM). Proliferation of “LAM” cells causes obstruction of airways leading to development of cystic lesions and fluid-filled cysts in the lymphatics. This is followed by a progressive decline in pulmonary function which can lead to respiratory failure necessitating oxygen supplementation, and may result in lung transplantation or death<sup>180</sup>. LAM can arise spontaneously or in association with TSC. LOH in *TSC2* has been detected in women with sporadic LAM<sup>26</sup>, suggesting a role for *TSC2* mutations in LAM pathogenesis. Immunohistochemical staining for VEGFR3 and VEGF-C is observed in both pulmonary and extrapulmonary lesions with a significant correlation between VEGF-C expression and severity of the disease<sup>181</sup>. Also, serum VEGF-D levels are increased in woman with sporadic LAM, suggesting dissemination of LAM cells may occur through lymphangiogenesis<sup>182-184</sup>.

## **Chapter 2: Experimental Methods**

### **Tumor sample and cell culture**

Samples of angiofibromas/fibrous plaques, periungual fibromas, and normal-appearing skin were obtained from adult TSC patients enrolled in an Institutional Review Board–approved protocol, 00-H-0051 at the National Heart, Lung, and Blood Institute, NIH. Written consent was obtained from all the patients. Skin samples from TSC patients were bisected and one portion was used for histology and the other for cell culture. To isolate fibroblast-like cells, the skin biopsies were placed in DMEM with 10% FBS in culture plates. The media were changed twice a week, until fibroblast migrated out to cover the dishes. The isolated fibroblasts were maintained in culture in DMEM supplemented with 10% FBS, penicillin (100U/ml) and streptomycin (100 µg/ml).

Keratinocytes were isolated from foreskins of unidentified normal neonates (provided by Dr Jonathan Vogel, NCI) and grown using standard methods. Briefly, tissues were treated overnight with Dispase (Becton Dickinson Labware) at 4 °C. Epidermal sheets were separated from dermal sheets and digested with 0.05% Trypsin 0.53 mM EDTA (Invitrogen) at 37 °C for 20 min. Cells were collected and placed on tissue culture dishes in keratinocyte serum-free media (Invitrogen) supplemented with bovine pituitary extract and recombinant epidermal growth factor.

### **Cytoplasm and Nuclear Fraction**

TSC tumor and TSC normal fibroblasts were grown in 10-cm tissue culture plates until 70-80% confluence in DMEM supplemented with 10% FBS. The media were replaced with fresh media and the cells were incubated under normoxic conditions for 24hrs or hypoxic conditions (1%O<sub>2</sub>) for 4 or 24hrs. To induce hypoxia, the cells were

placed in a modular chamber (Philips-Rothenburg, CA) and flushed with the hypoxic gas mixture (1% O<sub>2</sub>, 5% CO<sub>2</sub> and 94% N<sub>2</sub>) for about 5 min after which the plates were kept at 37°C and incubated for the indicated time points. Cells were lysed and the nuclear and cytoplasmic extracts were prepared using the NE-PER kit (Pierce) according to the manufacturer's protocol. The nuclear extracts were used to detect HIF-1 $\alpha$  protein and cytoplasmic extracts for phospho-S6 protein levels using Western blot.

### **Western Blot Analysis.**

Cells from TSC patient normal skin, angiofibroma, forehead plaques and periungual fibroma were grown in DMEM supplemented with 10% FBS until 70-80% confluent. Media was changed to serum-free DMEM for cell characterization and knockdown studies and maintained in culture for 24 hrs. Cells were lysed in protein extraction buffer (20 mM Tris, pH 7.5, 150 mM NaCl, 1% Nonidet P-40, 20 mM NaF, 2.5 mM Na<sub>2</sub>P<sub>4</sub>O<sub>7</sub>, 1mM  $\beta$ -glycerophosphate, 1mM benzamidine, 10 mM *p*-nitrophenyl phosphate, 1 mM phenylmethylsulfonyl fluoride). The protein concentration was measured using BCA protein assay (Pierce, Rockford, IL). Briefly, equal amounts of each protein were resolved by 10% sodium dodecyl sulfate-polyacrylamide gel electrophoresis and transferred onto 0.45um PVDF membranes (Invitrogen). The blots were probed with mouse anti-HIF-1 $\alpha$  (Novus biologicals), rabbit anti-tuberin (TSC2) C-20 (Santa Cruz, Santa Cruz, CA), anti-phospho-S6 ribosomal protein (Ser 235/236), anti-S6 ribosomal protein (Cell Signaling, Danvers, MA), anti-tubulin, and anti- $\beta$ -actin antibodies (Sigma, St. Louis, MO), horse radish peroxidase-conjugated secondary antibodies (GE healthcare) and Super Signal Pico chemiluminescence detection kit (Pierce). Band intensity was analyzed using image J software (Version 1.35s, National Institutes of Health, Bethesda, MD).

### ***TSC2* sequence analysis**

DNA was isolated from *TSC2*-null fibroblast-like cells and sequenced for *TSC2* mutations by Athena Diagnostics. A part of exon 10 of *TSC2* was amplified using AmpliTaq gold DNA polymerase (Applied Biosystems) and PCR primers 5'-TGGTGTCTATGAGATCGTCC-3' and 5'-AAGGAGCCGTTCGATGTT-3' (for G1074A). The PCR product was purified using the QIAquick Gel Extraction kit (QIAGEN) and sequenced using the 3130xl Genetic Analyzer (Applied Biosystems). To confirm DNA mutations using restricted enzyme digestion, PCR products were amplified using primers of 5'-TGGTGTCTATGAGATCGTCC-3' and 5'-AAGGAGCCGTTCGATGATGTT-3'. The products were digested with *BsmA1* for detecting G1074A, and separated by electrophoresis in 10%TBE gels.

### **Loss of heterozygosity analysis**

Genomic DNA was isolated from TSC patient cells using DNeasy Blood & Tissue kit (QIAGEN) and amplified by PCR with primers flanking microsatellite loci D16S291, D16S521 and D16S663 on chromosome 16p13<sup>185</sup>. One primer of each pair was fluorescently labeled with 6-FAM during synthesis (Invitrogen). PCR products were denatured in formamide containing GeneScan-500 (Rox) size standards and separated on the Genetic Analyzer 3100 (PE Biosystems) capillary electrophoresis system.

### **Creation of *in vitro* composites for xenografts.**

*TSC2*-null cells or TSC normal fibroblasts were mixed with 1 mg/ml of rat tail collagen type 1 (BD Biosciences, Bedford, MA) in 10% FBS/DMEM, and added to 6-well Transwell plates (Corning Incorporated, Corning, NY) at a density of  $0.5 \times 10^6$  cells per well. The dermal constructs were grown in 10% FBS/DMEM for 3 days and overlaid

with  $1 \times 10^6$  keratinocytes. The dermal-epidermal composites were incubated for 2 days submerged in a mixture of DMEM and Ham's F12 (3:1) (GIBCO/Invitrogen, Grand Island, NY) containing 0.1% FBS, after which the composites were brought to the air-liquid interface and grown for another 2 days in DMEM and Ham's F12 (1:1) containing 1% FBS before grafting.

### **Mouse grafting**

Female 6-8 week old Cr:NIH(S)-nu/nu mice (FCRDC, Frederick, MD) were anesthetized with a mixture of O<sub>2</sub> and isoflurane (2-4%). The grafting area on back of the mouse was washed with povidone and hydrogen peroxide topical solution (3%W/V). The graft area was carefully estimated, and skin was removed using curved scissors. Composites were placed on the graft bed in correct anatomical orientation, covered with sterile Vaseline gauze, and secured with bandages. The bandages were changed at 2 weeks and removed after 4 weeks.

### **Animal treatment**

Mice grafted with composites containing TSC2-null cells or TSC normal fibroblasts were treated with rapamycin (2 mg/kg) or vehicle (0.9% NaCl, 5% Polyethylene glycol and 5% Tween-80) every other day by intraperitoneal injection for 12 weeks, starting 5 weeks after grafting. All mouse experiments were conducted in accordance with relevant guidelines and regulations following protocol approval by the USUHS Institutional Animal Care and Use Committee. After treatment, grafts were harvested, one half for paraffin and the other half for frozen sections. Sections were stained with H&E or treated as described below.

## **Immunohistochemistry and quantification**

Paraffin sections of human normal and tumor tissues or xenografts were deparaffinized and treated for antigen retrieval by boiling in 10 mM sodium citrate buffer (pH 6.0) for 20 min. The tissue specimens were stained using human D2-40 (DakoCytomation), mouse D2-40 (Angio Bio.Co, CA), human LYVE-1 (R&D systems), human VEGFR3 (R&D systems), COX IV (Cell Signaling), CD-68 (DakoCytomation), mouse CD31 (Abcam) antibodies and VECTASTAIN ABC kit with Vector® Red (Vector Laboratories, Burlingame, CA) according to manufacturer's procedure. Frozen sections were fixed in acetone at -20°C for 10 min and then stained with Ki-67 (thermo scientific) and F4/80 (Abcam). The relative intensity of positive staining was measured using an Olympus BX40 light microscope (Olympus, Melville, NY) and the digital images were recorded using Openlab 4.0 software (Improvision, Lexington, MA). Measurements of lymphatic vessels in xenografts were performed only within the region of grafts shown to contain human cells.

## **Fluorescence *in situ* hybridization**

Four µm frozen sections were air-dried before incubating in 2X SSC buffer at 37°C for 20 min. Following sequential dehydration in ethanol, sections were treated with 10 mM HCl plus 0.006% pepsin at 37°C for 2.5 min and washed twice in PBS before dehydrating and air drying. Sections were denatured in 70% formamide, 2X SSC at 70°C for 2 min and dehydrated before hybridizing overnight with probe mixture (10.5 µl of hybridization buffer, and 2 µl of probe) at 37°C. The sample was washed twice at 37°C with 2X SSC/ 50% formamide and counterstained by applying 10 µl of DAPI (Vector Laboratories) on each target area. The probes used are Conc. Human Pan Centromeric



Paint, 1695-Cy3-02 (cat# SFP3339) and Conc. Mouse Pan Centromeric Paint-FITC, 1697-MF-02 (cat# MF-02) (Open Biosystems).

### **Y-chromosome fluorescence *in situ* hybridization**

The presence of male-derived human cells in xenografts was analyzed using the Vysis CEP Y (DYZ1) SpectrumOrange probe (Abbot Laboratories) according to the manufacturer's protocol. Briefly, 8- $\mu$ m cryosections were air-dried for 20 min before incubating in 2 $\times$  SSC at 37 °C for 20 min. Following sequential dehydration in ethanol, sections were treated with 10 mM HCl plus 0.006% pepsin at 37 °C for 5 min and washed twice in PBS before dehydrating and air-drying. Sections were denatured in 70% formamide, 2 $\times$  SSC at 73 °C for 5 min and dehydrated before hybridizing overnight with probe mixture (7  $\mu$ l of CEP hybridization buffer, 2  $\mu$ l of water and 1  $\mu$ l of probe) at 42 °C. The sample was washed twice at 68 °C with 2 $\times$  SSC, 0.1% NP-40 and counterstained by applying 10  $\mu$ l of DAPI (Vector Laboratories) on each target area.

### **Gene array analysis**

Gene array data deposited in the Gene Expression Omnibus (GEO) database<sup>26</sup>, [www.ncbi.nlm.nih.gov/geo](http://www.ncbi.nlm.nih.gov/geo) (GEO accession data set GDS3281), were analyzed for levels of *VEGF-A* genes in TSC angiofibroma cells, periungual fibroma cells and TSC normal fibroblasts.

### **SearchLight Protein Array**

Culture supernatants were collected after 24 hr incubation from three paired human normal and tumor fibroblasts (periungual fibroma and forehead plaques) grown in DMEM supplemented with 10% FBS. A simultaneous quantitative measurement was

performed for the following 6 proteins: angiopoietin-2, FGF, PDGFbb, VEGF, VEGF-C and VEGF-D using Pierce searchlight chemiluminescent protein array analysis.

## **ELISA**

Paired human normal and tumor fibroblasts (angiofibromas, periungual fibromas and forehead plaques) ( $2 \times 10^4$  cells/well) were grown overnight on 96-well plates in 10% FBS/DMEM. Media were replaced and the cells were incubated for an additional 24 h. For VEGF-A experiments, media were replaced and cells were grown in DMEM with 1% serum for 24 hr. Cell culture supernatants were then collected and levels of VEGF-A, HGF and VEGF-C were measured in the supernatants using ELISA specific for human VEGF-A, HGF and human VEGF-C (R&D systems) according to the manufacturer's protocol. Cellular lysates were prepared in protein extraction buffer as discussed above. Total cellular protein concentrations were quantified using the Bio-Rad *DC* Protein Assay (Bio-Rad). The paired normal and tumor fibroblasts were cultured in DMEM supplemented with 10%FBS until 80-90% confluent. The media were replaced and the cells were treated with 20 nm rapamycin (EMD chemicals, Inc.) for 24 hr after which cell culture supernatants were analyzed for HGF and VEGF-C using ELISA.

## **RT PCR**

Human cells ( $3 \times 10^4$  cells/plate) were grown on 10-cm plates in 10% FBS/DMEM until 80% confluency. Supernatants were collected and total RNA was extracted using RNeasy mini kit (Qiagen) and reverse transcribed using random primers and Multiscribe reverse transcriptase from High capacity cDNA archive kit (Applied biosystems). VEGF-C, VEGF-D and 18s rRNA were measured by RT PCR using the TaqMan universal master mix and with the respective assay-on-demand primers ( Applied Biosystems) on a

7700 Sequence Detector System (Applied Biosystems). The values are expressed relative to levels in the same cells of 18S.

### **ShRNA lentiviral transduction**

To knockdown TSC2 expression in neonatal foreskin fibroblasts, we used commercially available lentiviral particles carrying the pGIPZ-lentiviral shRNA vector containing a hairpin sequence targeting TSC2 (Open Biosystems). The fibroblasts were transduced by the lentiviral particles followed by puromycin selection (2ug/ml) starting 48 hrs post transduction. Cells stably expressing shRNA were pooled and maintained in puromycin. A pGIPZ lentivirus containing a non-silencing shRNA control with no homology to known mammalian genes was used as the negative control for the knockdown experiments. The neonatal fibroblasts transduced with TSC2 shRNA and control shRNA were grown until 80-90% confluent in DMEM supplemented with 10% FBS. The media were changed and the cells were maintained in serum free DMEM for 24hrs. The supernatants were collected and the cells were lysed in the lysis buffer as described before.

### **Statistics**

Statistical analysis was performed using SPSS 16.0. Data are represented as mean  $\pm$  SD and were analyzed with a two-tailed unpaired Student's *t*-test. When more than two groups were compared, two-way ANOVA was applied followed by post hoc comparison of the means for the lymphatic studies and Tukey-Kramer multiple pairwise comparison for the angiogenesis section. Differences between samples were considered statistically significant when  $p < 0.05$ .

## **Chapter 3: Results**

### **TSC patients and samples**

Samples were obtained from twenty adults with TSC, ranging from 20-53 years of age including nineteen women and one man. The mature age range and predominance of women in this patient population resulted from recruitment of patients with LAM, a pulmonary manifestation of TSC that occurs almost exclusively in adult women. At enrollment, these patients were evaluated for the presence of major and minor diagnostic features (Table 1). TSC was confirmed based on the presence of either at least 2 major or 1 major and 2 minor diagnostic features. Most patients had multiple major features and all had at least one skin feature. The samples used for the studies include nineteen samples of angiofibromas or forehead plaques from the head region and 20 samples of normal-appearing skin, mostly from the postauricular region. Nine of ten periungual fibromas were from the toes (Table 2).

**Table 1: TSC Features at the Time of Enrollment for 20 Adult Women\***

<b>MAJOR FEATURES</b>	<b>Number of patients (%)</b>
Facial angiofibromas or forehead plaque	20 (100%)
Nontraumatic ungual or periungual fibroma	63 (80%)
Hypomelanotic macules (3 or more)	14 (70%)
Shagreen patch (connective tissue nevus)	14 (70%)
Multiple retinal nodular hamartomas	5/12 (25%) <sup>±</sup>
Cortical tuber	18 (90%)
Subependymal nodule	7 (35%)
Subependymal giant cell astrocytoma	0/20 (0%) <sup>±</sup>
Cardiac rhabdomyoma, single or multiple	0/14 (0%) <sup>±</sup>
Lymphangioleiomyomatosis	18 (90%)
Renal angiomyolipomas	19 (95%)
<b>MINOR FEATURES</b>	
Multiple randomly distributed pits in dental enamel	17 (85%)
Hamartomatous rectal polyps	0/11 (0%) <sup>±</sup>
Bone cysts	ND
Cerebral white matter migration lines	ND
Gingival fibromas	12(60%)
Non-renal hamartoma	ND
Retinal achromic patch	0/12 (0%) <sup>±</sup>
“Confetti” skin lesions	7 (35%)
Multiple renal cysts	4 (20%)

\* TSC was confirmed in patients with at least 2 major features or 1 major and 2 minor features. The presence of lymphangioleiomyomatosis and renal angiomyolipomas in the same patient was counted as one major feature for diagnosis, since they occur together in sporadic lymphangioleiomyomatosis.

± Data were unavailable for some patients (total number is the denominator)

ND- Not Done

**Table 2: Locations and number of skin samples obtained from patients with tuberous sclerosis complex.**

<b>Lesion</b>	<b>Location</b>	<b>Number</b>
Normal-appearing skin	Postauricular	14
	Arm	2
	Back	5
Angiofibroma / Forehead plaque	Nose	10
	Forehead	6
	Other – neck, scalp	3
Periungual fibroma	Toe	9
	Finger	1

### **Part 1: Angiogenesis in TSC skin tumors**

**TSC skin tumors are highly vascular with constitutive mTOR activation and are enriched with mononuclear phagocytes**

Compared to normal-appearing skin from the patients (Figure 1a), TSC skin tumors, including angiofibromas, periungual fibromas and forehead plaques, show an altered histology with large fibroblast-like cells in a fibrous stroma and numerous vessels (Figure 1b). Staining with the vessel marker CD31 showed that TSC skin tumors have greater number of CD31- positive endothelial cells than patient's normal appearing skin (Figure 1c, d). In patient normal skin, cells positive for phospho-S6, a marker of mTOR activation, were present mainly in the granular layer of the epidermis with almost none in the dermis (Figure 1e). TSC skin tumors showed strong staining for phospho-S6 in the

epidermis and also in the large fibroblast-like cells in the dermis (Figure 1f). Staining with the nuclear antigen Ki-67, a marker of cell proliferation, showed greater numbers of positive cells in the basal layer of the epidermis of TSC skin tumors than normal skin (Figure 1g, h). These tumors also have increased number of stellate cells staining positive for CD68, a marker for monocyte/macrophage/DC cell lineage, than did patient's normal-appearing skin (Figure 1i, j). Results published from the laboratory also showed more intense staining for smooth muscle actin in the perivascular cells of angiofibromas and periungual fibromas than in normal-appearing skin<sup>186</sup>. These results along with others studies demonstrate that TSC skin tumors are comprised of an abnormal arrangement and number of fibroblast-like cells, fibrous tissue and vessels<sup>85, 87</sup>. In addition, they showed that these tumors contain increased numbers of mononuclear phagocytes accompanied by increased keratinocyte proliferation and mTOR activation. As shown below, the neoplastic cells (2-hit cells) are fibroblast-like cells. There is no evidence for 2-hit cells in the epidermis, and the epidermal changes may be due to the influence of tumor cells in the dermis<sup>187</sup>.

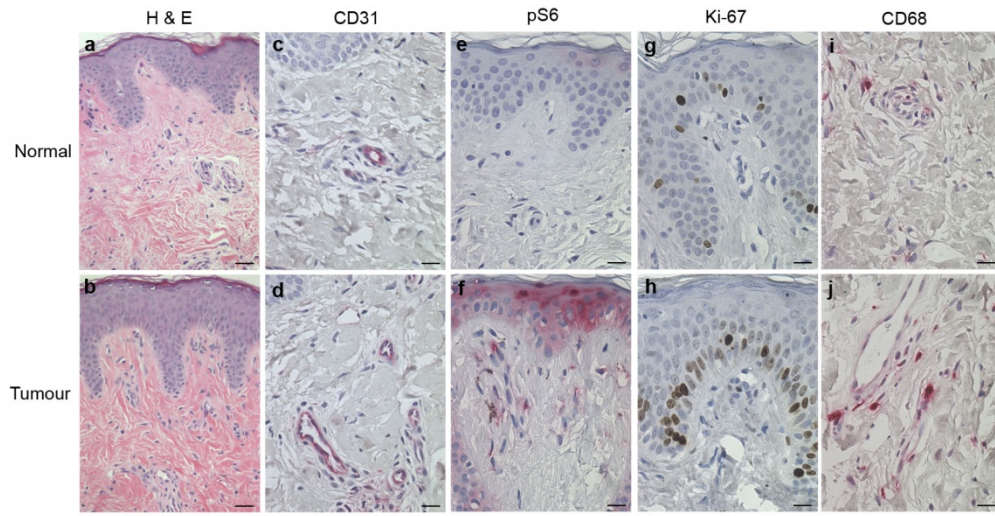


**Figure 1: Histological and immunohistological differences between TSC skin tumors and normal-appearing skin.** Reprinted from Li et al, *Nat Commun.* 2011; 2:235 with copyright permission from Nature Publishing Group.

a,b, H&E stained sections show increased vessels and fibrosis in fibrous plaques compared to normal skin from the same patient. c,d, A forehead plaque has more CD-31 positive vessels than normal-appearing skin. e,f, Greater immunoreactivity for pS6 in the epidermis and dermis of tumor than normal-appearing skin, indicating increased mTORC1 activity as expected due to loss of TSC1/TSC2 function in these TSC tumors. g,h, Ki-67 reactivity shows more positive cells in the epidermis of tumor than normal skin. i,j, Reactivity with anti-CD68 antibodies, a marker of mononuclear phagocytes, reveals a greater number of positive cells in the dermis of a forehead plaque than in normal-appearing skin. Scale bar, 35um. Similar results were obtained in 4 fibrous plaques, 3 angiofibromas, and 3 periungual fibromas from 7 patients. Staining performed by Ji-an Wang in our laboratory.



**Fibroblast-like cells from TSC skin tumors are null for TSC2 with constitutive mTOR activation.**

Fibroblast-like cells were cultured from both normal and tumor tissue explants (Figure 2). These cells express vimentin and HSP47, a collagen chaperone used as a marker for skin fibroblasts<sup>186</sup>. Fibroblast-like cells were screened for loss of TSC2 expression and increase in mTOR activation, as detected by hyperphosphorylation of ribosomal protein S6 using Western blot. Cells grown from TSC skin tumors showed undetectable or greatly decreased levels of TSC2. This was accompanied by greater phosphorylation of ribosomal protein S6 under serum starved conditions than in fibroblasts grown from the same patient's normal skin (Figure 3a-c). The *in vitro* studies performed in this thesis used fibroblast-like cells with undetectable or dramatically reduced expression of TSC2 and hyperphosphorylation of S6.

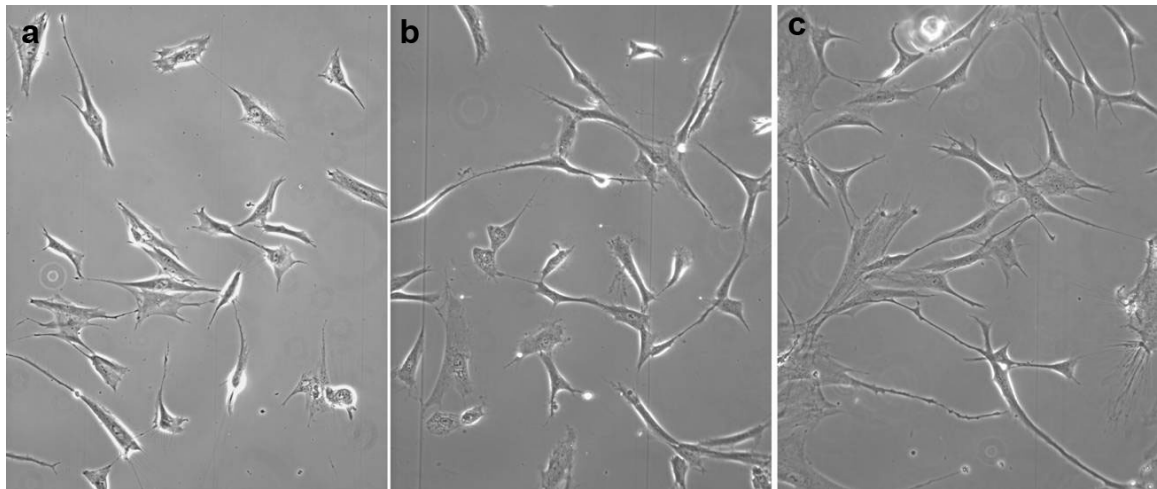


**Figure 2. Histological appearance of normal, TSC normal and TSC tumor cells.** Phase contrast microscopy shows that a) normal and b) TSC normal cells are spindle shaped while c) TSC tumor cells are spindle or polygonal in shape.

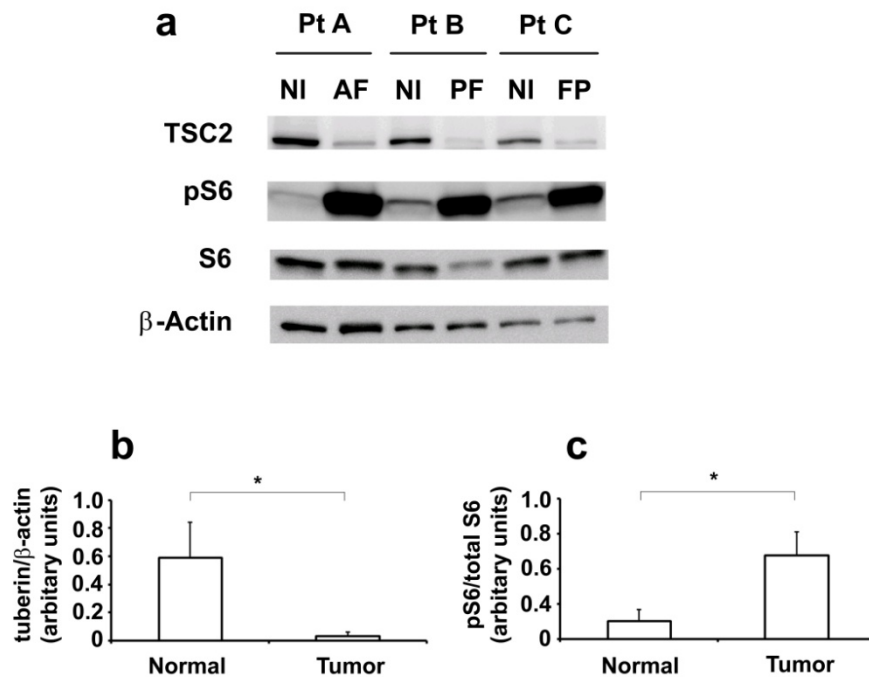


**Figure 3. Characterization of TSC skin tumor cells.** A) Western blots of TSC2, phosphorylated ribosomal protein S6 (pS6), total S6, and beta-actin in serum-starved angiofibroma (AF), periungual fibroma (PF), forehead plaque (FP), and TSC normal dermal fibroblasts (NI) from different patients (Pt A, Pt B, Pt C). Densitometric analysis of band intensities of B) tuberin relative to actin and C) pS6 relative to total S6 in Western blots of cells grown from 8 TSC tumors (2 AF, 3 PF, 3 FP) and TSC normal fibroblasts. \* $p < 0.0005$ .

### Fibroblast-like cells from TSC skin tumors are 2-hit cells

The genetic alterations in fibroblast-like cells were determined by sequence analysis, pursuing Knudson's two-hit hypothesis that both alleles are mutated in tumor cells.

Sequencing of the *TSC2* gene in a forehead plaque revealed a nonsense mutation in the *TSC2* gene, G1074A in exon 10, which converted UGG encoding tryptophan to UGA, a codon (Figure 4a). These cells also showed loss of heterozygosity (LOH) at three microsatellite markers flanking the *TSC2* gene (Figure 4b), rendering the cells homo- or hemizygous for the point mutation in exon 10. The mutation introduces a restriction

enzyme site for BsmA1 so that only the tumor DNA gets cleaved. The patient normal fibroblasts did not have the mutation and so are not cleaved with BsmA1. These results are consistent with mosaicism for the point mutation in this patient (Figure 4c). We used these TSC2-null cells for further *in vitro* studies and also to develop the xenograft mouse model.

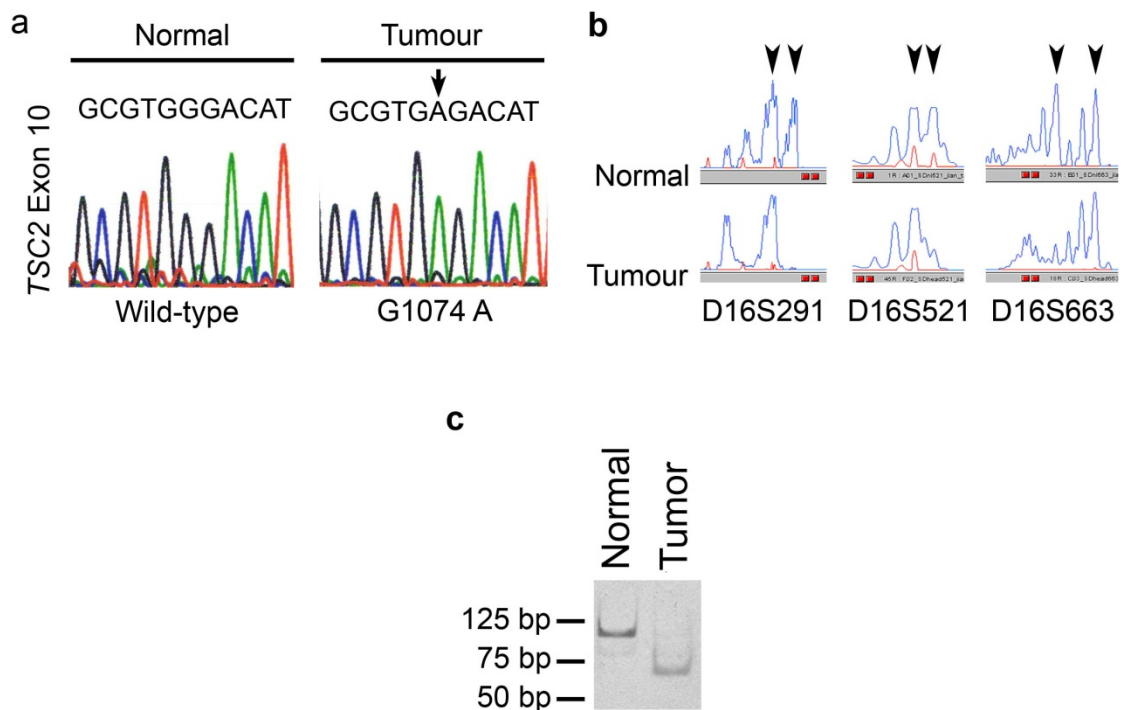


**Figure 4. Genetic analysis of TSC2-null fibroblast-like cells.** Reprinted from Li et al, *Nat Commun.* 2011;2:235 with copyright permission from Nature Publishing Group. a) Sequencing of DNA from TSC2-null cells from a forehead plaque revealed a single-base substitution (G1074A) in exon 10 of the *TSC2* gene. b) Analysis of microsatellite nucleotide-repeat polymorphisms flanking *TSC2* at 16p13.3. Alleles are marked with arrowheads for the patient's normal fibroblasts and TSC2-null cells. c) Restriction enzyme analysis of a part of exon 10 of *TSC2*, using PCR-amplified DNA from TSC normal fibroblasts (normal) and TSC2-null fibroblasts from a forehead plaque (tumor). The mutation introduces a restriction site for BsmA1, so that the tumor DNA, but not the normal DNA, is cleaved. Sequencing performed by Dr.Thangapazham, PCR and restriction digestion by Ji-an Wang.

### **Skin equivalents grafted onto nude mice to develop a xenograft mouse model of TSC skin tumors**

To test our hypothesis that TSC2-null cells are responsible for inducing various morphological changes observed in these skin tumors, we developed a xenograft mouse model. The model was developed by Dr. Shaowei Li in the laboratory and I assisted him and other members during grafting, treatment and graft harvest. For grafting, we used an extensively used system of *in vitro* constructed dermal-epidermal composites, which form stratified epithelia<sup>67</sup>. Fibroblast-like cells from the forehead plaque that are TSC2-null and TSC normal fibroblasts from the same patient were used to construct *in vitro* skin equivalents. Briefly, human neonatal foreskin keratinocytes with accompanying melanocytes were overlaid on a collagen matrix embedded with TSC2-null fibroblasts or TSC normal fibroblasts from the same patient to form the dermal-epidermal composites, which were grafted onto nude mice. After 17 weeks, the mice were sacrificed and the grafts were used for immunohistochemical analysis by paraffin embedding and frozen sections (Figure 5). There was no gross difference in size or appearance between the normal and tumor grafts. However, there were dramatic histological differences between normal and tumor grafts, as described below. An unexpected finding was that some grafts containing TSC2-null cells formed hair follicles<sup>67</sup>. The induction of *de novo* hair follicle neogenesis by TSC2-null cells has significant implications for TSC tumor formation, but it is outside the scope of this thesis and is covered only briefly.

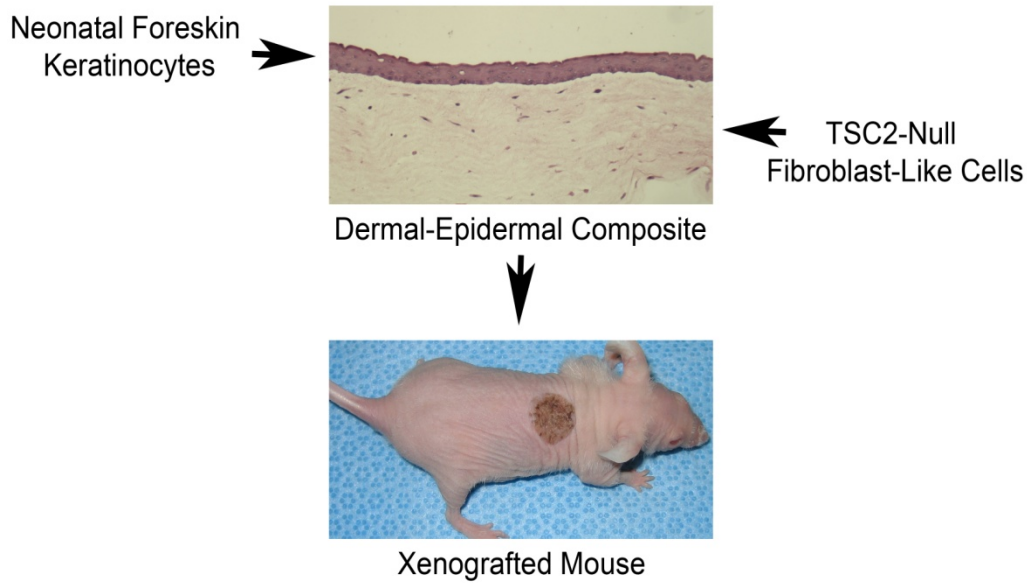


**Figure 5. Xenograft model of TSC skin hamartomas.** *Reprinted from Li et al, Nat Commun. 2011;2:235 with copyright permission from Nature Publishing Group.*

Fibroblast-like cells from skin hamartomas are overlaid with neonatal foreskin keratinocytes to form dermal-epidermal composites, that are grafted onto the backs of nude mice.

#### **Delineation of human and mouse cells in the xenografts**

To confirm the presence of human cells in the grafts, we immunostained the grafts with pan-human HLA class I monoclonal antibody. Immunoreactivity was observed in the follicles, epithelium and dermis, confirming the presence of human cells (Figure 6a). To distinguish between human foreskin keratinocytes and TSC2-null cells from female patients, we performed *in situ* hybridization using a probe for the human Y-chromosome. The probe hybridized to nuclei in the epidermis and the follicular epithelium but not to the nuclei of dermal cells (Figure 6b).

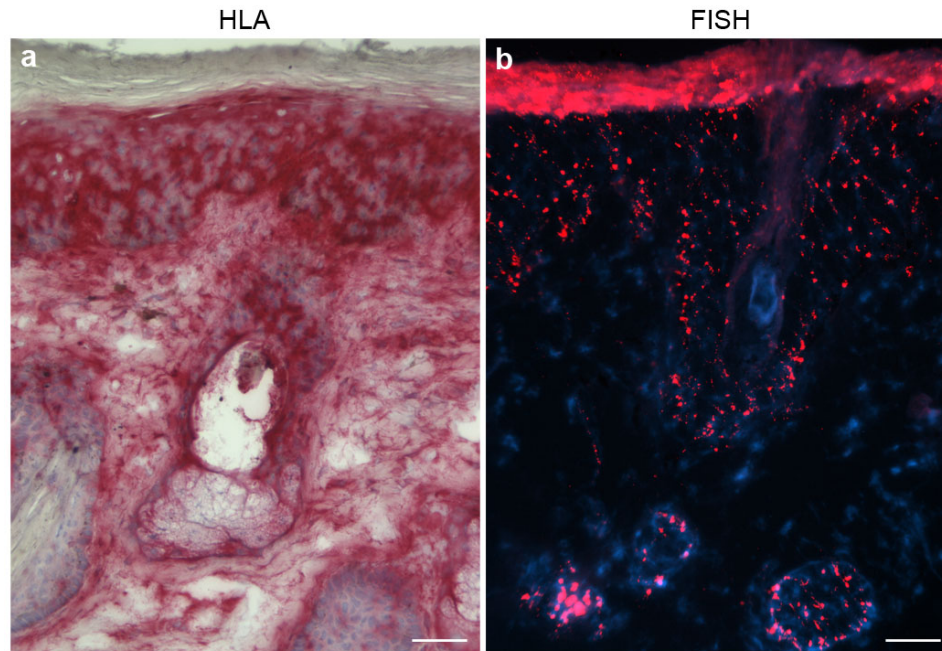


**Figure 6. TSC angiofibroma (AF) cells induce human hair follicle formation in xenografts.** Reprinted from Li et al, *Nat Commun.* 2011;2:235 with copyright permission from Nature Publishing Group.

a) TSC2-null fibroblast-like cells from an AF and neonatal foreskin keratinocytes were incorporated into dermal-epidermal composites and grafted onto mice. Reactivity with HLA antibody demonstrated the presence of human cells in the dermis, epidermis and hair follicles. b) Frozen sections of grafts were hybridized with a fluorescent probe of human Y chromosome. Red signals in the nuclei of epidermal and follicular epithelial cells demonstrate derivation from neonatal foreskin, but no signals are observed in dermal fibroblast-like cells from a female patient. Scale bar, 65µm. Staining performed by Ji-an Wang.

To further distinguish human and mouse cells in grafts, we performed fluorescence *in situ* hybridization using a Cy3 pan centromeric probe for human cells and a FITC pan centromeric probe to detect mouse cells. At the graft margin, there was a sharp demarcation in the epidermis between nuclei marked with the human probe (red) and mouse probe (green) (Figure 7a). In the dermis, the human probe hybridized to the nuclei of interstitial cells. The mouse probe marked sparse interstitial cells and cells lining vascular lumens (Figure 7a). Nuclei showed either red or green signals. In tumor grafts



with hair follicles, the human probe (red) hybridized to nuclei of cells comprising the hair follicle epithelium and perifollicular mesenchyme (Figure 7a). The mouse probe (green) hybridized to nuclei of endothelial cells lining vessels (Figure 7a-c), with some cells in a perivascular location showing red signals (Figure 7c). These results indicate that TSC2-null cells induce the formation of hair follicles that originate from human epidermal cells and induce vessel formation with vascular endothelial cells originating from the mouse.

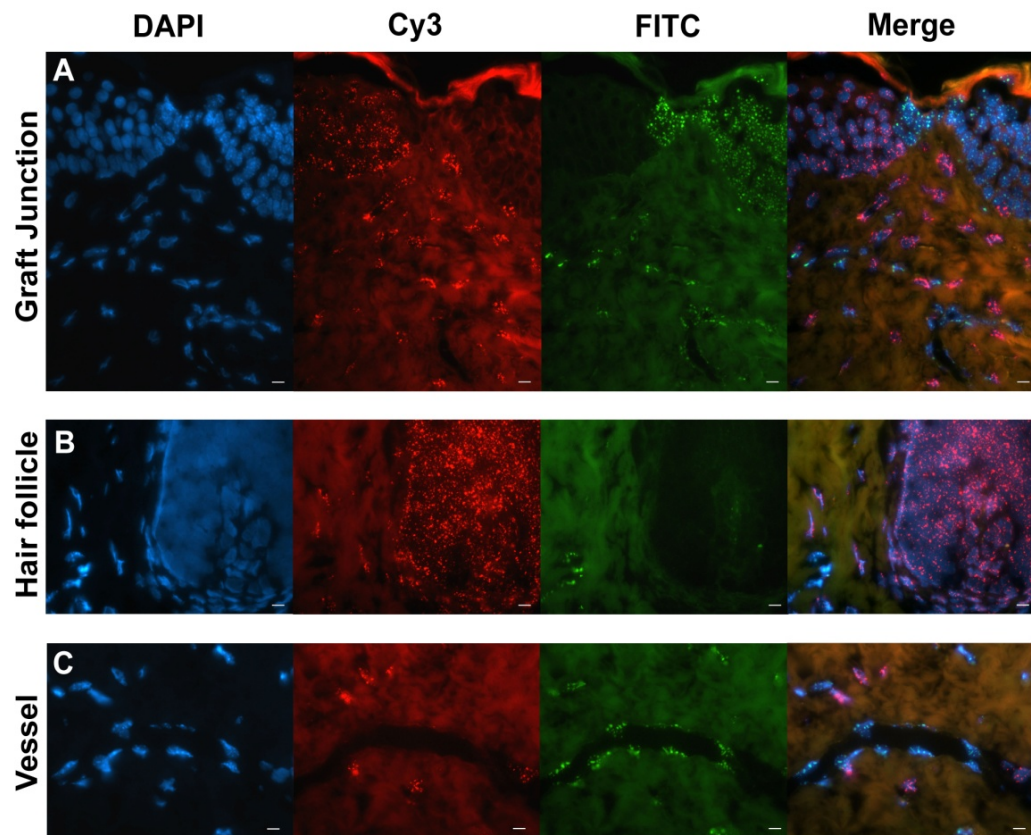


**Figure 7. Double FISH analysis on xenograft samples.** Double FISH analysis using human and mouse pan-centromeric probes on a tumor graft show A) human (red) and mouse (green) cells at the graft junction with the nuclei staining blue with DAPI, B) human cells (red) in the hair follicle suggesting a human origin, with the mouse cells lining the adjacent vessel (green), and C) The endothelial lining of the vessels react with mouse probe (green) but not with human probe (red), indicating that the vessels are derived from the mouse. *FISH performed by Jian-Wang and imaging by Sangeetha Rajesh.*

**Tumor grafts recapitulate hamartoma features of human tumors including hyperphosphorylation of S6, increased proliferation of epidermis, recruitment of mononuclear phagocytes and increased angiogenesis**

To determine the extent to which our xenograft model reproduces features of TSC skin tumors, we characterized the histological and immunohistochemical changes in fibrous plaques as a baseline for comparison. Presence of human cells was confirmed with an antibody to COX IV that is reactive with human but not mouse. COX-IV positive cells were present in the epithelium and dermis in both normal and tumor grafts (Figure 8a), as observed with pan-human HLA.

Staining the grafts for blood vessels showed that the tumor grafts possessed more CD31- positive blood vessels than normal grafts (Figure 8a). Quantitative analysis showed increased vessel area, higher vessel density and larger vessels in the tumor grafts than the normal grafts (Figure 8c-e).

Grafts containing TSC2-null fibroblasts revealed greater numbers of pS6-positive cells in the dermis than grafts with TSC normal fibroblasts. This is consistent with high mTORC1 activation observed in TSC skin tumors. The epidermis of tumor grafts also showed greater immunoreactivity for pS6 as well as greater proliferation as identified by greater number of Ki-67-positive cells than the normal grafts (Figure 8a). These epidermal changes are consistent with human tumors. A significant difference between the normal and tumor grafts with respect to pS6 and Ki-67 is represented graphically (Figure 8f-h). These findings indicate that TSC2-null fibroblasts stimulated proliferation and mTORC1 activation of the overlying epidermis as both tumor and normal grafts were generated with the same neonatal foreskin keratinocytes.



The increase in blood vasculature observed in tumor grafts was accompanied by increased numbers of F4/80-positive mononuclear phagocytes (Figure 8a, i). TSC2-null cells in the tumor grafts may directly induce angiogenesis by secreting paracrine factors or indirectly by recruiting pro-angiogenic mononuclear phagocytes.

Qualitatively similar changes were observed comparing TSC2-null cells from other patient fibrous plaques, angiofibromas and periungual fibroma with control grafts constructed from TSC normal fibroblasts. These results show that TSC2-null cells are sufficient to induce the hamartomatous features of TSC skin tumors. These observed features were consistent with human tumors further strengthening the validity of our xenograft model to study TSC skin tumors. This is the first novel model developed to study TSC skin tumors.

#### **Rapamycin reverses hamartoma features induced by TSC2-null cells.**

Our *in vitro* studies showed that rapamycin blocked mTORC1 activation in TSC2-null cells and decreased *in vitro* viability of TSC2-null cells to a greater extent than of TSC normal fibroblasts<sup>67</sup>. To study the effects of rapamycin *in vivo*, we administered rapamycin (2 mg/kg), or an equal volume of vehicle, by intraperitoneal injection on alternate days for 12 weeks, beginning 5 weeks after grafting, to nude mice grafted with composites containing either TSC2-null cells from a fibrous plaque or TSC normal fibroblasts. Mice were killed 24 h after the last injection for analysis of grafts by immunohistochemistry. There were no gross differences in size or appearance between tumor and normal grafts in mice with or without rapamycin treatment. Rapamycin decreased human dermal cell number in tumor xenografts as seen with the COX IV staining but had no significant effects on COX IV-positive human cells in normal

xenografts (Figure 8b). A similar pattern was observed by staining with the pan-human HLA class I monoclonal antibody<sup>67</sup> with a significant decrease in human cells with rapamycin only in the tumor grafts. The anti-angiogenic effect of rapamycin was observed by the dramatic decrease in vessel density, size and total area in the tumor grafts (Figure 8 c-e). *In vivo* penetration of rapamycin was further confirmed by a significant reduction in pS6 immunoreactivity in the dermal and epidermal cells in both normal and tumor grafts (Figure 8 f, g). Rapamycin also decreased the number of Ki-67-positive epidermal cells, and mononuclear phagocytes in the tumor grafts (Figure 8 h, i). These results suggest a cytostatic effect of rapamycin on TSC2-null cells and its anti-angiogenic effect in the xenografted TSC skin.

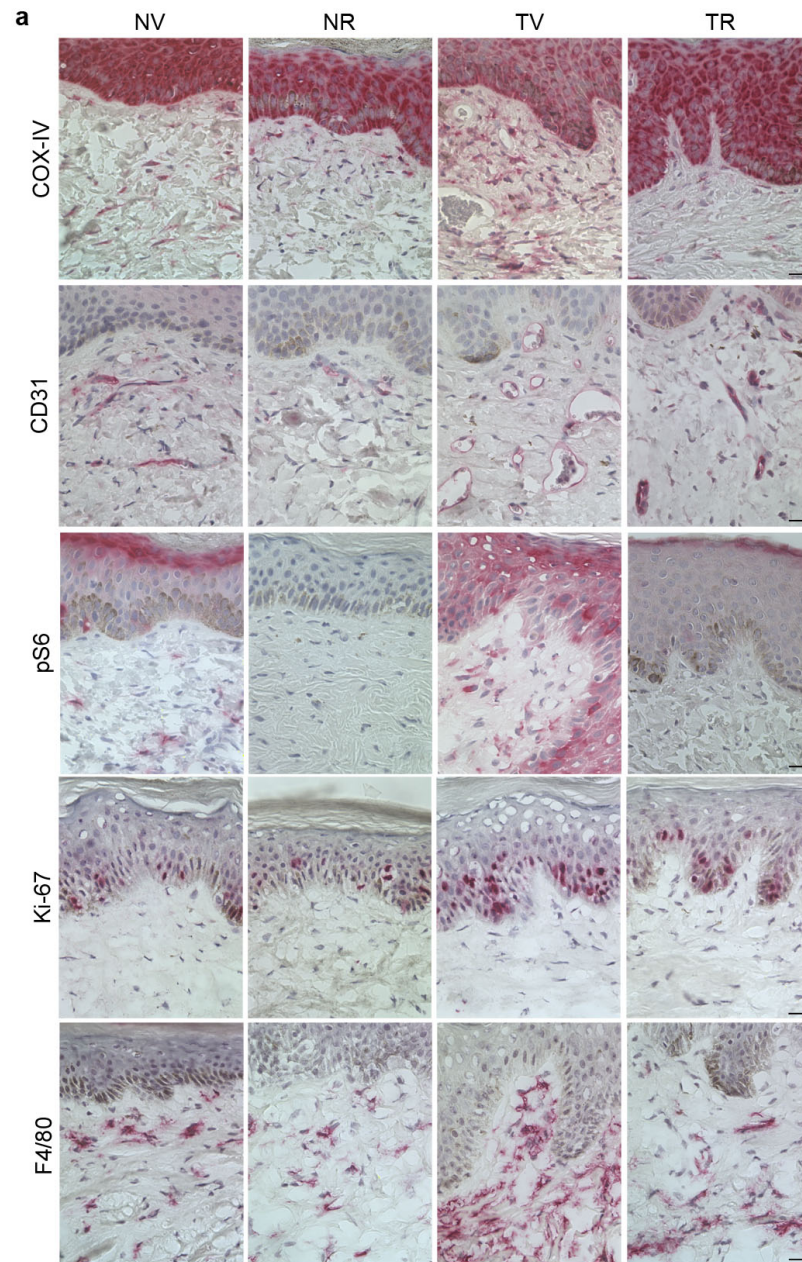


**Figure 8a. Tumor grafts replicate features of TSC skin tumors.** Reprinted from Li et al, *Nat Commun.* 2011;2:235 with copyright permission from Nature Publishing Group.. a) Immunohistochemistry for human COX-IV, pS6, Ki-67 (proliferation), F4/80 (phagocytes) and CD31 (vessels) in four experimental groups: NV, TSC normal fibroblasts with vehicle treatment; NR, TSC normal fibroblasts with rapamycin treatment; TV, TSC2-null cells with vehicle treatment; TR, TSC2-null cells with rapamycin treatment. Scale bar: 35  $\mu$ m.

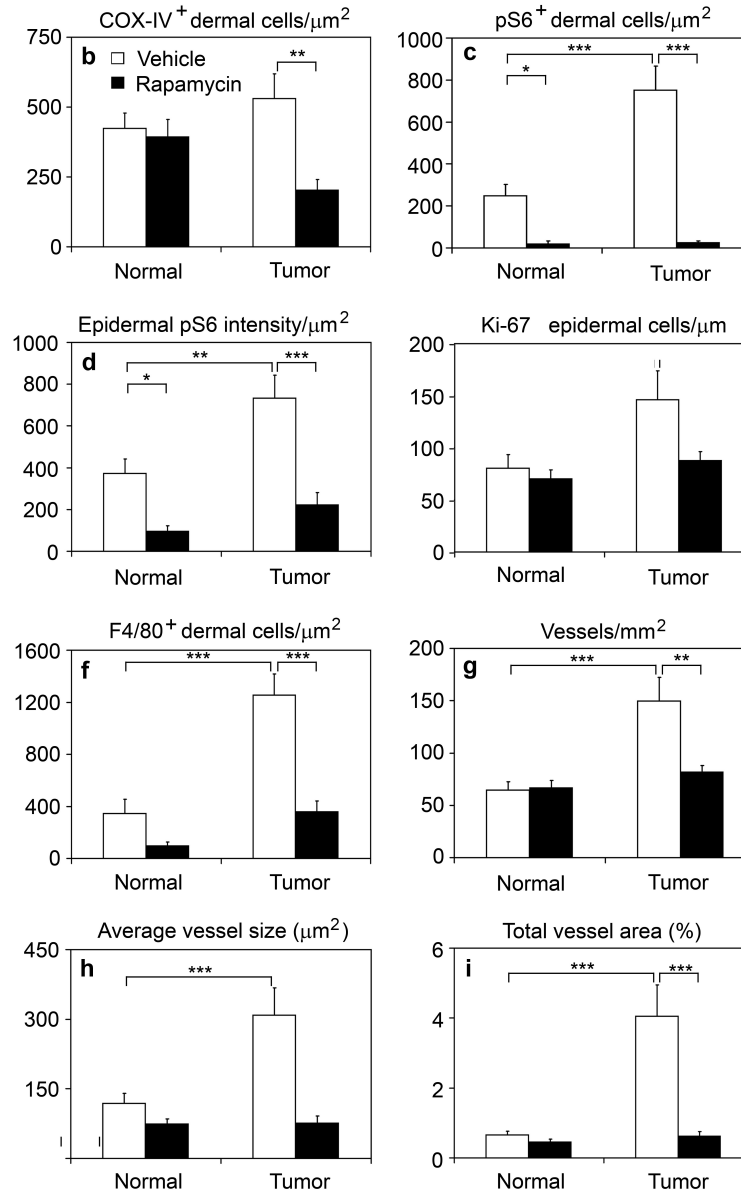


**Figure 8b. Effects of rapamycin on tumor and normal xenografts** Reprinted from Li et al, Nat Commun. 2011;2:235 with copyright permission from Nature Publishing Group

b) Staining was quantified as shown in b-i. White and black bars indicate means  $\pm$  s.e. for vehicle- and rapamycin-treated animals, respectively. (b) Density of dermal cells reactive with human-specific COX-IV. (c) Density of dermal cells reactive with pS6. (d) Intensity of staining for pS6 in the epidermis. (e) Numbers of non-follicular epidermal cells reactive with Ki-67 relative to epidermal length. (f) Density of dermal cells reactive with F4/80. (g) Density of CD-31 positive vessels. (h) Average cross-sectional area of CD-31 positive vessels. (i) The ratio of vessel area to dermal area within grafts. Numbers of mice were 13 for NV, 14 for NR, 12 for TV and 15 for TR. \* $P < 0.05$ ; \*\* $P < 0.01$ ; \*\*\* $P < 0.001$ .

Experiments performed by Dr.Li, Dr.Thangapazham, Ji-an Wang and Sangeetha Rajesh.

### **TSC2-null cells show greater basal and hypoxia-stimulated levels of HIF-1 $\alpha$ than TSC normal fibroblasts**

The increased vascularity observed in TSC skin tumors prompted us to determine the mechanisms involved in upregulating angiogenesis. The process of angiogenesis is regulated by paracrine factors acting on the endothelial cells. One of the main angiogenic factors is VEGFA which is transcriptionally regulated by HIF-1 $\alpha$ . We hypothesized that increased angiogenesis observed in TSC tumors may be due to increased expression of HIF-1  $\alpha$ . We cultured TSC2-null cells, TSC normal fibroblasts or normal human dermal fibroblasts under normoxic or hypoxic (1% oxygen) conditions. Under normoxic conditions, HIF-1 $\alpha$  levels were greater in TSC2-null cells than TSC normal fibroblasts or normal human dermal fibroblasts (Figure 9). This is consistent with the expected effect of mTORC1 activation on HIF-1 $\alpha$  levels in cells with loss of TSC2. HIF-1 $\alpha$  levels increased in all cells after 4 hr hypoxia. After 24 hr hypoxia, HIF-1 $\alpha$  levels had decreased in normal fibroblasts, while levels remained elevated in TSC normal fibroblasts and TSC2-null cells possibly indicating an effect due to haploinsufficiency of TSC2. Levels of phospho-S6 in the presence of 10% FBS were decreased by hypoxia in normal and TSC fibroblasts, but S6 continued to be phosphorylated in TSC2-null cells, indicating persistent mTORC1 activation (Figure 9). These results indicate that TSC2-null cells show increased baseline HIF-1 $\alpha$  levels, and prolonged elevation of HIF-1 $\alpha$  in response to hypoxia.

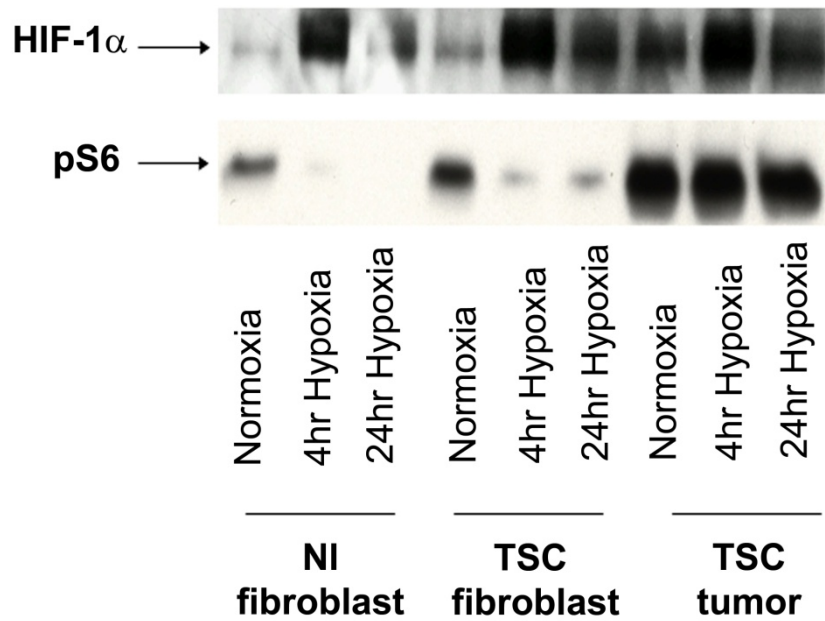


**Figure 9. HIF-1 $\alpha$  expression in normal fibroblasts, TSC fibroblasts and TSC2-null tumor fibroblasts.** Cells were grown to 80-90% confluence, fresh DMEM + 10% FBS was added, and the cells incubated under normoxic conditions for 24 hr or hypoxic conditions (1% O<sub>2</sub>) for 4 or 24 hr. HIF-1 $\alpha$  levels were measured in nuclear extracts and phospho-S6 was measured in cytoplasmic extracts using western blot. The same relative changes were observed using samples from three different patients.

## Summary 1

- Hamartomatous features of TSC skin tumors include increased vasculature, increased epidermal proliferation, hyperactivation of mTORC1 and increased numbers of mononuclear phagocytes.
- The neoplastic (2-hit) cells are fibroblast-like cells in the dermis that are null for *TSC2* with hyperphosphorylation of ribosomal protein S6.
- TSC2-null fibroblasts along with foreskin keratinocytes are used to form skin equivalents that are grafted onto nude mice to develop a TSC xenograft skin model.
- The xenograft model replicates hamartomatous features of TSC skin tumors, with increased angiogenesis, epidermal proliferation, activation of mTORC1 and infiltration of mononuclear phagocytes.
- Rapamycin treatment exerts anti-angiogenic effects in tumor grafts and decreases tumor cell number.
- One of the major pathways of angiogenesis activated in these tumors is HIF-1 $\alpha$ . TSC2 –null fibroblasts have high basal levels of HIF-1 $\alpha$  with persistent increase in HIF-1 $\alpha$  levels with hypoxia.

## **Part 2: Lymphangiogenesis in TSC skin tumors**

### **TSC skin tumors show greater lymphangiogenesis than normal skin**

To assess lymphatic involvement in TSC skin tumors, we performed immunohistochemical analysis using D2-40, a commercially available monoclonal antibody specific for lymphatic endothelial cells, on paraffin sections of TSC skin tumors and normal-appearing skin. Immunohistochemical analysis was performed on fifteen angiofibromas/fibrous plaques, six periungual fibromas and fifteen samples of normal-appearing skin (Figure 10a). Normal-appearing skin had few vessels with narrow lumens (Figure 10a, left panel) while the tumors had numerous and larger vessels (Figure 10a, middle and right panels). Interspersed with the D2-40 stained vessels were unstained vessels, consistent with the specificity of the marker for lymphatic but not blood vessels. We grouped forehead plaque and angiofibroma data for morphometric analysis as forehead plaques are histologically similar to angiofibromas and are grouped together for the purpose of clinical analysis<sup>13</sup>. Morphometric analysis for the three lymphatic parameters namely vessel area, vessel density and vessel size was done using Openlab software. Quantitation showed a significant increase in the dermal area covered by lymphatic vessels in the angiofibromas/forehead plaques compared to normal-appearing skin (Figure 10b). Fibrous plaques and periungual fibromas also showed greater vessel density (Figure 10c) and average vessel size (Figure 10d) than normal-appearing skin. Qualitatively similar results were obtained when sections of angiofibromas (n=3), periungual fibromas (n=3), and patient normal skin (n=3) from 3 TSC patients were stained using lymphatic markers LYVE-1 or VEGFR3.



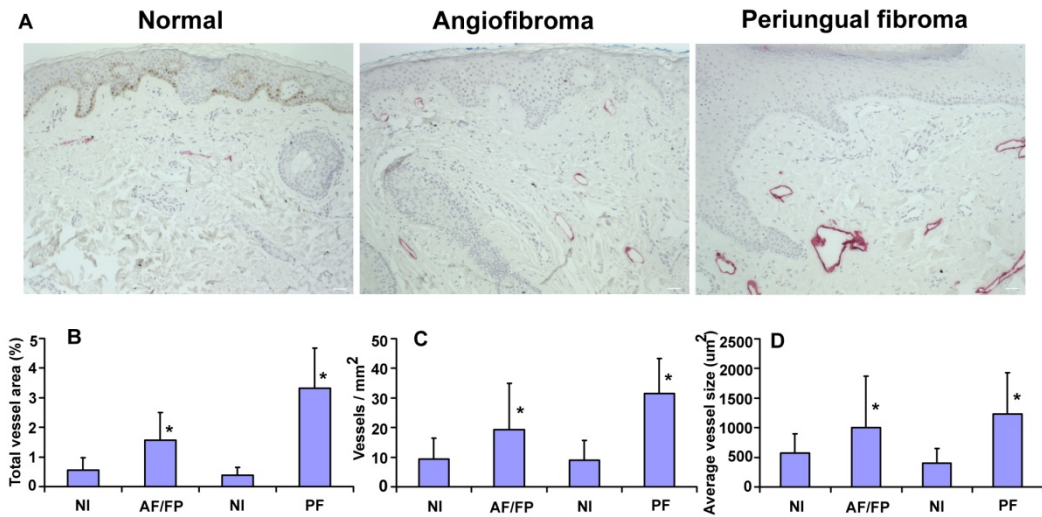


**Figure 10. D2-40 positive vessels in TSC skin tumors and patient normal-appearing skin.** A) Immunohistochemistry on paired paraffin sections of patient normal skin and TSC skin tumors was performed using D2-40 antibody and Vectastain ABC-AP using Vector Red substrate. Scale bar, 35 µm. Lymphatic endothelial cells of TSC skin tumors (staining red) were denser and larger than in patient normal skin. (B) Total lymphatic vessel area, (C) lymphatic vessel density and (D) average lymphatic vessel size in samples obtained from fifteen TSC patients including fifteen facial angiofibromas or fibrous plaques (AF/FP), six periungual fibromas (PF) and fifteen samples of patient normal skin (NI). Total vessel area (%) denotes total area of the vessels/dermal area. Data are expressed as mean ± SD. (\*,  $p < 0.05$ ).

### Periungual fibromas from patients on rapamycin treatment trend towards decreased lymphatic vessels

Rapamycin, a specific inhibitor of mTOR is shown to possess anti-lymphangiogenic properties in addition to its anti-angiogenic effects<sup>188</sup>. Our next step was to determine the extent of lymphatic involvement in patients taking rapamycin. We performed immunohistochemical analysis using D2-40 on the paraffin sections of periungual fibromas from two patients on rapamycin treatment. We found modest decrease in area,

lymphatic vessel density and size in both patients compared to untreated periungual fibromas (n=6) from six TSC patients (Figure 11a-c).

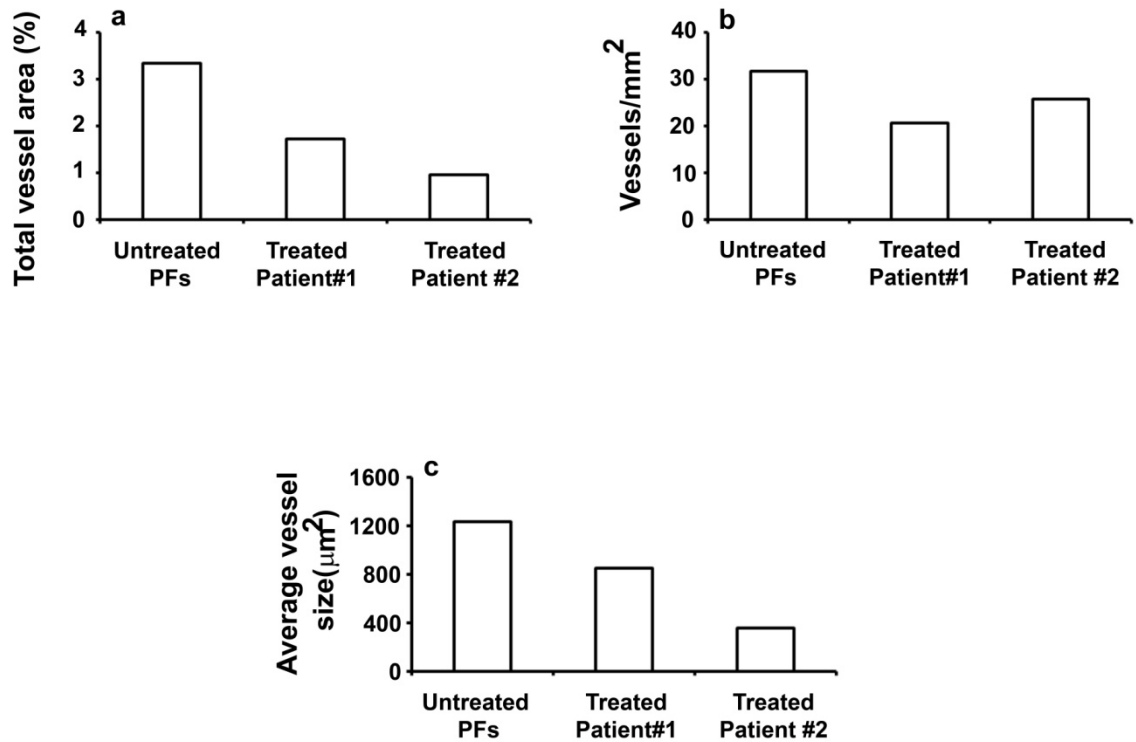


**Figure 11. Effect of rapamycin on lymphangiogenesis in TSC skin tumors:**

Immunohistochemistry was performed using D2-40 antibody and Vectastain ABC-AP using Vector Red substrate on paraffin sections of six periungual fibromas from 6 TSC patients and 2 periungual fibromas from two patients on rapamycin treatment. Scale bar, 35 µm. Quantitation of the lymphatic parameters, a) Total lymphatic vessel area, b) lymphatic vessel density and c) average lymphatic vessel. Total vessel area (%) denotes total area of the vessels/dermal area. Data are expressed as mean ± SD. (\*,  $p < 0.05$ ).

### **Lymphatics invade grafts containing human cells**

We used the xenograft model to study lymphangiogenesis. The junction between human and mouse epidermis was apparent at the margins of the grafts in H&E stained sections. Hair follicles were present in tumor but not normal grafts (Figure 12a, d). Staining with an anti-human COX IV antibody confirmed the presence of human cells in the graft epidermis and dermis, with a clear demarcation between human and mouse cells at the peripheral and deep margins of the grafts (Figure 12b, e). Lymphatic endothelial cell marker D2-40 stained endothelial cells forming lumens within the graft as well as numerous cells just outside the graft margin (Figure 12c, f).

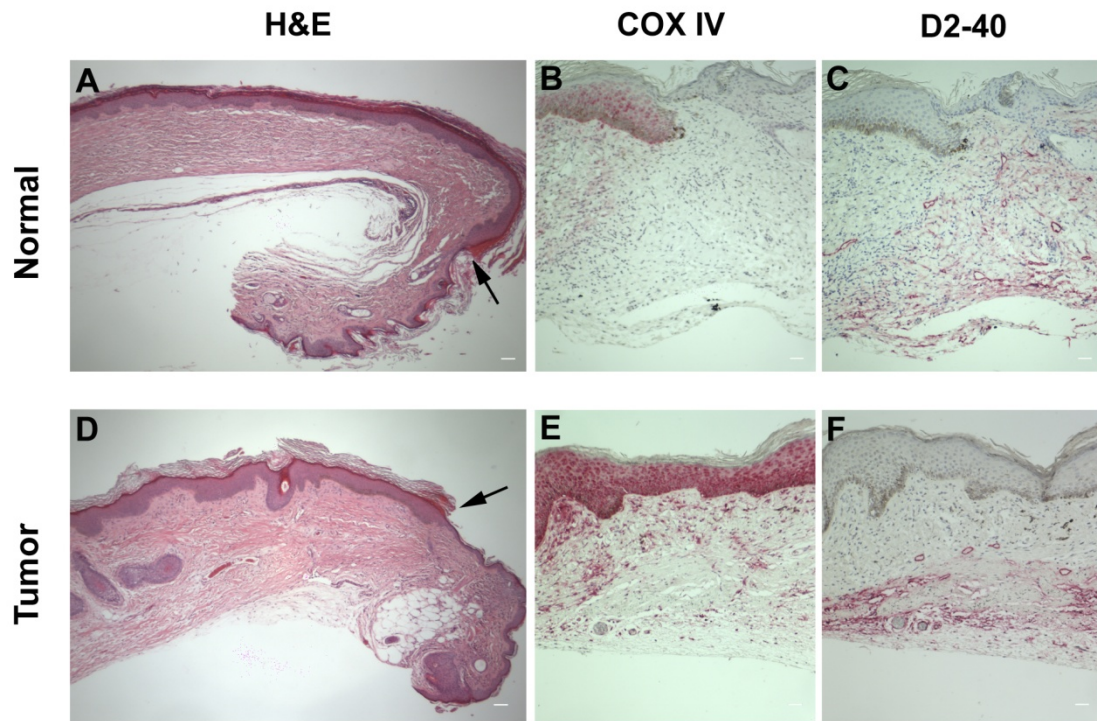


**Figure 12. Pathological analysis of the grafted tissue.** A) H&E staining of a graft composed of TSC normal fibroblast and human neonatal keratinocytes showing the human mouse junction (arrow). B, E) Epithelial cells in the epidermis and the fibroblasts in the upper dermis are immunoreactive to human-specific anti-COX IV antibody (red). The flanking mouse epidermal cells and mouse fibroblasts in the lower dermis are not reactive. D) H&E staining of a graft composed of TSC tumor fibroblasts and human neonatal keratinocytes showing the human mouse junction (arrow). C, F) Some vessels in the graft dermis are immunoreactive to D2-40.

### **Rapamycin dramatically decreases lymphangiogenesis in the normal and tumor grafts**

To determine the effects of rapamycin on lymphangiogenesis in the xenograft model, grafted mice were treated with rapamycin for 12 weeks, beginning 5 weeks after grafting. Rapamycin treatment dramatically decreased vessel density, size and area in both normal and tumor grafts (Figure 13a-d). As mentioned before, rapamycin decreased human dermal cells only in tumor xenografts, suggesting that the anti-lymphangiogenic effects of rapamycin in normal grafts are caused by direct effects on the lymphatic endothelium.

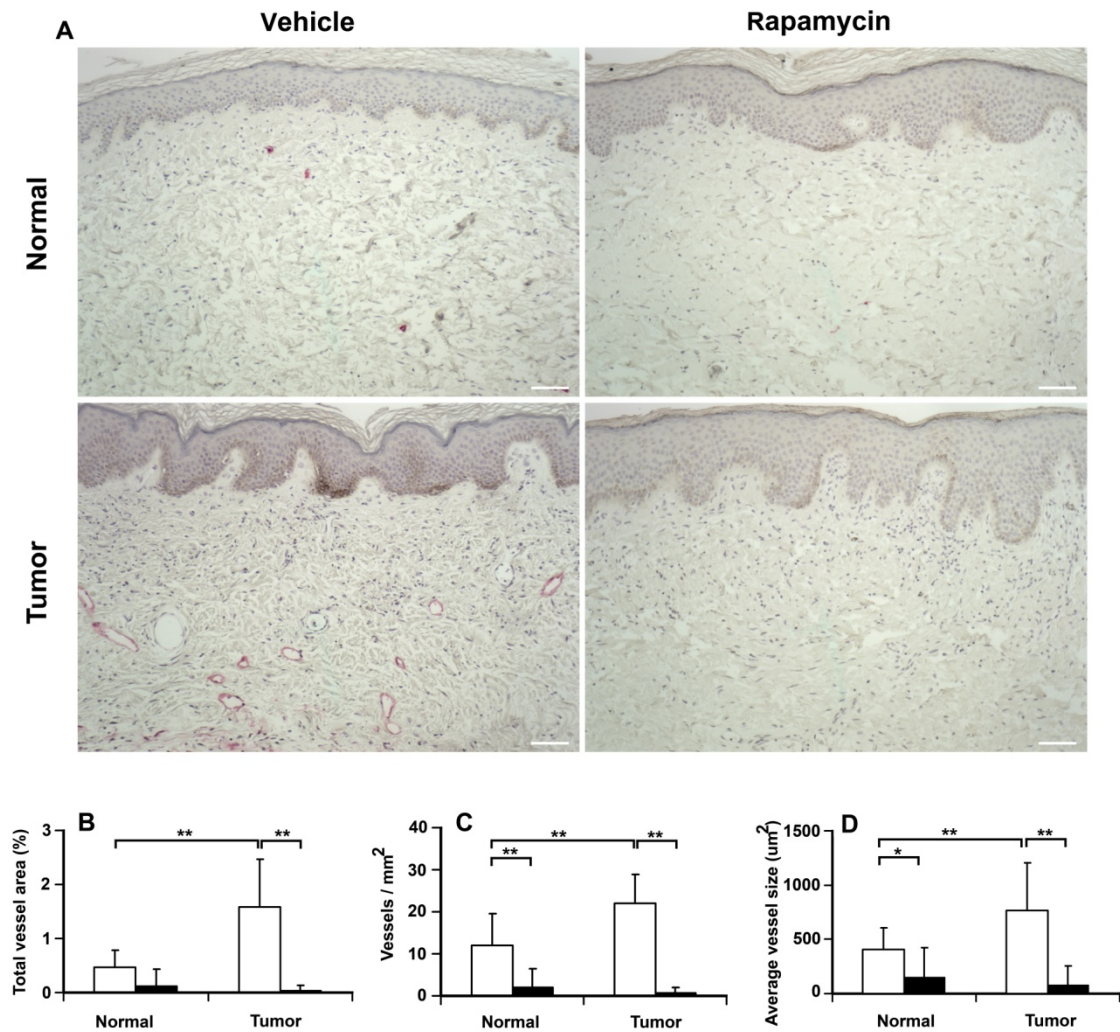


**Figure 13. Lymphatic vessels in xenografted mice treated with or without rapamycin.** Pictures show representative immunohistochemical D2-40 staining of A) normal and tumor grafts obtained from rapamycin-treated and untreated mice. Scale bar, 35  $\mu$ m. Tumor xenografts had numerous and larger vessels than normal grafts, and rapamycin almost completely abrogated lymphatic vessel formation. B) total lymphatic vessel area, (C) lymphatic vessel density and (D) average lymphatic vessel size. Numbers of mice studied were: 13 TSC normal fibroblasts with vehicle treatment; 14 TSC normal fibroblasts with rapamycin treatment; 10 TSC2- null fibroblasts with vehicle treatment; and 14 TSC2-null fibroblasts with rapamycin treatment. Data are expressed as mean  $\pm$  SD. (\*,  $p < 0.05$  and \*\*,  $p < 0.0001$ ).

## **Summary 2**

- TSC skin tumors showed greater lymphangiogenesis than normal skin.
- Rapamycin treatment in patients tends to decrease lymphangiogenesis.
- The TSC xenograft model recapitulates the human tumors with increased lymphangiogenesis in the tumor grafts. It clearly demonstrates that the TSC2 null cells are the inciting cells that induce lymphangiogenesis in these tumor grafts.
- Rapamycin treatment dramatically decreased lymphangiogenesis in both normal and tumor grafts in the xenograft model.

### **Part 3: a) Angiogenic and lymphangiogenic factors in TSC skin tumors**

#### **TSC skin tumor cells secrete increased amounts of HGF and VEGF-C**

With this exciting data about lymphangiogenesis in TSC skin tumors, our next step was to identify the factors secreted by these tumor cells that are responsible for inducing lymphangiogenesis. The expression of lymphangiogenic factors including VEGF-C, VEGF-D, VEGF-A, angiopoietin-2, FGF, and PDGFbb, was measured in culture supernatants using a multiplex chemiluminescent protein array. Tumor fibroblasts released at least 1.5-fold more VEGF-C than normal fibroblasts in 2/3 tumors, and at least 1.5-fold more VEGF-A than normal fibroblasts in 1/3 tumors. Levels of VEGF-D and angiopoietin-2 were below the limit of detection, and levels of the other factors were similar in supernatants of tumor and normal cells. Microarray analysis using total RNA from periungual fibroma showed about 4.27-fold increase in HGF and 5.7-fold increase in VEGF-C levels in TSC tumors compared to normal fibroblasts. To determine if TSC skin tumors overexpress HGF and VEGF-C, paired samples of TSC normal (n=8) and tumor fibroblasts (2 angiofibromas, 3 periungual fibromas, 3 forehead plaques) were

cultured in DMEM with 10% FBS for 24hr. HGF and VEGF-C protein levels were then measured in culture supernatants using ELISA and the results were normalized to the total cellular protein levels. TSC tumor fibroblasts released significantly higher levels of HGF ( $p=0.028$ ) into the medium compared to TSC normal fibroblasts (Figures 14a). RT-PCR for HGF in these paired normal and tumor fibroblasts did not show an induction of *HGF* mRNA (Figure 14b). The secretion of VEGF-C was also upregulated in the tumor fibroblasts than TSC normal fibroblasts ( $5800\pm3200$  and  $4400\pm2000$  pg VEGF-C/mg total cellular protein, respectively) (Figure 15a). We also measured *VEGF-C* mRNA by RT-PCR in these paired normal and tumor fibroblasts (464 and 530 VEGF-C (pg)/18S rRNA (ng), respectively) and did not see an induction of *VEGF-C* content (Figure 15b). These results further confirm our preliminary studies that TSC2-null fibroblast-like cells secrete relatively higher levels of the lymphatic factors HGF and VEGF-C than TSC normal fibroblasts.

### **VEGF-A in TSC skin tumors**

Studies have linked the loss of TSC1/TSC2 gene expression to secretion of the angiogenic factor vascular endothelial growth factor, VEGF-A<sup>189</sup>. We investigated the possibility of a direct correlation between HIF-1 $\alpha$  and VEGF-A levels in these tumors as increased expression of HIF-1 $\alpha$  leads to activation of its target genes. We measured *VEGF-A* RNA levels in the fibroblast-like tumor cells grown from four AFs, three PFs, and normal fibroblasts from four patients using Affymetrix arrays. Unexpectedly, *VEGF-A* levels did not reach the 2-fold cut off in the arrays (Figure 16a). We also tested the induction of VEGF-A by ELISA in the culture supernatants. The tumor fibroblasts did



not secrete more VEGF-A than normal fibroblasts, consistent with our array data (Figure 16b).

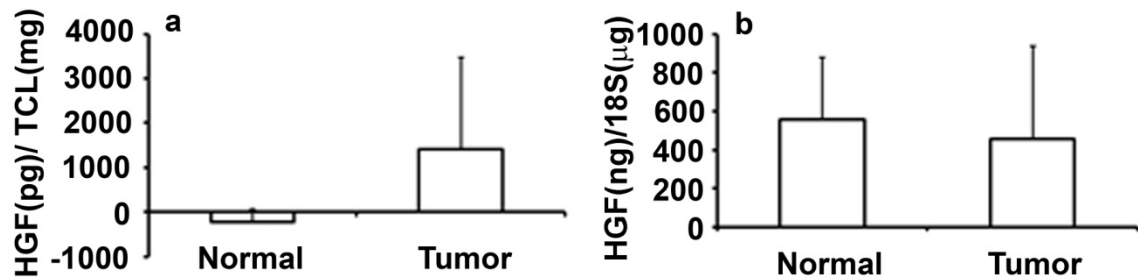


**Figure 14. HGF expression in TSC skin tumors.** Fibroblasts from eight pairs of normal-appearing skin and TSC tumors, including angiofibromas, periungual fibromas and forehead plaques were cultured in DMEM with 10%FBS for 24 hr. a) The supernatants were then collected for measurement of HGF production using ELISA. The results are normalized to the total cellular protein in the lysate (TCL). b) RT-PCR of HGF was performed in the RNA extracted from the eight paired fibroblasts. Data are expressed as mean  $\pm$  SD. (\*,  $p < 0.05$ ).

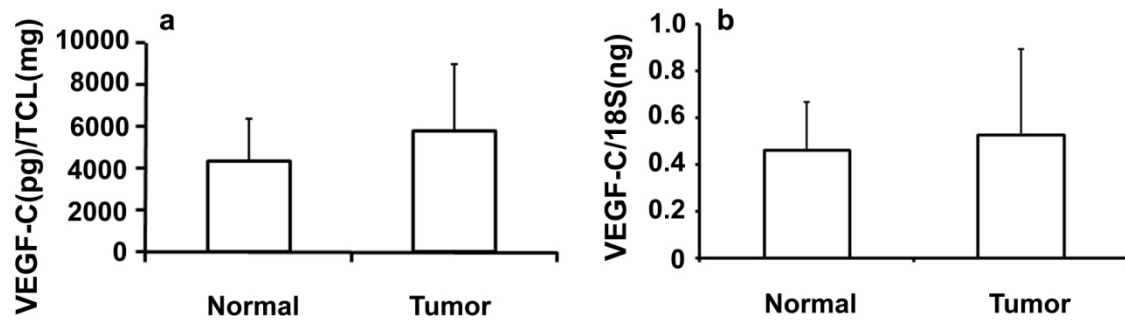


**Figure 15. VEGF-C expression in TSC skin tumors.** Fibroblasts were cultured from eight pairs of TSC tumor and TSC normal tissue explants obtained from eight patients. a) ELISA quantification of VEGF-C levels were performed in culture supernatants of the eight paired fibroblasts. The results are normalized to the total cellular protein in the lysate. b) RT-PCR of VEGF-C was performed in the RNA extracted from the eight paired fibroblasts. Data are expressed as mean  $\pm$  SD. (\*,  $p < 0.05$ ).

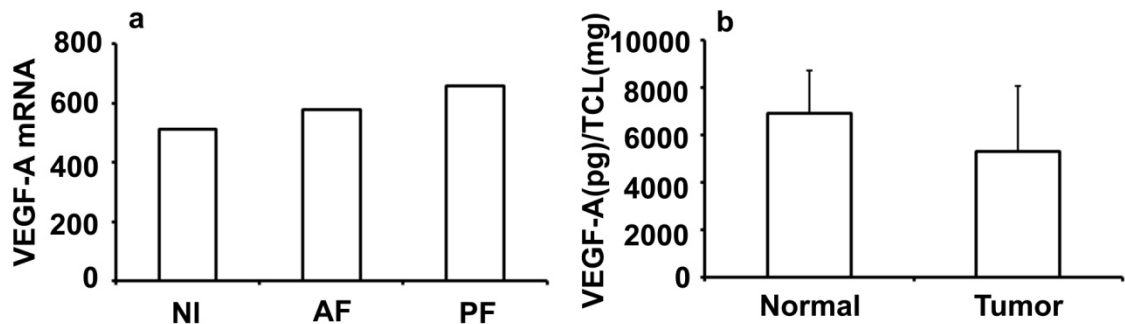


**Figure 16. Expression levels of VEGF-A in TSC skin tumors.** a) Gene expression of *VEGFA* in fibroblast-like cells grown from four angiofibromas (AF), three periungual fibromas (PF), and normal fibroblasts (NI) from four patients analyzed by using Affymetrix GeneChips. b) Quantification of VEGF-A levels using ELISA was performed in culture supernatants of fifteen pairs of TSC tumor fibroblasts and TSC normal fibroblasts obtained from thirteen patients. The results are normalized to the total cellular protein in the lysates.

### **Part 3: b) Regulation of lymphangiogenic factor expression in TSC skin tumors.**

#### **TSC2 knockdown increases HGF secretion in neonatal fibroblasts**

Because HGF and VEGF-C are upregulated in TSC skin tumors, we wanted to determine whether TSC2 regulates expression of these lymphatic factors. A lentiviral approach was used to stably knockdown the expression of TSC2. Neonatal foreskin fibroblasts were transduced with virus particles carrying pGIPZ-lentiviral shRNA vector with TSC2 shRNA or with virus particles carrying a control construct containing a shRNA that recognizes no human sequence (shNT). Cells retaining the shRNA were selected with puromycin. The selected TSC2 shRNA and control shRNA transduced fibroblasts retained eGFP over several passages. The efficiency of silencing was determined by Western blot analysis. Transduction with TSC2 shRNA almost completely reduced the expression of TSC2 with an increase in phosphorylation of ribosomal protein S6 indicative of mTORC1 activation compared to control fibroblasts. Total S6 levels were unchanged in both control and TSC2 shRNA transduced fibroblasts (Figure 17).

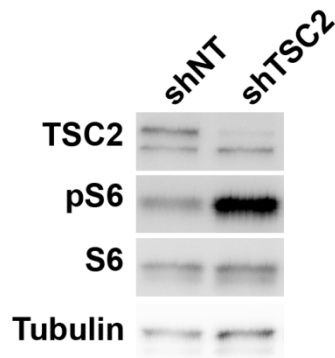


**Figure 17. Effect of TSC2 knockdown on TSC2 and phosphorylation of ribosomal protein S6 in neonatal fibroblasts.** Western blots of TSC2, phosphorylated ribosomal protein S6 (pS6), total S6, and tubulin in neonatal foreskin fibroblasts transduced with viral particles carrying either a control shRNA vector or shTSC2 vector. Tubulin is used as a loading control. Similar results were obtained in duplicate transductions. *Transduction performed by Dr.Thangapazham.*

Neonatal fibroblasts transduced with the lentivirus carrying the shRNA directed against TSC2 released more HGF into culture supernatants than fibroblasts containing the control vector (Figure 18). In contrast, *TSC2* knockdown did not alter the levels of VEGF-C secreted by neonatal fibroblasts (Figure 19). A similar pattern was observed with transient transfection of neonatal and adult fibroblasts with a siRNA construct specific to TSC2. Western blots showed about 50% TSC2 knockdown in both neonatal and adult fibroblasts with TSC2 siRNA but not with control siRNA. Knockdown of TSC2 was accompanied by an increase in pS6 expression as an indication of increased mTOR activation when compared to the controls. This downregulation of TSC2 was paralleled with an increase in HGF secretion in the culture supernatants of both neonatal and adult fibroblasts. However, there was no stimulatory effect on VEGF-C secretion

with TSC2 knockdown (data not shown). Together the *in vitro* TSC2 knockdown studies demonstrate that enhanced expression of HGF observed in these skin tumors is regulated in a TSC2-dependent mechanism. In contrast, it appears that VEGF-C levels in TSC tumor cells are regulated by some mechanism independent of TSC2 loss.

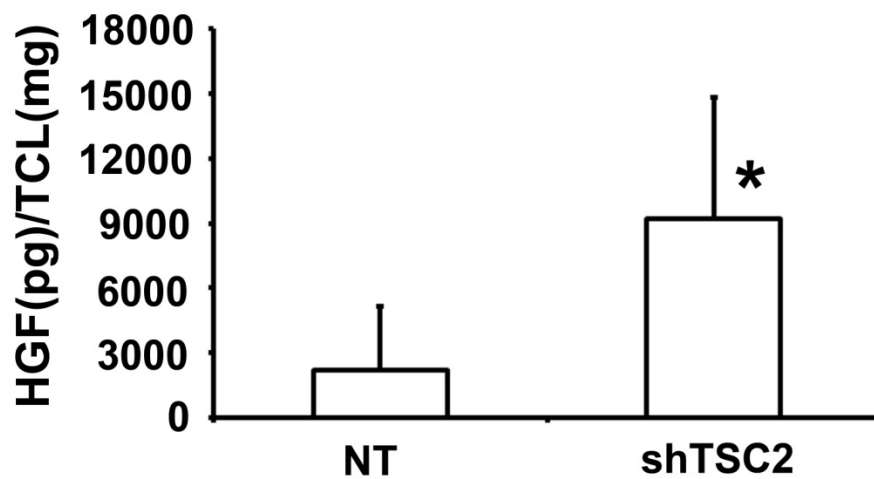


**Figure 18. Effect of TSC2 knockdown on HGF production.** Culture supernatants were obtained from neonatal foreskin fibroblasts transduced with viral particles carrying either a control shRNA vector or shTSC2 vector cultured in serum-free DMEM for about 24hr. The supernatants were then analyzed for HGF production using ELISA. The results are normalized to the total cellular protein in the lysate. Data are expressed as mean  $\pm$  SD of three separate experiments. (\*,  $p < 0.05$ ).

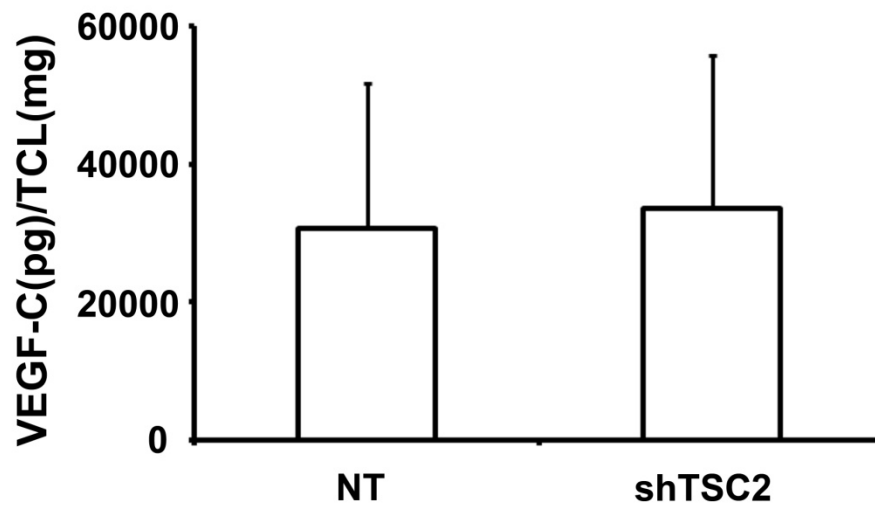


**Figure 19. Effect of TSC2 knockdown on VEGF-C production.** Neonatal foreskin fibroblasts transduced with viral particles carrying either a control shRNA vector or shTSC2 vector were cultured in serum-free DMEM for about 24hr. The culture supernatants were then collected and analyzed for VEGF-C production using ELISA. The results are normalized to the total cellular protein in the lysate. Data are expressed as mean  $\pm$  SD of three separate experiments. (\*,  $p < 0.05$ ).

### **mTORC1-independent regulation of HGF and VEGF-C in TSC skin tumors**

Our *in vivo* studies indicated dramatic anti-lymphangiogenic effects of rapamycin on TSC xenografts. To investigate the role of mTORC1 in regulating expression of the lymphangiogenic factors HGF and VEGF-C, we used rapamycin, one of the best studied inhibitors of mTORC1. Normal and tumor fibroblasts were incubated for 24 hr with 20 nM rapamycin and levels of HGF and VEGF-C in culture supernatants were measured by ELISA. Tumor fibroblasts secreted higher levels of HGF and VEGF-C than normal fibroblasts. Rapamycin treatment did not affect levels of HGF released by the tumor cells (Figure 20). There was also no significant difference in VEGF-C release between 20 nM rapamycin treated and untreated normal and tumor fibroblasts (Figure 21). Thus, the levels of HGF and VEGF-C secreted by the TSC tumor fibroblasts were insensitive to rapamycin treatment.

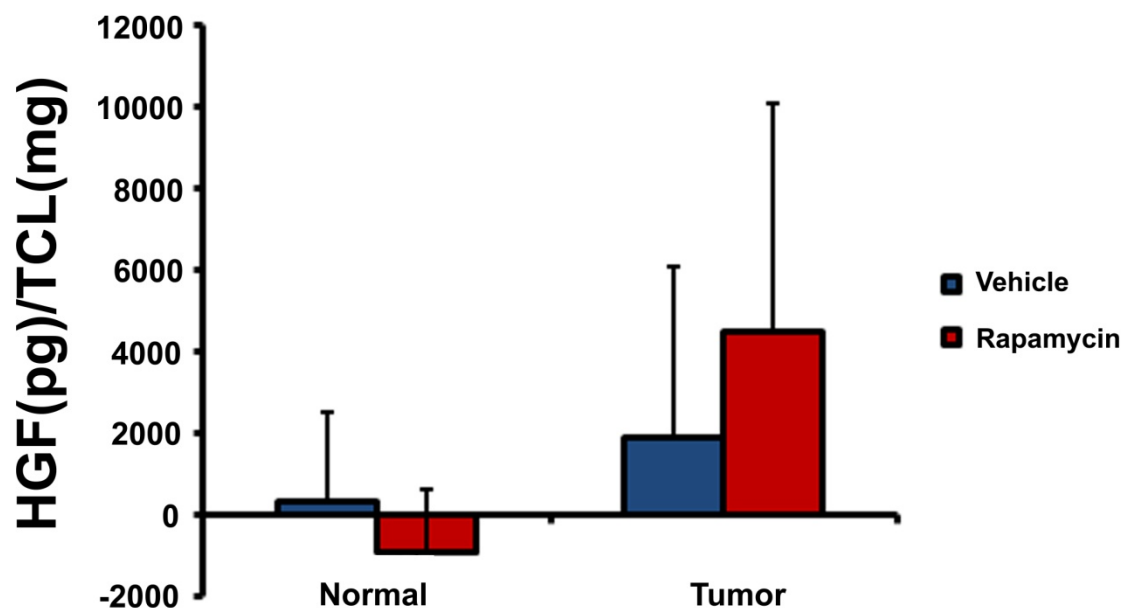


**Figure 20. Effect of rapamycin on HGF production.** Culture supernatants were collected from TSC normal and tumor fibroblasts (2AFs, 3PFs and 3FPs) obtained from eight patients. HGF levels in the supernatants were measured in duplicate using ELISA after incubating equal number of cells for 24 hr in DMEM with or without rapamycin at 20 nM. HGF concentration is normalized to the total cellular protein (TCL) and is reported as the mean  $\pm$  SD.



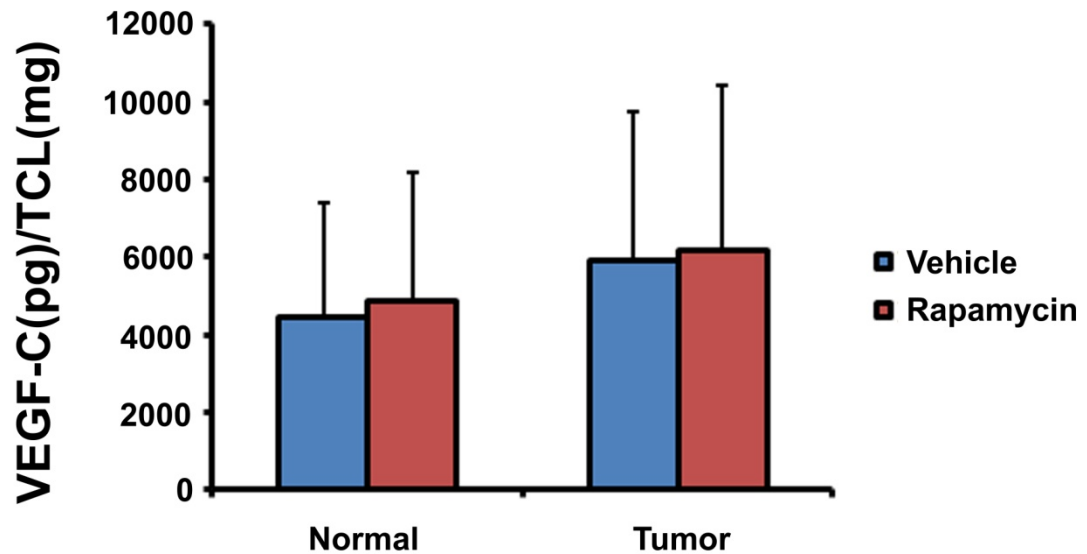


**Figure 21. Effect of rapamycin on VEGF-C production.** Culture supernatants were collected from TSC normal and tumor fibroblasts (2AFs, 3PFs and 3FPs) obtained from eight patient biopsies. VEGF-C levels in the supernatants were measured in duplicates using ELISA after incubating equal number of cells for 24 hr in DMEM with or without rapamycin at 20 nM. The results are normalized to the total cellular protein (TCL) and is reported as the mean  $\pm$  SD.

### Summary 3

- TSC tumor fibroblasts overexpressed the lymphangiogenic factors HGF and VEGF-C
- Knockdown of *TSC2* increased HGF secretion
- VEGF-C levels were unaffected by *TSC2* knockdown
- Rapamycin did not affect the secretion of either HGF or VEGF-C

## **Chapter 4: Discussion**

Identification of the TSC genes associated with the development of TSC has accelerated basic research and improved our understanding of the pathogenesis of this disorder. The TSC1-TSC2 complex is mainly involved in regulating mTOR, a serine/threonine kinase which has central roles in cell size, growth, protein synthesis and transcription. TSC tumors exhibit hyperactivation of mTOR, which in cancers, has been associated with survival, growth, proliferation, angiogenesis, and migration of tumor cells. We sought to elucidate the biochemical and cellular mechanisms by which mTOR signaling contributes to increased growth and vascularity of TSC tumors, with the expectation that a better understanding of TSC pathogenesis would lead to new drug targets and more effective therapies.

TSC skin tumors range from being minimally troubling to disfiguring and painful lesions that dramatically impact patients' quality of life. All of the patients in our study had at least one major skin lesion characteristic of TSC, including facial angiofibromas or forehead plaques, ungual fibromas, hypomelanotic macules and shagreen patches. Many of these patients had endured multiple surgeries that left permanent scarring and abnormal pigmentation. These limitations and disadvantages of surgical treatments have stimulated great interest in developing new medical treatments. The discovery of mTOR activation in TSC tumors prompted clinical trials of the mTOR inhibitor rapamycin. This class of mTOR inhibitors is now the leading approach for the medical treatment of TSC tumors, and yet these drugs are only partially effective and have numerous side effects. By determining the effects of rapamycin on TSC tumors, we sought to identify new avenues to augment therapeutic effectiveness. We found that angiogenesis and

lymphangiogenesis are major components of TSC tumors and important targets of rapamycin.

### **TSC skin tumors are highly vascular**

Angiogenesis is a complex process that is important for many physiological and pathological processes including embryogenesis, reproductive cycle and tumor growth and survival. Early evidence for angiogenesis in TSC skin tumors was obtained using routine histology. The facial lesions in particular showed increased vessels and fibrosis and consequently were called angiofibromas. Our laboratory later showed that TSC skin tumors show greater numbers of vessels positive for CD31 than normal skin<sup>67</sup>. CD31 is platelet endothelial cell adhesion molecule-1 that serves as an indicator of angiogenesis in many tumors<sup>190</sup>. These results confirm and extend previous findings that TSC-associated lesions of the skin, brain and kidney show a high degree of neovascularization<sup>105</sup>.

Previous studies in the laboratory showed that not all vessels stain positive for CD34, a blood vessel endothelial cell marker<sup>180</sup>. This suggested the possibility that lymphatic vessels make up a significant proportion of the vasculature. Indeed, earlier histological examination had suggested the presence of lymphatic vessels interspersed with blood vessels<sup>86</sup>. By staining for markers of lymphatic endothelial cells, we became the first to demonstrate increased lymphangiogenesis in these skin tumors. The lymphatic vessels in these TSC skin tumors were larger and denser than in patient normal-appearing skin. The magnitude of these changes was similar to those observed in malignant and metastatic melanomas<sup>191-193</sup>. The lymphatic vessel density observed in the normal skin from TSC patients was comparable to that obtained from normal volunteers<sup>194</sup>. Therefore,

angiogenesis and lymphangiogenesis can be characteristics of benign tumors and is not restricted to cancers with a propensity to metastasis.

**Biallelic TSC2 mutations are observed in fibroblast-like cells and not vessels.**

The cellular heterogeneity of TSC skin tumors confounded efforts to determine which cell population, if any, showed loss of the wild type allele, in accordance with Knudson's two-hit hypothesis. Earlier studies in this laboratory demonstrated that two-hit cells are present in the dermis and are not detected in the epidermal keratinocytes<sup>187</sup>. Here we show that fibroblast-like cells sustain two-hits in TSC skin tumors. Fibroblast-like cells from angiofibromas, periungual fibromas and forehead plaques showed low or undetectable levels of TSC2 with hyperphosphorylation of ribosomal protein S6 under serum-starved conditions. Biallelic mutations in TSC2 were demonstrated in fibroblast-like cells from a forehead plaque and periungual fibroma<sup>67</sup>. Cells grown from angiofibromas and periungual fibromas have shown loss of heterozygosity (LOH) at the TSC2 locus (Wang and Darling, unpublished data). In contrast, there is no evidence for genetically altered blood vessels in TSC skin tumors, since LOH was not observed in microdissected endothelial cells (Wang and Darling, unpublished). Similar findings were obtained in renal angiomyolipomas; LOH was observed in smooth muscle cells, fat cells, and thickened vessel walls, but not in vascular endothelial cells<sup>195</sup>. Together, these results suggest that fibroblast-like cells in the dermis of TSC skin tumors orchestrate the formation of TSC skin tumors and induce angiogenesis and lymphangiogenesis.

## **TSC2-null fibroblast-like cells are the inciting cells for TSC skin tumor development**

A number of animal models including rats and mice have been developed to study TSC tumors and the effect of drugs *in vivo*. These models develop tumors of the kidney, lungs, heart and brain<sup>196</sup> but do not develop the characteristic skin lesions. To overcome this barrier to studying TSC skin tumorigenesis, we developed a novel xenograft model in which dermal-epidermal composites, composed of TSC2-null fibroblast-like cells overlaid with neonatal foreskin keratinocytes, were grafted onto nude mice. Tumor grafts with TSC2-null cells showed increased activation of mTORC1 compared to grafts with fibroblasts from patient normal-appearing skin (normal grafts). Tumor grafts also had larger and more numerous blood vessels than normal grafts. Tumor grafts contained larger and denser lymphatic vessels than normal grafts. Thus, tumor xenografts replicated features of TSC skin tumors and TSC2-null cells induced angiogenesis and lymphangiogenesis. Angiogenesis plays a crucial role in tumor growth and progression. Increased microvessel density is a prognostic tool for activated angiogenesis in a variety of cancers<sup>197</sup>. The increased angiogenesis observed in the human TSC skin tumors could be recapitulated in the tumor xenografts suggesting a role for angiogenesis in the growth of TSC tumors. In LAM, lymphangiogenesis has been implicated in disease progression and dissemination<sup>181, 198</sup>. In TSC skin tumors it is possible that lymphatic vessels serve other functions to support tumor growth, for example by releasing paracrine growth factors or regulating tumor edema or inflammation.

Identification of the TSC2-null tumor cells as the inciting cells that convey signals to other cells for inducing angiogenesis and lymphangiogenesis is a major breakthrough in TSC skin tumor research. Studies focused on these cells would enable identification of

soluble factors and the signaling pathways that cooperate or synergize with each other in stimulating angiogenesis and lymphangiogenesis. This will lead to identification of drug targets, development of targeted therapies and better monitoring of responses to treatment.

Thus, these benign tumors provide a model of how tumor cells with mTOR activation may stimulate angiogenesis as well as lymphangiogenesis.

### **Cells contributing to angiogenesis and lymphangiogenesis in TSC skin tumors**

The induction of angiogenesis and lymphangiogenesis in tumor xenografts may occur as a direct response to TSC2-null cells or indirectly through the involvement of other cells types. Other cells with possible roles in vessel formation in TSC skin tumors include macrophages and epidermal cells, since they constitute a significant proportion of the cells.

### **Mononuclear phagocytes**

In cancer, the tumor microenvironment plays major roles in tumor growth and metastasis. Interaction between cancer cells and activated stromal cells, such as macrophages, lymphocytes, natural killer cells, fibroblasts and endothelial cells, plays prominent role in tumor cell-proliferation, migration, invasion and angiogenesis. TSC skin tumors contain increased numbers of mononuclear phagocytes, as detected by staining with CD68, a monocyte/dendritic cell marker. Cortical tubers of TSC also have increased numbers of CD68-positive cells<sup>199</sup>. In our xenograft model, tumor grafts showed greater numbers of mononuclear phagocytes than normal grafts. This is significant since the number of tumor-associated macrophages (TAMs) correlates with tumor vascularity and tumor progression in a number of cancers<sup>200</sup>. TAMs release diverse

factors that stimulate angiogenesis including growth factors such as VEGF, bFGF, EGF, and TGF- $\alpha$ , as well as tissue-degrading enzymes<sup>200</sup>. Furthermore, CD68-positive mononuclear phagocytes recruited into the tumor microenvironment may release lymphangiogenic factors. TAMs have been shown to stimulate lymphangiogenesis in other tumors by release of VEGF-C, VEGF-D<sup>201</sup> and HGF<sup>202</sup>.

Earlier studies in our laboratory showed that TSC skin tumors overexpress the angiogenic factors MCP-1 and epiregulin<sup>186, 187</sup>. MCP-1 is a chemokine that stimulates angiogenesis directly and through recruitment of monocytes<sup>203</sup>. Thus, MCP-1 produced from the tumor cells may attract the mononuclear phagocytes, which are pro-angiogenic and pro-lymphangiogenic, into the tumor microenvironment. These TAMs could be partly responsible for the increased vascularity of TSC skin tumors.

### **Epidermal cells**

Keratinocytes are major sources of VEGF production and are important players in wound angiogenesis<sup>204</sup>. They are also highly pro-angiogenic, secreting angiogenic factors such as VEGF, IL-8, TNF- $\alpha$  in a psoriatic skin lesion<sup>205, 206</sup>. TSC skin tumors show increased keratinocyte proliferation, as detected by staining with Ki-67. One of the characteristic features of TSC skin tumors is increased epidermal thickness<sup>87</sup> and the increased keratinocyte proliferation observed in these TSC skin tumors correlates with the increased thickness of the overlying epidermis. Proliferation of epidermis was observed in angiofibroma and periungual fibroma lesions<sup>187</sup>. Hyperplasia of the overlying epidermis was also observed in the tumor grafts in comparison to the normal grafts. Previous studies in the laboratory have shown that the TSC tumor cells overexpress the angiogenic factor epiregulin. Epiregulin is an EGF family member and EGFR signaling

has been implicated in tumor angiogenesis<sup>187</sup>. *In vitro* and *in vivo* studies have shown that epiregulin stimulates epidermal cell proliferation and thickness<sup>207, 208</sup>. So the TSC tumor cells might induce overgrowth of the epidermal keratinocytes resulting in continued expression of angiogenic factors that stimulates TSC tumor growth.

The increased epidermal proliferation was also associated with induction of hair follicles only in the tumor grafts. Thus, the TSC2-null cells contribute to the disorganized overgrowth of the overlying epidermis and also induce follicular neogenesis.

### **Rapamycin as a therapeutic agent for TSC skin tumors**

Studies of TSC2-null fibroblast-like cells incubated with rapamycin demonstrated that rapamycin reduced mTORC1 activation and cell proliferation *in vitro*, but studies using the xenograft model were necessary to determine *in vivo* response of TSC2-cells within a representative tumor microenvironment. In both tumor and normal grafts, rapamycin inhibited mTORC1 signaling, as indicated by decreased phosphorylation of ribosomal protein S6. Tumor grafts also showed decreased numbers of TSC2-null cells and mononuclear phagocytes, and decreased epidermal proliferation. Angiogenesis in tumor grafts was significantly decreased by rapamycin, without any effect on the blood vessels in normal grafts. These results suggest that the decreased redness and size of TSC skin lesions observed in patients receiving systemic<sup>78</sup> or topical<sup>209</sup> rapamycin may result from both anti-tumor cell effects and anti-angiogenic effects. Rapamycin has been shown to decrease VEGF-A overexpressed by *Tsc2*<sup>-/-</sup> mouse embryonic fibroblasts<sup>210</sup>. Thus, the anti-angiogenic effects of rapamycin may be due to direct inhibition of vascular endothelium and/or indirect effects, such as diminished release of angiogenic factors by TSC2-null cells or recruitment of proangiogenic mononuclear cells.



Rapamycin markedly reduced the number and size of the lymphatic vessels in both normal and tumor grafts. The effects of rapamycin on lymphatic vessels differed from its effects on blood vessels, since rapamycin decreased lymphangiogenesis in both tumor and normal grafts, whereas angiogenesis was decreased only in tumor grafts. This may indicate that rapamycin broadly inhibits lymphangiogenesis but selectively inhibits tumor-cell specific aspects of angiogenesis. Macrophages are also actively involved in lymphangiogenesis by secreting lymphatic factors VEGF-C and VEGF-D. Rapamycin analog everolimus has been shown to decrease macrophage recruitment and accumulation in carotid lesions<sup>211</sup>. It has been shown that rapamycin at concentrations as low as 1 ng/ml inhibits the *in vitro* proliferation and migration of human dermal lymphatic endothelial cells in response to VEGF-C<sup>212</sup> and also inhibits VEGF-C expression in pancreatic tumor cells<sup>188</sup>. Thus, the anti-lymphangiogenic effects of rapamycin in TSC skin tumors may be due to its direct effects on the LECs or indirectly by blocking expression of the soluble factors by tumor cells and decreasing infiltration of mononuclear phagocytes.

Rapamycin thus exerts its anti-angiogenic, anti-lymphangiogenic and anti-tumor effects in the TSC xenograft model. However, it did not eradicate all the tumor cells. This cytostatic effect of rapamycin on the tumor cells could account for the need for continuous treatment without which the tumors reoccur. The mechanism of action of rapamycin in these tumors could be due to shut down of the tumor blood and lymphatic vessels, which in turn decreases tumor growth, and also due to a direct anti-proliferative effect on the tumor cells.

## **Angiogenic and lymphangiogenic factors in TSC skin tumors**

The foregoing studies demonstrated that TSC2-null cells induce angiogenesis and lymphangiogenesis, and suggested that the mechanism is at least partly through direct effects of the tumor cells on the vascular endothelium. We used genomic and proteomic screens to identify candidate angiogenic and lymphangiogenic factors, including VEGF-A, Angiopoietin 2, FGF, HGF, VEGF-C, VEGF-D and PDGFbb. These identified VEGF-A, VEGF-C, and HGF as candidate factors.

VEGF-A is a major angiogenic factor, and loss of TSC1/TSC2 function has been associated with increased production of VEGF-A<sup>189, 210</sup>. In spite of these skin tumors being highly vascular and angiogenic, we found that VEGF-A mRNA and protein levels were not consistently or significantly higher in the tumor fibroblasts than TSC normal fibroblasts. Other angiogenic factors may be important, and previous studies in our laboratory showed that TSC skin tumors overexpressed the angiogenic factors MCP-1 and epiregulin<sup>186, 187</sup>. As mentioned earlier, MCP-1 and epiregulin may induce angiogenesis indirectly, through effects on macrophages and epidermal cells, respectively. They also may directly stimulate angiogenesis. MCP-1 induced endothelial cell sprouting and migration in cells of different origin including HUVEC and HMECs<sup>203</sup>. Epiregulin induced neovasculature of breast cancer cells by promoting assembly of dilated, tortuous and leaky tumor blood vessels<sup>213</sup>.

A possible mechanism for lymphangiogenesis in TSC skin tumors is increased release of lymphangiogenic factors by tumor cells, since TSC2-null cells produced more HGF and VEGF-C than normal fibroblasts. HGF and VEGF-C have been shown to directly promote proliferation, migration and survival of lymphatic endothelial cells.

Recently, HGF and VEGF-C have been reported to play a role in the pathogenesis of cortical tubers. Enhanced expression of HGF and c-met was shown in human SEGAs and cortical tubers and also in a TSC1 conditional knockout mouse cortex (TSC1 (GFAP) CKO) mouse<sup>214</sup>. An upregulation of VEGF-C and VEGFR3 was also found in the cortical tubers of TSC<sup>215</sup> and pulmonary and extrapulmonary lung lesions<sup>181</sup>. The severity of pulmonary LAM correlates with the levels of VEGF-C expression<sup>181</sup>.

Therefore TSC2-null tumor cells can secrete angiogenic and lymphangiogenic factors that directly stimulate the growth of blood and lymphatic vessels, thereby inducing TSC tumor growth. These results show that the interaction between the fibroblast-like tumor cells and the endothelial cells might be an important aspect of TSC tumor growth and proliferation. The soluble factors identified may be potential therapeutic targets leading to effective treatment for TSC and other similar human pathologies.

#### **HIF-1 $\alpha$ might contribute to tumor growth in TSC skin tumors**

Normal skin is generally mildly hypoxic with oxygen levels between 1.5% - 5%. Mild hypoxia stimulates growth and expression of angiogenic factors through HIF<sup>116</sup>. The effects of hypoxia on TSC tumor growth, by regulating angiogenic and lymphangiogenic factors, are not well elucidated. We observed that TSC tumor fibroblasts show high basal levels of HIF-1 $\alpha$ , which remained persistent under prolonged hypoxia. The high HIF-1 $\alpha$  levels also correlated with sustained activation of mTOR under hypoxia. Abnormal accumulation of HIF-1 $\alpha$ , with an increase in phosphorylation of S6, has been shown in TSC2-deficient MEFs<sup>216</sup>. mTOR exerts a positive feedback by acting upstream of HIF-1 $\alpha$  and enhances its stability and function<sup>217</sup>. Our data indicate TSC2-null tumor fibroblasts

that have high mTOR activation also have high HIF-1 $\alpha$  expression through a positive feedback mechanism. The high levels of HIF-1 $\alpha$  could account for the highly vascular nature of these tumors as tumors with high mTOR activity are highly vascularized<sup>189, 218</sup>.

Hypoxic activation of HIF-1 $\alpha$  triggers the expression of angiogenic factors including VEGF-A. Elevated VEGF-A levels have been associated with poor prognosis and response to treatment<sup>219</sup>. There was no positive correlation between HIF-1 $\alpha$  and VEGF-A levels in these skin tumors. HIF-1 $\alpha$  independent regulation of VEGF-A has been reported in colon cancer<sup>220</sup>. VEGF-A has also been shown to be regulated by other signaling pathways including Wnt and K-ras<sup>221</sup>.

HIF-1 $\alpha$  could also induce angiogenesis and lymphangiogenesis by upregulating other soluble factors such as MCP-1<sup>186, 222</sup>, VEGF-C and HGF. HIF-1 $\alpha$  indirectly activates HGF by activating its target gene, hepatocyte growth factor activator (HGFA). HGFA is a serine protease that converts pro-HGF into its mature form<sup>223</sup>. Hypoxia has been reported to increase the transcripts encoding VEGF-C, VEGF-D and VEGFR3 in venous endothelial cells<sup>224</sup>. A correlation between HIF-1 $\alpha$ , and VEGF-C and lymph node metastasis was observed in human esophageal cancer and breast cancers, suggesting a regulatory role of HIF-1 $\alpha$  in tumor lymphangiogenesis<sup>225, 226</sup>.

Hypoxia was also shown to recruit macrophages to stimulate tumor progression<sup>227</sup>. TAMs accumulate in highly hypoxic regions and express HIF-1 $\alpha$ . HIF-1 $\alpha$  knockout studies showed that HIF-1 $\alpha$  is indispensable for the TAMs to exert their angiogenic properties<sup>228</sup>. Thus, hypoxia by inducing HIF-1 $\alpha$ , which triggers expression of soluble factors, and recruiting macrophages might play an important role in TSC tumor growth.

## Regulation of the lymphangiogenic factors HGF and VEGF-C

To explore the relationship between loss of TSC2 and the production of HGF and VEGF-C, we knocked down *TSC2* using siRNA and, in separate experiments, shRNA. Knockdown of *TSC2* in neonatal fibroblasts stimulated production of HGF but did not increase VEGF-C production. This suggests that HGF is regulated in a TSC2-dependent manner while regulation of VEGF-C is by TSC2-independent mechanisms. The difference in VEGF-C expression in our experiments between TSC2-null and TSC2 knockdown fibroblasts may be due to differences in cell type, anatomical location of the fibroblasts, or insufficient knockdown of *TSC2*. A number of other mechanisms have been reported to upregulate VEGF-C including microenvironment stress like hyperthermia and oxidative stress<sup>229</sup>, heparanase in a xenograft model of head and neck cancers<sup>230</sup>, and proinflammatory cytokines IL-1 $\beta$  and TNF- $\alpha$ <sup>231, 232</sup>. Preliminary studies in the laboratory indicate increased expression of COX-2 by TSC tumor cells, and TNF- $\alpha$  also increased secretion of VEGF-C (unpublished data).

Rapamycin did not significantly affect HGF or VEGF-C production by TSC2-null skin tumor cells. This suggests that upregulation of these factors in TSC2-null cells is by a mechanism independent of mTORC1 activity. One possible mechanism could be that secretion of these factors by the TSC2-null cells is regulated in a mTORC2-dependent manner. Either a prolonged treatment with rapamycin or an inhibitor of both mTORC1 and mTORC2 might downregulate the expression of HGF and VEGF-C. Although mTOR is the major signaling pathway in TSC2-null cells, rapamycin-insensitive, mTORC1-independent effects on gene expression have already been reported. VEGF upregulation observed in TSC2-/- MEFs was only partially downregulated with

rapamycin, even at concentrations sufficient to inhibit mTOR<sup>210</sup>. A similar pattern was observed in a TSC2- null AML cell line where upregulation of several genes including MMP-2 was not affected by rapamycin<sup>233</sup>.

There are several potential explanations for the marked anti-lymphangiogenic effects of rapamycin on xenografts despite having no effects on the production of lymphangiogenic factors. Rapamycin decreased the number of tumor cells in xenografts, which presumably decreased the total amount of lymphangiogenic factors produced. In addition, rapamycin decreased the numbers of CD68-positive macrophages in tumor xenografts, which is expected to block macrophage-stimulated lymphangiogenesis. The most powerful effects of lymphangiogenesis may be through direct effects on the lymphatic endothelium and by recruitment of pro-lymphangiogenic mononuclear phagocytes.

The observations that HGF and VEGF-C are regulated by mechanisms that are rapamycin-insensitive indicate the need for further studies to identify means of blocking production of the lymphangiogenic factors. The current medical treatments for TSC tumors are directed solely at inhibiting mTORC1. However our results emphasize the need to focus on mTORC1-independent pathways, which might be equally important for TSC pathogenesis.

### **A model for angiogenesis and lymphangiogenesis in TSC skin tumors**

Based on the above studies, we propose a model for increased angiogenesis and lymphangiogenesis in TSC skin tumors, which involves TSC2-null tumor cells, TAMs and keratinocytes (Figure 22). This model highlights the importance of paracrine factors

and the tumor microenvironment for induction of angiogenesis and lymphangiogenesis in TSC tumors, and provides new potential targets for therapeutic intervention.

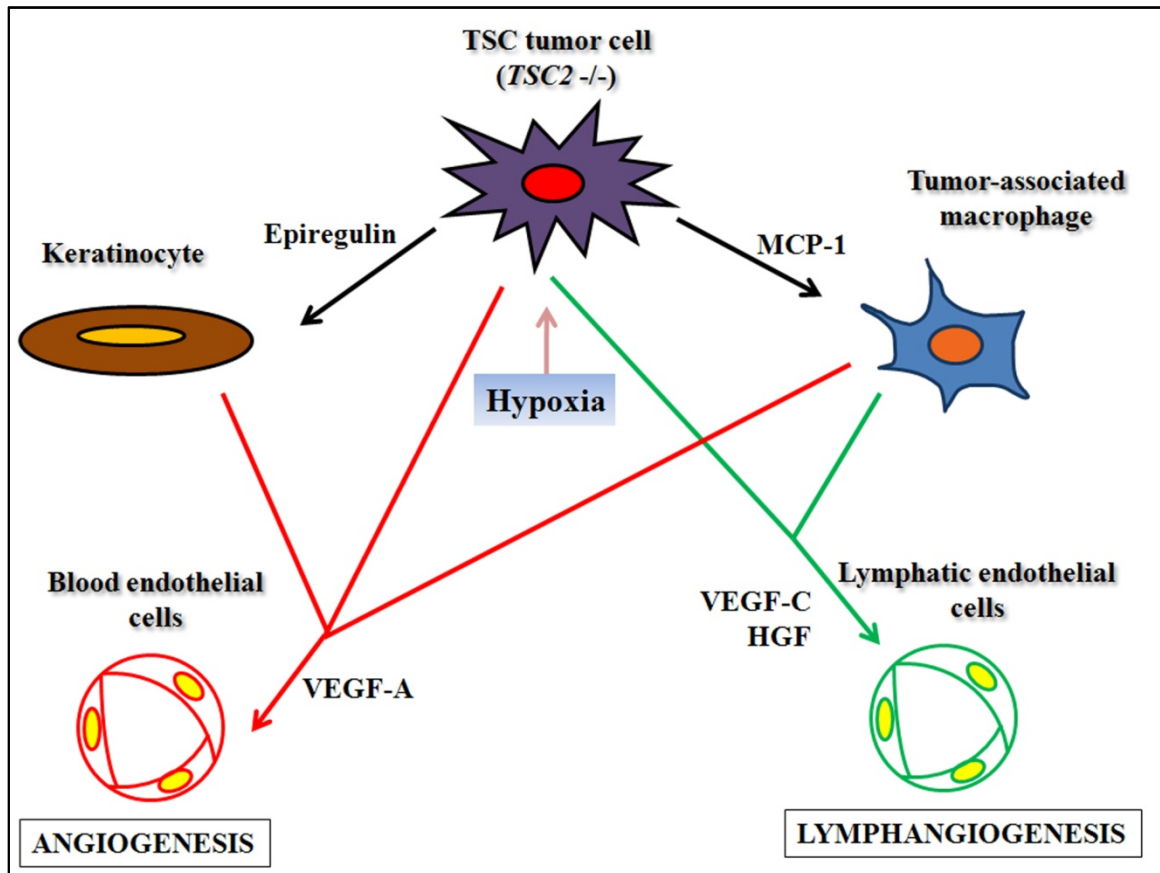


**Figure 22. Model for angiogenesis and lymphangiogenesis in TSC skin tumors.** TSC2-null tumor cells induce angiogenesis and lymphangiogenesis by a) secreting soluble factors namely VEGF-A, VEGF-C and HGF, b) producing the angiogenic factor MCP-1 that acts as a chemoattractant and recruits mononuclear phagocytes, which in turn release soluble factors including VEGF-A, VEGF-C and HGF thereby stimulating both angiogenesis and lymphangiogenesis, c) secreting epiregulin, a EGF growth factor that stimulates proliferation of keratinocytes, which further induces angiogenesis by secreting the major angiogenic factor VEGF-A, d) abnormal responses to hypoxia, which induces tumor fibroblasts to express hypoxia inducible factor, HIF-1 $\alpha$ , which triggers expression of the genes VEGF-A, HGF, VEGF-C and can also recruit TAMs, leading to angiogenesis and lymphangiogenesis.

## **Targeting angiogenesis and lymphangiogenesis in TSC skin tumors**

Studies have shown the importance of angiogenesis for tumor growth, without which tumors are unable to grow more than 2mm in diameter<sup>234-236</sup>. Rapamycin dramatically inhibits neoangiogenesis and lymphangiogenesis in TSC skin tumor xenografts, but does not completely eradicate the tumor cells. This cytostatic effect of rapamycin on tumor cells, the ability of tumors to regrow in patients when rapamycin is discontinued and the potential adverse effects of rapamycin suggests the inadequacy of rapamycin treatment alone and the need for finding better treatment strategies including combination therapies.

A number of anti-angiogenic and anti-lymphangiogenic therapies are already being developed and tested clinically. The strategy includes either directly targeting the endothelial receptors or indirectly by neutralizing the functions of soluble factors. Potential therapies found to be effective in animal models include soluble versions of cell surface receptors VEGFR-1, VEGFR-2, and VEGFR-3, monoclonal antibodies to the soluble factors including VEGF-A, VEGF-D, MCP-1, and HGF and small molecular inhibitors of tyrosine kinase receptors or downstream signaling molecules. One of the monoclonal antibodies that is FDA approved as an anti-angiogenic therapy to treat patients with metastatic colorectal cancer is Bevacizumab. Small molecule tyrosine kinase inhibitors that block both VEGFR-3 and VEGFR-2 are under evaluation in clinical trials as anti-cancer therapeutics<sup>237</sup>. The experimental and clinicopathological studies show that the VEGF signaling pathway may be a promising target and justifies its testing in the clinic.



In conclusion, TSC2-null fibroblast-like cells induce features characteristic of TSC skin tumors including angiogenesis and lymphangiogenesis. The TSC2-null fibroblast-like cells exhibit mTOR activation with increased HIF-1 $\alpha$  expression and produce many soluble factors including HGF, VEGF-C, MCP-1 and epiregulin. Angiogenesis and lymphangiogenesis are commonly linked with metastasis of various cancers<sup>238, 239</sup> and this benign skin tumor model provides an opportunity to elucidate additional roles of blood vessels and lymphatics in tumors with mTOR activation, such as responses to therapies. Identifying angiogenic and lymphangiogenic factors and their mechanisms would have a great impact on understanding TSC tumor growth. Rapamycin blocked angiogenesis and lymphangiogenesis in the xenografts, without being cytotoxic to the tumor cells. Therefore, combination therapies using chemotherapeutic agents along with anti-angiogenic and anti-lymphangiogenic agents may prove to be a more effective method of treatment of TSC tumors and cancer in general.

## CHAPTER 5: References

1. Jordan WM: Familial tuberous sclerosis, Br Med J 1956, 2:132-135
2. SE M: Hamartial nature of tuberous sclerosis complex and its bearings on the tumor problem: report of a case with tumor anomaly of the kidney and adenoma sebaceum, Archives of Internal Medicine 1942, 69:589–623
3. Gomez MR: Phenotypes of the tuberous sclerosis complex with a revision of diagnostic criteria, Ann N Y Acad Sci 1991, 615:1-7
4. Osborne JP, Fryer A, Webb D: Epidemiology of tuberous sclerosis, Ann N Y Acad Sci 1991, 615:125-127
5. Wiederholt WC, Gomez MR, Kurland LT: Incidence and prevalence of tuberous sclerosis in Rochester, Minnesota, 1950 through 1982, Neurology 1985, 35:600-603
6. Mizuguchi M, Takashima S: Neuropathology of tuberous sclerosis, Brain Dev 2001, 23:508-515
7. DiMario FJ, Jr.: Brain abnormalities in tuberous sclerosis complex, J Child Neurol 2004, 19:650-657
8. Rakowski SK, Winterkorn EB, Paul E, Steele DJ, Halpern EF, Thiele EA: Renal manifestations of tuberous sclerosis complex: Incidence, prognosis, and predictive factors, Kidney Int 2006, 70:1777-1782
9. Hancock E, Osborne J: Lymphangiomyomatosis: a review of the literature, Respir Med 2002, 96:1-6
10. Webb DW, Clarke A, Fryer A, Osborne JP: The cutaneous features of tuberous sclerosis: a population study, Br J Dermatol 1996, 135:1-5

11. Jozwiak S, Kotulska K, Kasprzyk-Obara J, Domanska-Pakiela D, Tomyn-Drabik M, Roberts P, Kwiatkowski D: Clinical and genotype studies of cardiac tumors in 154 patients with tuberous sclerosis complex, *Pediatrics* 2006, 118:e1146-1151
12. Shepherd CW, Gomez MR, Lie JT, Crowson CS: Causes of death in patients with tuberous sclerosis, *Mayo Clin Proc* 1991, 66:792-796
13. Roach ES, Gomez MR, Northrup H: Tuberous sclerosis complex consensus conference: revised clinical diagnostic criteria, *J Child Neurol* 1998, 13:624-628
14. Identification and characterization of the tuberous sclerosis gene on chromosome 16, *Cell* 1993, 75:1305-1315
15. van Slegtenhorst M, de Hoogt R, Hermans C, Nellist M, Janssen B, Verhoef S, Lindhout D, van den Ouweland A, Halley D, Young J, Burley M, Jeremiah S, Woodward K, Nahmias J, Fox M, Ekong R, Osborne J, Wolfe J, Povey S, Snell RG, Cheadle JP, Jones AC, Tachataki M, Ravine D, Sampson JR, Reeve MP, Richardson P, Wilmer F, Munro C, Hawkins TL, Sepp T, Ali JB, Ward S, Green AJ, Yates JR, Kwiatkowska J, Henske EP, Short MP, Haines JH, Jozwiak S, Kwiatkowski DJ: Identification of the tuberous sclerosis gene TSC1 on chromosome 9q34, *Science* 1997, 277:805-808
16. Krymskaya VP: Tumour suppressors hamartin and tuberlin: intracellular signalling, *Cell Signal* 2003, 15:729-739
17. McCall T, Chin SS, Salzman KL, Fults DW: Tuberous sclerosis: a syndrome of incomplete tumor suppression, *Neurosurg Focus* 2006, 20:E3
18. Jones AC, Shyamsundar MM, Thomas MW, Maynard J, Idziaszczyk S, Tomkins S, Sampson JR, Cheadle JP: Comprehensive mutation analysis of TSC1 and TSC2-and

- phenotypic correlations in 150 families with tuberous sclerosis, *Am J Hum Genet* 1999, 64:1305-1315
19. Dabora SL, Jozwiak S, Franz DN, Roberts PS, Nieto A, Chung J, Choy YS, Reeve MP, Thiele E, Egelhoff JC, Kasprzyk-Obara J, Domanska-Pakiela D, Kwiatkowski DJ: Mutational analysis in a cohort of 224 tuberous sclerosis patients indicates increased severity of TSC2, compared with TSC1, disease in multiple organs, *Am J Hum Genet* 2001, 68:64-80
  20. Sancak O, Nellist M, Goedbloed M, Elfferich P, Wouters C, Maat-Kievit A, Zonnenberg B, Verhoef S, Halley D, van den Ouweland A: Mutational analysis of the TSC1 and TSC2 genes in a diagnostic setting: genotype--phenotype correlations and comparison of diagnostic DNA techniques in Tuberous Sclerosis Complex, *Eur J Hum Genet* 2005, 13:731-741
  21. Kwiatkowska J, Jozwiak S, Hall F, Henske EP, Haines JL, McNamara P, Braiser J, Wigowska-Sowinska J, Kasprzyk-Obara J, Short MP, Kwiatkowski DJ: Comprehensive mutational analysis of the TSC1 gene: observations on frequency of mutation, associated features, and nonpenetrance, *Ann Hum Genet* 1998, 62:277-285
  22. Knudson AG, Jr.: Mutation and cancer: statistical study of retinoblastoma, *Proc Natl Acad Sci U S A* 1971, 68:820-823
  23. Carbonara C, Longa L, Grosso E, Borrone C, Garre MG, Brisigotti M, Migone N: 9q34 loss of heterozygosity in a tuberous sclerosis astrocytoma suggests a growth suppressor-like activity also for the TSC1 gene, *Hum Mol Genet* 1994, 3:1829-1832
  24. Green AJ, Smith M, Yates JR: Loss of heterozygosity on chromosome 16p13.3 in hamartomas from tuberous sclerosis patients, *Nat Genet* 1994, 6:193-196

25. Henske EP, Neumann HP, Scheithauer BW, Herbst EW, Short MP, Kwiatkowski DJ: Loss of heterozygosity in the tuberous sclerosis (TSC2) region of chromosome band 16p13 occurs in sporadic as well as TSC-associated renal angiomyolipomas, *Genes Chromosomes Cancer* 1995, 13:295-298
26. Smolarek TA, Wessner LL, McCormack FX, Mylet JC, Menon AG, Henske EP: Evidence that lymphangiomyomatosis is caused by TSC2 mutations: chromosome 16p13 loss of heterozygosity in angiomyolipomas and lymph nodes from women with lymphangiomyomatosis, *Am J Hum Genet* 1998, 62:810-815
27. Plank TL, Logginidou H, Klein-Szanto A, Henske EP: The expression of hamartin, the product of the TSC1 gene, in normal human tissues and in TSC1- and TSC2-linked angiomyolipomas, *Mod Pathol* 1999, 12:539-545
28. Aicher LD, Campbell JS, Yeung RS: Tuberin phosphorylation regulates its interaction with hamartin. Two proteins involved in tuberous sclerosis, *J Biol Chem* 2001, 276:21017-21021
29. Wienecke R, Maize JC, Jr., Shoarinejad F, Vass WC, Reed J, Bonifacino JS, Resau JH, de Gunzburg J, Yeung RS, DeClue JE: Co-localization of the TSC2 product tuberin with its target Rap1 in the Golgi apparatus, *Oncogene* 1996, 13:913-923
30. Lou D, Griffith N, Noonan DJ: The tuberous sclerosis 2 gene product can localize to nuclei in a phosphorylation-dependent manner, *Mol Cell Biol Res Commun* 2001, 4:374-380
31. Astrinidis A, Senapedis W, Henske EP: Hamartin, the tuberous sclerosis complex 1 gene product, interacts with polo-like kinase 1 in a phosphorylation-dependent manner, *Hum Mol Genet* 2006, 15:287-297

32. Tapon N, Ito N, Dickson BJ, Treisman JE, Hariharan IK: The Drosophila tuberous sclerosis complex gene homologs restrict cell growth and cell proliferation, *Cell* 2001, 105:345-355
33. Dan HC, Sun M, Yang L, Feldman RI, Sui XM, Ou CC, Nellist M, Yeung RS, Halley DJ, Nicosia SV, Pledger WJ, Cheng JQ: Phosphatidylinositol 3-kinase/Akt pathway regulates tuberous sclerosis tumor suppressor complex by phosphorylation of tuberin, *J Biol Chem* 2002, 277:35364-35370
34. Manning BD, Tee AR, Logsdon MN, Blenis J, Cantley LC: Identification of the tuberous sclerosis complex-2 tumor suppressor gene product tuberin as a target of the phosphoinositide 3-kinase/akt pathway, *Mol Cell* 2002, 10:151-162
35. Potter CJ, Pedraza LG, Xu T: Akt regulates growth by directly phosphorylating Tsc2, *Nat Cell Biol* 2002, 4:658-665
36. Gao X, Zhang Y, Arrazola P, Hino O, Kobayashi T, Yeung RS, Ru B, Pan D: Tsc tumour suppressor proteins antagonize amino-acid-TOR signalling, *Nat Cell Biol* 2002, 4:699-704
37. Inoki K, Li Y, Zhu T, Wu J, Guan KL: TSC2 is phosphorylated and inhibited by Akt and suppresses mTOR signalling, *Nat Cell Biol* 2002, 4:648-657
38. Hay N, Sonenberg N: Upstream and downstream of mTOR, *Genes Dev* 2004, 18:1926-1945
39. Inoki K, Zhu T, Guan KL: TSC2 mediates cellular energy response to control cell growth and survival, *Cell* 2003, 115:577-590

40. Roux PP, Ballif BA, Anjum R, Gygi SP, Blenis J: Tumor-promoting phorbol esters and activated Ras inactivate the tuberous sclerosis tumor suppressor complex via p90 ribosomal S6 kinase, *Proc Natl Acad Sci U S A* 2004, 101:13489-13494
41. Ma L, Chen Z, Erdjument-Bromage H, Tempst P, Pandolfi PP: Phosphorylation and functional inactivation of TSC2 by Erk implications for tuberous sclerosis and cancer pathogenesis, *Cell* 2005, 121:179-193
42. Miloloza A, Kubista M, Rosner M, Hengstschlager M: Evidence for separable functions of tuberous sclerosis gene products in mammalian cell cycle regulation, *J Neuropathol Exp Neurol* 2002, 61:154-163
43. Kobayashi T, Minowa O, Sugitani Y, Takai S, Mitani H, Kobayashi E, Noda T, Hino O: A germ-line Tsc1 mutation causes tumor development and embryonic lethality that are similar, but not identical to, those caused by Tsc2 mutation in mice, *Proc Natl Acad Sci U S A* 2001, 98:8762-8767
44. Yeung RS: Multiple roles of the tuberous sclerosis complex genes, *Genes Chromosomes Cancer* 2003, 38:368-375
45. Brown EJ, Albers MW, Shin TB, Ichikawa K, Keith CT, Lane WS, Schreiber SL: A mammalian protein targeted by G1-arresting rapamycin-receptor complex, *Nature* 1994, 369:756-758
46. Ma XM, Blenis J: Molecular mechanisms of mTOR-mediated translational control, *Nat Rev Mol Cell Biol* 2009, 10:307-318
47. Loewith R, Jacinto E, Wullschleger S, Lorberg A, Crespo JL, Bonenfant D, Oppliger W, Jenoe P, Hall MN: Two TOR complexes, only one of which is rapamycin sensitive, have distinct roles in cell growth control, *Mol Cell* 2002, 10:457-468

48. Pause A, Methot N, Svitkin Y, Merrick WC, Sonenberg N: Dominant negative mutants of mammalian translation initiation factor eIF-4A define a critical role for eIF-4F in cap-dependent and cap-independent initiation of translation, *EMBO J* 1994, 13:1205-1215
49. Fingar DC, Blenis J: Target of rapamycin (TOR): an integrator of nutrient and growth factor signals and coordinator of cell growth and cell cycle progression, *Oncogene* 2004, 23:3151-3171
50. Wullschleger S, Loewith R, Hall MN: TOR signaling in growth and metabolism, *Cell* 2006, 124:471-484
51. Guertin DA, Sabatini DM: Defining the role of mTOR in cancer, *Cancer Cell* 2007, 12:9-22
52. Kim DH, Sarbassov DD, Ali SM, King JE, Latek RR, Erdjument-Bromage H, Tempst P, Sabatini DM: mTOR interacts with raptor to form a nutrient-sensitive complex that signals to the cell growth machinery, *Cell* 2002, 110:163-175
53. Saucedo LJ, Gao X, Chiarelli DA, Li L, Pan D, Edgar BA: Rheb promotes cell growth as a component of the insulin/TOR signalling network, *Nat Cell Biol* 2003, 5:566-571
54. Stocker H, Radimerski T, Schindelholtz B, Wittwer F, Belawat P, Daram P, Breuer S, Thomas G, Hafen E: Rheb is an essential regulator of S6K in controlling cell growth in *Drosophila*, *Nat Cell Biol* 2003, 5:559-565
55. Zhang Y, Gao X, Saucedo LJ, Ru B, Edgar BA, Pan D: Rheb is a direct target of the tuberous sclerosis tumour suppressor proteins, *Nat Cell Biol* 2003, 5:578-581



56. Manning BD, Cantley LC: Rheb fills a GAP between TSC and TOR, Trends Biochem Sci 2003, 28:573-576
57. Tee AR, Blenis J, Proud CG: Analysis of mTOR signaling by the small G-proteins, Rheb and RhebL1, FEBS Lett 2005, 579:4763-4768
58. Sarbassov DD, Ali SM, Kim DH, Guertin DA, Latek RR, Erdjument-Bromage H, Tempst P, Sabatini DM: Rictor, a novel binding partner of mTOR, defines a rapamycin-insensitive and raptor-independent pathway that regulates the cytoskeleton, Curr Biol 2004, 14:1296-1302
59. Sarbassov DD, Guertin DA, Ali SM, Sabatini DM: Phosphorylation and regulation of Akt/PKB by the rictor-mTOR complex, Science 2005, 307:1098-1101
60. Huang J, Dibble CC, Matsuzaki M, Manning BD: The TSC1-TSC2 complex is required for proper activation of mTOR complex 2, Mol Cell Biol 2008, 28:4104-4115
61. Singh K, Sun S, Vezina C: Rapamycin (AY-22,989), a new antifungal antibiotic. IV. Mechanism of action, J Antibiot (Tokyo) 1979, 32:630-645
62. Jozwiak J, Jozwiak S, Oldak M: Molecular activity of sirolimus and its possible application in tuberous sclerosis treatment, Med Res Rev 2006, 26:160-180
63. Kunz J, Hall MN: Cyclosporin A, FK506 and rapamycin: more than just immunosuppression, Trends Biochem Sci 1993, 18:334-338
64. Chen J, Zheng XF, Brown EJ, Schreiber SL: Identification of an 11-kDa FKBP12-rapamycin-binding domain within the 289-kDa FKBP12-rapamycin-associated protein and characterization of a critical serine residue, Proc Natl Acad Sci U S A 1995, 92:4947-4951

65. Koltin Y, Faucette L, Bergsma DJ, Levy MA, Cafferkey R, Koser PL, Johnson RK, Livi GP: Rapamycin sensitivity in *Saccharomyces cerevisiae* is mediated by a peptidyl-prolyl cis-trans isomerase related to human FK506-binding protein, *Mol Cell Biol* 1991, 11:1718-1723
66. Oshiro N, Yoshino K, Hidayat S, Tokunaga C, Hara K, Eguchi S, Avruch J, Yonezawa K: Dissociation of raptor from mTOR is a mechanism of rapamycin-induced inhibition of mTOR function, *Genes Cells* 2004, 9:359-366
67. Li S, Thangapazham RL, Wang JA, Rajesh S, Kao TC, Sperling L, Moss J, Darling TN: Human TSC2-null fibroblast-like cells induce hair follicle neogenesis and hamartoma morphogenesis, *Nat Commun* 2011, 2:235
68. Guertin DA, Sabatini DM: An expanding role for mTOR in cancer, *Trends Mol Med* 2005, 11:353-361
69. Humar R, Kiefer FN, Berns H, Resink TJ, Battegay EJ: Hypoxia enhances vascular cell proliferation and angiogenesis in vitro via rapamycin (mTOR)-dependent signaling, *FASEB J* 2002, 16:771-780
70. Ballou LM, Lin RZ: Rapamycin and mTOR kinase inhibitors, *J Chem Biol* 2008, 1:27-36
71. Moses JW, Leon MB, Popma JJ, Fitzgerald PJ, Holmes DR, O'Shaughnessy C, Caputo RP, Kereiakes DJ, Williams DO, Teirstein PS, Jaeger JL, Kuntz RE: Sirolimus-eluting stents versus standard stents in patients with stenosis in a native coronary artery, *N Engl J Med* 2003, 349:1315-1323
72. Lee L, Sudentas P, Donohue B, Asrican K, Worku A, Walker V, Sun Y, Schmidt K, Albert MS, El-Hashemite N, Lader AS, Onda H, Zhang H, Kwiatkowski DJ, Dabora

SL: Efficacy of a rapamycin analog (CCI-779) and IFN-gamma in tuberous sclerosis mouse models, *Genes Chromosomes Cancer* 2005, 42:213-227

73. Kenerson H, Dundon TA, Yeung RS: Effects of rapamycin in the Eker rat model of tuberous sclerosis complex, *Pediatr Res* 2005, 57:67-75

74. Kenerson HL, Aicher LD, True LD, Yeung RS: Activated mammalian target of rapamycin pathway in the pathogenesis of tuberous sclerosis complex renal tumors, *Cancer Res* 2002, 62:5645-5650

75. Franz DN, Leonard J, Tudor C, Chuck G, Care M, Sethuraman G, Dinopoulos A, Thomas G, Crone KR: Rapamycin causes regression of astrocytomas in tuberous sclerosis complex, *Ann Neurol* 2006, 59:490-498

76. Herry I, Neukirch C, Debray MP, Mignon F, Crestani B: Dramatic effect of sirolimus on renal angiomyolipomas in a patient with tuberous sclerosis complex, *Eur J Intern Med* 2007, 18:76-77

77. Wienecke R, Fackler I, Linsenmaier U, Mayer K, Licht T, Kretzler M: Antitumoral activity of rapamycin in renal angiomyolipoma associated with tuberous sclerosis complex, *Am J Kidney Dis* 2006, 48:e27-29

78. Hofbauer GF, Marcollo-Pini A, Corsenca A, Kistler AD, French LE, Wuthrich RP, Serra AL: The mTOR inhibitor rapamycin significantly improves facial angiofibroma lesions in a patient with tuberous sclerosis, *Br J Dermatol* 2008, 159:473-475

79. McCormack FX, Inoue Y, Moss J, Singer LG, Strange C, Nakata K, Barker AF, Chapman JT, Brantly ML, Stocks JM, Brown KK, Lynch JP, 3rd, Goldberg HJ, Young LR, Kinder BW, Downey GP, Sullivan EJ, Colby TV, McKay RT, Cohen MM, Korbee

- L, Taveira-DaSilva AM, Lee HS, Krischer JP, Trapnell BC: Efficacy and safety of sirolimus in lymphangioleiomyomatosis, *N Engl J Med* 2011, 364:1595-1606
80. Wee SA, Fangman B: Tuberous sclerosis, *Dermatol Online J* 2007, 13:22
81. Darling TN: Hamartomas and tubers from defects in hamartin-tuberin, *J Am Acad Dermatol* 2004, 51:S9-11
82. Jozwiak S, Schwartz RA, Janniger CK, Michalowicz R, Chmielik J: Skin lesions in children with tuberous sclerosis complex: their prevalence, natural course, and diagnostic significance, *Int J Dermatol* 1998, 37:911-917
83. Jimbow K: Tuberous sclerosis and guttate leukodermas, *Semin Cutan Med Surg* 1997, 16:30-35
84. Kobayasi T, Wolf-Jurgensen P, Danielsen L: Ultrastructure of shagreen patch, *Acta Derm Venereol* 1973, 53:275-278
85. Nickel WR, Reed WB: Tuberous sclerosis. Special reference to the microscopic alterations in the cutaneous hamartomas, *Arch Dermatol* 1962, 85:209-226
86. Sanchez NP, Wick MR, Perry HO: Adenoma sebaceum of Pringle: a clinicopathologic review, with a discussion of related pathologic entities, *J Cutan Pathol* 1981, 8:395-403
87. Reed RJ, Ackerman AB: Pathology of the adventitial dermis. Anatomic observations and biologic speculations, *Hum Pathol* 1973, 4:207-217
88. Schwartz RA, Fernandez G, Kotulska K, Jozwiak S: Tuberous sclerosis complex: advances in diagnosis, genetics, and management, *J Am Acad Dermatol* 2007, 57:189-202

89. Kint A, Baran R: Histopathologic study of Koenen tumors. Are they different from acquired digital fibrokeratoma?, *J Am Acad Dermatol* 1988, 18:369-372
90. Papadavid E, Markey A, Bellaney G, Walker NP: Carbon dioxide and pulsed dye laser treatment of angiofibromas in 29 patients with tuberous sclerosis, *Br J Dermatol* 2002, 147:337-342
91. Carmeliet P: Angiogenesis in health and disease, *Nat Med* 2003, 9:653-660
92. Folkman J: Tumor angiogenesis: therapeutic implications, *N Engl J Med* 1971, 285:1182-1186
93. Breier G, Risau W: The role of vascular endothelial growth factor in blood vessel formation, *Trends Cell Biol* 1996, 6:454-456
94. Tischer E, Mitchell R, Hartman T, Silva M, Gospodarowicz D, Fiddes JC, Abraham JA: The human gene for vascular endothelial growth factor. Multiple protein forms are encoded through alternative exon splicing, *J Biol Chem* 1991, 266:11947-11954
95. Hicklin DJ, Ellis LM: Role of the vascular endothelial growth factor pathway in tumor growth and angiogenesis, *J Clin Oncol* 2005, 23:1011-1027
96. Rini BI, Small EJ: Biology and clinical development of vascular endothelial growth factor-targeted therapy in renal cell carcinoma, *J Clin Oncol* 2005, 23:1028-1043
97. Ferrara N: Vascular endothelial growth factor: basic science and clinical progress, *Endocr Rev* 2004, 25:581-611
98. Carmeliet P, Ferreira V, Breier G, Pollefeyt S, Kieckens L, Gertsenstein M, Fahrig M, Vandenhoek A, Harpal K, Eberhardt C, Declercq C, Pawling J, Moons L,

- Collen D, Risau W, Nagy A: Abnormal blood vessel development and lethality in embryos lacking a single VEGF allele, *Nature* 1996, 380:435-439
99. Ferrara N: Vascular endothelial growth factor, *Eur J Cancer* 1996, 32A:2413-2422
100. Flamme I, von Reutern M, Drexler HC, Syed-Ali S, Risau W: Overexpression of vascular endothelial growth factor in the avian embryo induces hypervascularization and increased vascular permeability without alterations of embryonic pattern formation, *Dev Biol* 1995, 171:399-414
101. Plate KH, Breier G, Weich HA, Mennel HD, Risau W: Vascular endothelial growth factor and glioma angiogenesis: coordinate induction of VEGF receptors, distribution of VEGF protein and possible in vivo regulatory mechanisms, *Int J Cancer* 1994, 59:520-529
102. Dvorak HF: Vascular permeability factor/vascular endothelial growth factor: a critical cytokine in tumor angiogenesis and a potential target for diagnosis and therapy, *J Clin Oncol* 2002, 20:4368-4380
103. Kim KJ, Li B, Winer J, Armanini M, Gillett N, Phillips HS, Ferrara N: Inhibition of vascular endothelial growth factor-induced angiogenesis suppresses tumour growth in vivo, *Nature* 1993, 362:841-844
104. Millauer B, Shawver LK, Plate KH, Risau W, Ullrich A: Glioblastoma growth inhibited in vivo by a dominant-negative Flk-1 mutant, *Nature* 1994, 367:576-579
105. Arbiser JL, Brat D, Hunter S, D'Armiento J, Henske EP, Arbiser ZK, Bai X, Goldberg G, Cohen C, Weiss SW: Tuberous sclerosis-associated lesions of the kidney, brain, and skin are angiogenic neoplasms, *J Am Acad Dermatol* 2002, 46:376-380

106. Nguyen-Vu PA, Fackler I, Rust A, DeClue JE, Sander CA, Volkenandt M, Flaig M, Yeung RS, Wienecke R: Loss of tuberlin, the tuberous-sclerosis-complex-2 gene product is associated with angiogenesis, *J Cutan Pathol* 2001, 28:470-475
107. Wang GL, Jiang BH, Rue EA, Semenza GL: Hypoxia-inducible factor 1 is a basic-helix-loop-helix-PAS heterodimer regulated by cellular O<sub>2</sub> tension, *Proc Natl Acad Sci U S A* 1995, 92:5510-5514
108. Yang J, Zhang L, Erbel PJ, Gardner KH, Ding K, Garcia JA, Bruick RK: Functions of the Per/ARNT/Sim domains of the hypoxia-inducible factor, *J Biol Chem* 2005, 280:36047-36054
109. Huang LE, Gu J, Schau M, Bunn HF: Regulation of hypoxia-inducible factor 1 $\alpha$  is mediated by an O<sub>2</sub>-dependent degradation domain via the ubiquitin-proteasome pathway, *Proc Natl Acad Sci U S A* 1998, 95:7987-7992
110. Jewell UR, Gassmann M: Mammalian gene expression in hypoxic conditions, *Zoology (Jena)* 2001, 104:192-197
111. Bruick RK: Oxygen sensing in the hypoxic response pathway: regulation of the hypoxia-inducible transcription factor, *Genes Dev* 2003, 17:2614-2623
112. Maltepe E, Schmidt JV, Baunoch D, Bradfield CA, Simon MC: Abnormal angiogenesis and responses to glucose and oxygen deprivation in mice lacking the protein ARNT, *Nature* 1997, 386:403-407
113. Maltepe E, Simon MC: Oxygen, genes, and development: an analysis of the role of hypoxic gene regulation during murine vascular development, *J Mol Med (Berl)* 1998, 76:391-401

114. Semenza GL: Regulation of mammalian O<sub>2</sub> homeostasis by hypoxia-inducible factor 1, *Annu Rev Cell Dev Biol* 1999, 15:551-578
115. Semenza GL: Expression of hypoxia-inducible factor 1: mechanisms and consequences, *Biochem Pharmacol* 2000, 59:47-53
116. Semenza GL: Targeting HIF-1 for cancer therapy, *Nat Rev Cancer* 2003, 3:721-732
117. Sakuda H, Nakashima Y, Kuriyama S, Sueishi K: Media conditioned by smooth muscle cells cultured in a variety of hypoxic environments stimulates in vitro angiogenesis. A relationship to transforming growth factor-beta 1, *Am J Pathol* 1992, 141:1507-1516
118. Phillips PG, Birnby LM, Narendran A: Hypoxia induces capillary network formation in cultured bovine pulmonary microvessel endothelial cells, *Am J Physiol* 1995, 268:L789-800
119. Liu Y, Cox SR, Morita T, Kourembanas S: Hypoxia regulates vascular endothelial growth factor gene expression in endothelial cells. Identification of a 5' enhancer, *Circ Res* 1995, 77:638-643
120. Forsythe JA, Jiang BH, Iyer NV, Agani F, Leung SW, Koos RD, Semenza GL: Activation of vascular endothelial growth factor gene transcription by hypoxia-inducible factor 1, *Mol Cell Biol* 1996, 16:4604-4613
121. Zagzag D, Zhong H, Scalzitti JM, Laughner E, Simons JW, Semenza GL: Expression of hypoxia-inducible factor 1alpha in brain tumors: association with angiogenesis, invasion, and progression, *Cancer* 2000, 88:2606-2618



122. Iyer NV, Kotch LE, Agani F, Leung SW, Laughner E, Wenger RH, Gassmann M, Gearhart JD, Lawler AM, Yu AY, Semenza GL: Cellular and developmental control of O<sub>2</sub> homeostasis by hypoxia-inducible factor 1 alpha, *Genes Dev* 1998, 12:149-162
123. Maxwell PH, Dachs GU, Gleadle JM, Nicholls LG, Harris AL, Stratford IJ, Hankinson O, Pugh CW, Ratcliffe PJ: Hypoxia-inducible factor-1 modulates gene expression in solid tumors and influences both angiogenesis and tumor growth, *Proc Natl Acad Sci U S A* 1997, 94:8104-8109
124. Sabin FR: The Method of Growth of the Lymphatic System, *Science* 1916, 44:145-158
125. Huntington G MC: The anatomy and development of the jugular lymph sac in the domestic cat (*Felis domestica*), *American Journal of Anatomy* 1910, 10:177-311
126. Witte MH, Bernas MJ, Martin CP, Witte CL: Lymphangiogenesis and lymphangiodysplasia: from molecular to clinical lymphology, *Microsc Res Tech* 2001, 55:122-145
127. Leak LV, Burke JF: Electron microscopic study of lymphatic capillaries in the removal of connective tissue fluids and particulate substances, *Lymphology* 1968, 1:39-52
128. Casley-Smith JR, Florey HW: The structure of normal small lymphatics, *Q J Exp Physiol Cogn Med Sci* 1961, 46:101-106
129. Leak LV: Electron microscopic observations on lymphatic capillaries and the structural components of the connective tissue-lymph interface, *Microvasc Res* 1970, 2:361-391

130. Karpanen T, Alitalo K: Molecular biology and pathology of lymphangiogenesis, *Annu Rev Pathol* 2008, 3:367-397
131. Schoppmann SF: Lymphangiogenesis, inflammation and metastasis, *Anticancer Res* 2005, 25:4503-4511
132. Karpanen T, Makinen T: Regulation of lymphangiogenesis--from cell fate determination to vessel remodeling, *Exp Cell Res* 2006, 312:575-583
133. Oliver G: Lymphatic vasculature development, *Nat Rev Immunol* 2004, 4:35-45
134. Petrova TV, Makinen T, Makela TP, Saarela J, Virtanen I, Ferrell RE, Finegold DN, Kerjaschki D, Yla-Herttuala S, Alitalo K: Lymphatic endothelial reprogramming of vascular endothelial cells by the Prox-1 homeobox transcription factor, *EMBO J* 2002, 21:4593-4599
135. Jurisic G, Detmar M: Lymphatic endothelium in health and disease, *Cell Tissue Res* 2009, 335:97-108
136. Wigle JT, Harvey N, Detmar M, Lagutina I, Grosveld G, Gunn MD, Jackson DG, Oliver G: An essential role for Prox1 in the induction of the lymphatic endothelial cell phenotype, *EMBO J* 2002, 21:1505-1513
137. Jackson DG, Prevo R, Clasper S, Banerji S: LYVE-1, the lymphatic system and tumor lymphangiogenesis, *Trends Immunol* 2001, 22:317-321
138. Luong MX, Tam J, Lin Q, Hagendoorn J, Moore KJ, Padera TP, Seed B, Fukumura D, Kuchelapati R, Jain RK: Lack of lymphatic vessel phenotype in LYVE-1/CD44 double knockout mice, *J Cell Physiol* 2009, 219:430-437
139. Breiteneder-Geleff S, Matsui K, Soleiman A, Meraner P, Poczewski H, Kalt R, Schaffner G, Kerjaschki D: Podoplanin, novel 43-kd membrane protein of glomerular

epithelial cells, is down-regulated in puromycin nephrosis, *Am J Pathol* 1997, 151:1141-1152

140. Schacht V, Ramirez MI, Hong YK, Hirakawa S, Feng D, Harvey N, Williams M, Dvorak AM, Dvorak HF, Oliver G, Detmar M: T1alpha/podoplanin deficiency disrupts normal lymphatic vasculature formation and causes lymphedema, *EMBO J* 2003, 22:3546-3556

141. Dumont DJ, Jussila L, Taipale J, Lymboussaki A, Mustonen T, Pajusola K, Breitman M, Alitalo K: Cardiovascular failure in mouse embryos deficient in VEGF receptor-3, *Science* 1998, 282:946-949

142. Tammela T, Enholm B, Alitalo K, Paavonen K: The biology of vascular endothelial growth factors, *Cardiovasc Res* 2005, 65:550-563

143. Kreuger J, Nilsson I, Kerjaschki D, Petrova T, Alitalo K, Claesson-Welsh L: Early lymph vessel development from embryonic stem cells, *Arterioscler Thromb Vasc Biol* 2006, 26:1073-1078

144. Makinen T, Veikkola T, Mustjoki S, Karpanen T, Catimel B, Nice EC, Wise L, Mercer A, Kowalski H, Kerjaschki D, Stacker SA, Achen MG, Alitalo K: Isolated lymphatic endothelial cells transduce growth, survival and migratory signals via the VEGF-C/D receptor VEGFR-3, *EMBO J* 2001, 20:4762-4773

145. Veikkola T, Jussila L, Makinen T, Karpanen T, Jeltsch M, Petrova TV, Kubo H, Thurston G, McDonald DM, Achen MG, Stacker SA, Alitalo K: Signalling via vascular endothelial growth factor receptor-3 is sufficient for lymphangiogenesis in transgenic mice, *EMBO J* 2001, 20:1223-1231

146. Lee J, Gray A, Yuan J, Luoh SM, Avraham H, Wood WI: Vascular endothelial growth factor-related protein: a ligand and specific activator of the tyrosine kinase receptor Flt4, *Proc Natl Acad Sci U S A* 1996, 93:1988-1992
147. Joukov V, Sorsa T, Kumar V, Jeltsch M, Claesson-Welsh L, Cao Y, Saksela O, Kalkkinen N, Alitalo K: Proteolytic processing regulates receptor specificity and activity of VEGF-C, *EMBO J* 1997, 16:3898-3911
148. McColl BK, Baldwin ME, Roufail S, Freeman C, Moritz RL, Simpson RJ, Alitalo K, Stacker SA, Achen MG: Plasmin activates the lymphangiogenic growth factors VEGF-C and VEGF-D, *J Exp Med* 2003, 198:863-868
149. Cao Y, Linden P, Farnebo J, Cao R, Eriksson A, Kumar V, Qi JH, Claesson-Welsh L, Alitalo K: Vascular endothelial growth factor C induces angiogenesis in vivo, *Proc Natl Acad Sci U S A* 1998, 95:14389-14394
150. Karkkainen MJ, Haiko P, Sainio K, Partanen J, Taipale J, Petrova TV, Jeltsch M, Jackson DG, Talikka M, Rauvala H, Betsholtz C, Alitalo K: Vascular endothelial growth factor C is required for sprouting of the first lymphatic vessels from embryonic veins, *Nat Immunol* 2004, 5:74-80
151. Kuchler AM, Gjini E, Peterson-Maduro J, Cancilla B, Wolburg H, Schulte-Merker S: Development of the zebrafish lymphatic system requires VEGFC signaling, *Curr Biol* 2006, 16:1244-1248
152. Baldwin ME, Halford MM, Roufail S, Williams RA, Hibbs ML, Grail D, Kubo H, Stacker SA, Achen MG: Vascular endothelial growth factor D is dispensable for development of the lymphatic system, *Mol Cell Biol* 2005, 25:2441-2449

153. Skobe M, Hamberg LM, Hawighorst T, Schirner M, Wolf GL, Alitalo K, Detmar M: Concurrent induction of lymphangiogenesis, angiogenesis, and macrophage recruitment by vascular endothelial growth factor-C in melanoma, *Am J Pathol* 2001, 159:893-903
154. Stacker SA, Caesar C, Baldwin ME, Thornton GE, Williams RA, Prevo R, Jackson DG, Nishikawa S, Kubo H, Achen MG: VEGF-D promotes the metastatic spread of tumor cells via the lymphatics, *Nat Med* 2001, 7:186-191
155. Nagy JA, Vasile E, Feng D, Sundberg C, Brown LF, Detmar MJ, Lawitts JA, Benjamin L, Tan X, Manseau EJ, Dvorak AM, Dvorak HF: Vascular permeability factor/vascular endothelial growth factor induces lymphangiogenesis as well as angiogenesis, *J Exp Med* 2002, 196:1497-1506
156. Hirakawa S, Kodama S, Kunstfeld R, Kajiya K, Brown LF, Detmar M: VEGF-A induces tumor and sentinel lymph node lymphangiogenesis and promotes lymphatic metastasis, *J Exp Med* 2005, 201:1089-1099
157. Nakamura T, Nishizawa T, Hagiya M, Seki T, Shimonishi M, Sugimura A, Tashiro K, Shimizu S: Molecular cloning and expression of human hepatocyte growth factor, *Nature* 1989, 342:440-443
158. Russell WE, McGowan JA, Bucher NL: Partial characterization of a hepatocyte growth factor from rat platelets, *J Cell Physiol* 1984, 119:183-192
159. Montesano R, Matsumoto K, Nakamura T, Orci L: Identification of a fibroblast-derived epithelial morphogen as hepatocyte growth factor, *Cell* 1991, 67:901-908
160. Gao CF, Vande Woude GF: HGF/SF-Met signaling in tumor progression, *Cell Res* 2005, 15:49-51

161. Naka D, Ishii T, Yoshiyama Y, Miyazawa K, Hara H, Hishida T, Kidamura N: Activation of hepatocyte growth factor by proteolytic conversion of a single chain form to a heterodimer, *J Biol Chem* 1992, 267:20114-20119
162. Naldini L, Tamagnone L, Vigna E, Sachs M, Hartmann G, Birchmeier W, Daikuhara Y, Tsubouchi H, Blasi F, Comoglio PM: Extracellular proteolytic cleavage by urokinase is required for activation of hepatocyte growth factor/scatter factor, *EMBO J* 1992, 11:4825-4833
163. Bottaro DP, Rubin JS, Faletto DL, Chan AM, Kmieciak TE, Vande Woude GF, Aaronson SA: Identification of the hepatocyte growth factor receptor as the c-met proto-oncogene product, *Science* 1991, 251:802-804
164. Stella MC, Comoglio PM: HGF: a multifunctional growth factor controlling cell scattering, *Int J Biochem Cell Biol* 1999, 31:1357-1362
165. Zhang YW, Su Y, Volpert OV, Vande Woude GF: Hepatocyte growth factor/scatter factor mediates angiogenesis through positive VEGF and negative thrombospondin 1 regulation, *Proc Natl Acad Sci U S A* 2003, 100:12718-12723
166. Yamashita J, Ogawa M, Yamashita S, Nomura K, Kuramoto M, Saishoji T, Shin S: Immunoreactive hepatocyte growth factor is a strong and independent predictor of recurrence and survival in human breast cancer, *Cancer Res* 1994, 54:1630-1633
167. Humphrey PA, Zhu X, Zarnegar R, Swanson PE, Ratliff TL, Vollmer RT, Day ML: Hepatocyte growth factor and its receptor (c-MET) in prostatic carcinoma, *Am J Pathol* 1995, 147:386-396
168. Parr C, Watkins G, Mansel RE, Jiang WG: The hepatocyte growth factor regulatory factors in human breast cancer, *Clin Cancer Res* 2004, 10:202-211

169. Kajiya K, Hirakawa S, Ma B, Drinnenberg I, Detmar M: Hepatocyte growth factor promotes lymphatic vessel formation and function, *EMBO J* 2005, 24:2885-2895
170. Kunstfeld R, Hirakawa S, Hong YK, Schacht V, Lange-Asschenfeldt B, Velasco P, Lin C, Fiebiger E, Wei X, Wu Y, Hicklin D, Bohlen P, Detmar M: Induction of cutaneous delayed-type hypersensitivity reactions in VEGF-A transgenic mice results in chronic skin inflammation associated with persistent lymphatic hyperplasia, *Blood* 2004, 104:1048-1057
171. Javerzat S, Auguste P, Bikfalvi A: The role of fibroblast growth factors in vascular development, *Trends Mol Med* 2002, 8:483-489
172. Matsuo M, Yamada S, Koizumi K, Sakurai H, Saiki I: Tumour-derived fibroblast growth factor-2 exerts lymphangiogenic effects through Akt/mTOR/p70S6kinase pathway in rat lymphatic endothelial cells, *Eur J Cancer* 2007, 43:1748-1754
173. Cao R, Brakenhielm E, Pawliuk R, Wariaro D, Post MJ, Wahlberg E, Leboulch P, Cao Y: Angiogenic synergism, vascular stability and improvement of hind-limb ischemia by a combination of PDGF-BB and FGF-2, *Nat Med* 2003, 9:604-613
174. Anan K, Morisaki T, Katano M, Ikubo A, Kitsuki H, Uchiyama A, Kuroki S, Tanaka M, Torisu M: Vascular endothelial growth factor and platelet-derived growth factor are potential angiogenic and metastatic factors in human breast cancer, *Surgery* 1996, 119:333-339
175. Travers MT, Barrett-Lee PJ, Berger U, Luqmani YA, Gazet JC, Powles TJ, Coombes RC: Growth factor expression in normal, benign, and malignant breast tissue, *Br Med J (Clin Res Ed)* 1988, 296:1621-1624

176. Boes M, Dake BL, Bar RS: Interactions of cultured endothelial cells with TGF-beta, bFGF, PDGF and IGF-I, *Life Sci* 1991, 48:811-821
177. Reinmuth N, Fan F, Liu W, Parikh AA, Stoeltzing O, Jung YD, Bucana CD, Radinsky R, Gallick GE, Ellis LM: Impact of insulin-like growth factor receptor-I function on angiogenesis, growth, and metastasis of colon cancer, *Lab Invest* 2002, 82:1377-1389
178. Akagi Y, Liu W, Zebrowski B, Xie K, Ellis LM: Regulation of vascular endothelial growth factor expression in human colon cancer by insulin-like growth factor-I, *Cancer Res* 1998, 58:4008-4014
179. Bjorndahl M, Cao R, Nissen LJ, Clasper S, Johnson LA, Xue Y, Zhou Z, Jackson D, Hansen AJ, Cao Y: Insulin-like growth factors 1 and 2 induce lymphangiogenesis in vivo, *Proc Natl Acad Sci U S A* 2005, 102:15593-15598
180. Glasgow CG, Taveira-Dasilva AM, Darling TN, Moss J: Lymphatic involvement in lymphangioleiomyomatosis, *Ann N Y Acad Sci* 2008, 1131:206-214
181. Kumasaka T, Seyama K, Mitani K, Sato T, Souma S, Kondo T, Hayashi S, Minami M, Uekusa T, Fukuchi Y, Suda K: Lymphangiogenesis in lymphangioleiomyomatosis: its implication in the progression of lymphangioleiomyomatosis, *Am J Surg Pathol* 2004, 28:1007-1016
182. Young LR, Inoue Y, McCormack FX: Diagnostic potential of serum VEGF-D for lymphangioleiomyomatosis, *N Engl J Med* 2008, 358:199-200
183. Glasgow CG, Avila NA, Lin JP, Stylianou MP, Moss J: Serum vascular endothelial growth factor-D levels in patients with lymphangioleiomyomatosis reflect lymphatic involvement, *Chest* 2009, 135:1293-1300



184. Glasgow CG, Taveira-DaSilva A, Pacheco-Rodriguez G, Steagall WK, Tsukada K, Cai X, El-Chemaly S, Moss J: Involvement of lymphatics in lymphangioleiomyomatosis, *Lymphat Res Biol* 2009, 7:221-228
185. Crooks DM, Pacheco-Rodriguez G, DeCastro RM, McCoy JP, Jr., Wang JA, Kumaki F, Darling T, Moss J: Molecular and genetic analysis of disseminated neoplastic cells in lymphangioleiomyomatosis, *Proc Natl Acad Sci U S A* 2004, 101:17462-17467
186. Li S, Takeuchi F, Wang JA, Fuller C, Pacheco-Rodriguez G, Moss J, Darling TN: MCP-1 overexpressed in tuberous sclerosis lesions acts as a paracrine factor for tumor development, *J Exp Med* 2005, 202:617-624
187. Li S, Takeuchi F, Wang JA, Fan Q, Komurasaki T, Billings EM, Pacheco-Rodriguez G, Moss J, Darling TN: Mesenchymal-epithelial interactions involving epiregulin in tuberous sclerosis complex hamartomas, *Proc Natl Acad Sci U S A* 2008, 105:3539-3544
188. Kobayashi S, Kishimoto T, Kamata S, Otsuka M, Miyazaki M, Ishikura H: Rapamycin, a specific inhibitor of the mammalian target of rapamycin, suppresses lymphangiogenesis and lymphatic metastasis, *Cancer Sci* 2007, 98:726-733
189. El-Hashemite N, Walker V, Zhang H, Kwiatkowski DJ: Loss of Tsc1 or Tsc2 induces vascular endothelial growth factor production through mammalian target of rapamycin, *Cancer Res* 2003, 63:5173-5177
190. Wang D, Stockard CR, Harkins L, Lott P, Salih C, Yuan K, Buchsbaum D, Hashim A, Zayzafoon M, Hardy RW, Hameed O, Grizzle W, Siegal GP: Immunohistochemistry in the evaluation of neovascularization in tumor xenografts, *Biotech Histochem* 2008, 83:179-189

191. Dadras SS, Paul T, Bertoncini J, Brown LF, Muzikansky A, Jackson DG, Ellwanger U, Garbe C, Mihm MC, Detmar M: Tumor lymphangiogenesis: a novel prognostic indicator for cutaneous melanoma metastasis and survival, *Am J Pathol* 2003, 162:1951-1960
192. Shields JD, Borsetti M, Rigby H, Harper SJ, Mortimer PS, Levick JR, Orlando A, Bates DO: Lymphatic density and metastatic spread in human malignant melanoma, *Br J Cancer* 2004, 90:693-700
193. Giorgadze TA, Zhang PJ, Pasha T, Coogan PS, Acs G, Elder DE, Xu X: Lymphatic vessel density is significantly increased in melanoma, *J Cutan Pathol* 2004, 31:672-677
194. Moussai D, Mitsui H, Pettersen JS, Pierson KC, Shah KR, Suarez-Farinas M, Cardinale IR, Bluth MJ, Krueger JG, Carucci JA: The human cutaneous squamous cell carcinoma microenvironment is characterized by increased lymphatic density and enhanced expression of macrophage-derived VEGF-C, *J Invest Dermatol* 2011, 131:229-236
195. Karbowniczek M, Yu J, Henske EP: Renal angiomyolipomas from patients with sporadic lymphangiomyomatosis contain both neoplastic and non-neoplastic vascular structures, *Am J Pathol* 2003, 162:491-500
196. Kwiatkowski DJ: Animal models of lymphangiomyomatosis (LAM) and tuberous sclerosis complex (TSC), *Lymphat Res Biol* 2010, 8:51-57
197. Hlatky L, Hahnfeldt P, Folkman J: Clinical application of antiangiogenic therapy: microvessel density, what it does and doesn't tell us, *J Natl Cancer Inst* 2002, 94:883-893

198. Kumasaka T, Seyama K, Mitani K, Souma S, Kashiwagi S, Hebisawa A, Sato T, Kubo H, Gomi K, Shibuya K, Fukuchi Y, Suda K: Lymphangiogenesis-mediated shedding of LAM cell clusters as a mechanism for dissemination in lymphangioliomyomatosis, *Am J Surg Pathol* 2005, 29:1356-1366
199. Maldonado M, Baybis M, Newman D, Kolson DL, Chen W, McKhann G, 2nd, Gutmann DH, Crino PB: Expression of ICAM-1, TNF-alpha, NF kappa B, and MAP kinase in tubers of the tuberous sclerosis complex, *Neurobiol Dis* 2003, 14:279-290
200. Kitadai Y: Angiogenesis and lymphangiogenesis of gastric cancer, *J Oncol* 2010, 2010:468725
201. Schoppmann SF, Birner P, Stockl J, Kalt R, Ullrich R, Caucig C, Kriehuber E, Nagy K, Alitalo K, Kerjaschki D: Tumor-associated macrophages express lymphatic endothelial growth factors and are related to peritumoral lymphangiogenesis, *Am J Pathol* 2002, 161:947-956
202. Wang R, Zhang J, Chen S, Lu M, Luo X, Yao S, Liu S, Qin Y, Chen H: Tumor-associated macrophages provide a suitable microenvironment for non-small lung cancer invasion and progression, *Lung Cancer* 2011,
203. Salcedo R, Ponce ML, Young HA, Wasserman K, Ward JM, Kleinman HK, Oppenheim JJ, Murphy WJ: Human endothelial cells express CCR2 and respond to MCP-1: direct role of MCP-1 in angiogenesis and tumor progression, *Blood* 2000, 96:34-40
204. Brown LF, Yeo KT, Berse B, Yeo TK, Senger DR, Dvorak HF, van de Water L: Expression of vascular permeability factor (vascular endothelial growth factor) by epidermal keratinocytes during wound healing, *J Exp Med* 1992, 176:1375-1379

205. Nickoloff BJ, Mitra RS, Varani J, Dixit VM, Polverini PJ: Aberrant production of interleukin-8 and thrombospondin-1 by psoriatic keratinocytes mediates angiogenesis, *Am J Pathol* 1994, 144:820-828
206. Creamer D, Sullivan D, Bicknell R, Barker J: Angiogenesis in psoriasis, *Angiogenesis* 2002, 5:231-236
207. Shirakata Y, Komurasaki T, Toyoda H, Hanakawa Y, Yamasaki K, Tokumaru S, Sayama K, Hashimoto K: Epiregulin, a novel member of the epidermal growth factor family, is an autocrine growth factor in normal human keratinocytes, *J Biol Chem* 2000, 275:5748-5753
208. Draper BK, Komurasaki T, Davidson MK, Nanney LB: Topical epiregulin enhances repair of murine excisional wounds, *Wound Repair Regen* 2003, 11:188-197
209. Haemel AK, O'Brian AL, Teng JM: Topical rapamycin: a novel approach to facial angiofibromas in tuberous sclerosis, *Arch Dermatol* 2010, 146:715-718
210. Brugarolas JB, Vazquez F, Reddy A, Sellers WR, Kaelin WG, Jr.: TSC2 regulates VEGF through mTOR-dependent and -independent pathways, *Cancer Cell* 2003, 4:147-158
211. Baetta R, Granata A, Canavesi M, Ferri N, Arnaboldi L, Bellosta S, Pfister P, Corsini A: Everolimus inhibits monocyte/macrophage migration in vitro and their accumulation in carotid lesions of cholesterol-fed rabbits, *J Pharmacol Exp Ther* 2009, 328:419-425
212. Huber S, Bruns CJ, Schmid G, Hermann PC, Conrad C, Niess H, Huss R, Graeb C, Jauch KW, Heeschen C, Guba M: Inhibition of the mammalian target of rapamycin impedes lymphangiogenesis, *Kidney Int* 2007, 71:771-777

213. Gupta GP, Nguyen DX, Chiang AC, Bos PD, Kim JY, Nadal C, Gomis RR, Manova-Todorova K, Massague J: Mediators of vascular remodelling co-opted for sequential steps in lung metastasis, *Nature* 2007, 446:765-770
214. Parker WE, Orlova KA, Heuer GG, Baybis M, Aronica E, Frost M, Wong M, Crino PB: Enhanced epidermal growth factor, hepatocyte growth factor, and vascular endothelial growth factor expression in tuberous sclerosis complex, *Am J Pathol* 2011, 178:296-305
215. Zhang CQ, Shu HF, Yin Q, An N, Xu SL, Yin JB, Song YC, Liu SY, Yang H: Expression and cellular distribution of vascular endothelial growth factor-C system in cortical tubers of the tuberous sclerosis complex, *Brain Pathol* 2011,
216. Brugarolas J, Lei K, Hurley RL, Manning BD, Reiling JH, Hafen E, Witters LA, Ellisen LW, Kaelin WG, Jr.: Regulation of mTOR function in response to hypoxia by REDD1 and the TSC1/TSC2 tumor suppressor complex, *Genes Dev* 2004, 18:2893-2904
217. Hudson CC, Liu M, Chiang GG, Otterness DM, Loomis DC, Kaper F, Giaccia AJ, Abraham RT: Regulation of hypoxia-inducible factor 1alpha expression and function by the mammalian target of rapamycin, *Mol Cell Biol* 2002, 22:7004-7014
218. Gomez-Manzano C, Fueyo J, Jiang H, Glass TL, Lee HY, Hu M, Liu JL, Jasti SL, Liu TJ, Conrad CA, Yung WK: Mechanisms underlying PTEN regulation of vascular endothelial growth factor and angiogenesis, *Ann Neurol* 2003, 53:109-117
219. Carmeliet P: VEGF as a key mediator of angiogenesis in cancer, *Oncology* 2005, 69 Suppl 3:4-10

220. Mizukami Y, Li J, Zhang X, Zimmer MA, Iliopoulos O, Chung DC: Hypoxia-inducible factor-1-independent regulation of vascular endothelial growth factor by hypoxia in colon cancer, *Cancer Res* 2004, 64:1765-1772
221. Zhang X, Gaspard JP, Chung DC: Regulation of vascular endothelial growth factor by the Wnt and K-ras pathways in colonic neoplasia, *Cancer Res* 2001, 61:6050-6054
222. Mojsilovic-Petrovic J, Callaghan D, Cui H, Dean C, Stanimirovic DB, Zhang W: Hypoxia-inducible factor-1 (HIF-1) is involved in the regulation of hypoxia-stimulated expression of monocyte chemoattractant protein-1 (MCP-1/CCL2) and MCP-5 (Ccl12) in astrocytes, *J Neuroinflammation* 2007, 4:12
223. Kitajima Y, Ide T, Ohtsuka T, Miyazaki K: Induction of hepatocyte growth factor activator gene expression under hypoxia activates the hepatocyte growth factor/c-Met system via hypoxia inducible factor-1 in pancreatic cancer, *Cancer Sci* 2008, 99:1341-1347
224. Nilsson I, Shibuya M, Wennstrom S: Differential activation of vascular genes by hypoxia in primary endothelial cells, *Exp Cell Res* 2004, 299:476-485
225. Katsuta M, Miyashita M, Makino H, Nomura T, Shinji S, Yamashita K, Tajiri T, Kudo M, Ishiwata T, Naito Z: Correlation of hypoxia inducible factor-1alpha with lymphatic metastasis via vascular endothelial growth factor-C in human esophageal cancer, *Exp Mol Pathol* 2005, 78:123-130
226. Schoppmann SF, Fenzl A, Schindl M, Bachleitner-Hofmann T, Nagy K, Gnant M, Horvat R, Jakesz R, Birner P: Hypoxia inducible factor-1alpha correlates with VEGF-

C expression and lymphangiogenesis in breast cancer, *Breast Cancer Res Treat* 2006, 99:135-141

227. Murdoch C, Lewis CE: Macrophage migration and gene expression in response to tumor hypoxia, *Int J Cancer* 2005, 117:701-708

228. Werno C, Menrad H, Weigert A, Dehne N, Goerdt S, Schledzewski K, Kzhyskowska J, Brune B: Knockout of HIF-1alpha in tumor-associated macrophages enhances M2 polarization and attenuates their pro-angiogenic responses, *Carcinogenesis* 2010, 31:1863-1872

229. Cohen B, Addadi Y, Sapoznik S, Meir G, Kalchenko V, Harmelin A, Ben-Dor S, Neeman M: Transcriptional regulation of vascular endothelial growth factor C by oxidative and thermal stress is mediated by lens epithelium-derived growth factor/p75, *Neoplasia* 2009, 11:921-933

230. Cohen-Kaplan V, Naroditsky I, Zetser A, Ilan N, Vlodavsky I, Doweck I: Heparanase induces VEGF C and facilitates tumor lymphangiogenesis, *Int J Cancer* 2008, 123:2566-2573

231. Ristimaki A, Narko K, Enholm B, Joukov V, Alitalo K: Proinflammatory cytokines regulate expression of the lymphatic endothelial mitogen vascular endothelial growth factor-C, *J Biol Chem* 1998, 273:8413-8418

232. Cha HS, Bae EK, Koh JH, Chai JY, Jeon CH, Ahn KS, Kim J, Koh EM: Tumor necrosis factor-alpha induces vascular endothelial growth factor-C expression in rheumatoid synoviocytes, *J Rheumatol* 2007, 34:16-19

233. Lee PS, Tsang SW, Moses MA, Trayer-Gibson Z, Hsiao LL, Jensen R, Squillace R, Kwiatkowski DJ: Rapamycin-insensitive up-regulation of MMP2 and other genes in

- tuberous sclerosis complex 2-deficient lymphangioleiomyomatosis-like cells, *Am J Respir Cell Mol Biol* 2010, 42:227-234
234. Folkman J, Hahnfeltdt P, Hlatky L: Cancer: looking outside the genome, *Nat Rev Mol Cell Biol* 2000, 1:76-79
235. Naumov GN, Akslen LA, Folkman J: Role of angiogenesis in human tumor dormancy: animal models of the angiogenic switch, *Cell Cycle* 2006, 5:1779-1787
236. Chaplain MA: Mathematical modelling of angiogenesis, *J Neurooncol* 2000, 50:37-51
237. Williams SP, Karnezis T, Achen MG, Stacker SA: Targeting lymphatic vessel functions through tyrosine kinases, *J Angiogenes Res* 2010, 2:13
238. Stacker SA, Achen MG: From anti-angiogenesis to anti-lymphangiogenesis: emerging trends in cancer therapy, *Lymphat Res Biol* 2008, 6:165-172
239. Pepper MS, Tille JC, Nisato R, Skobe M: Lymphangiogenesis and tumor metastasis, *Cell Tissue Res* 2003, 314:167-177



## COPYRIGHT PERMISSIONS

### **Chapter 1: Introduction**

**Figure 1. Schematic representation of the structural-functional domains of hamartin (A) and tuberin (B).** *Reprinted from Cellular Signalling, 15(8), Vera P. Krymskaya, 729-39, Copyright (2003), with permission from Elsevier.*

**Figure 3. Structure of rapamycin.** *Reprinted from [www.dominiosweb.org/drugs/rapamycin](http://www.dominiosweb.org/drugs/rapamycin). The structure is in public domain in Wikipedia and can be used without permission.*

**Figure 4. *In vitro* effects of rapamycin in TSC.** *Reprinted from Li et al, Nat Commun. 2011;2:235. Authors of articles published by Nature Publishing Group do not need to seek permission to re-use of their material as long as the journal is credited with initial publication.*

**Figure 6. Receptor binding specificities of VEGF family members.** *Hicklin DJ, Ellis LM, Role of the Vascular Endothelial Growth Factor Pathway in Tumor Growth and Angiogenesis, Journal of clinical oncology, 23(5), 2005:1011-27. "Reprinted with permission. © 2008 American Society of Clinical Oncology. All rights reserved".*

**Figure 7. Hypoxic regulation of the hypoxia-inducible factor-1 $\alpha$  (HIF-1 $\alpha$ ).** *Reproduced from Arthritis research and therapy, Hitchon and El-Gabalawy, 2004;6(6):265-78. Reproduction of figures is permitted without formal written permission from the publisher BioMed Central, provided the figure is original.*

### **Chapter 3: Results**

**Figure 1. Histological and immunohistological differences between TSC skin tumors and normal-appearing skin.** *Reprinted from Li et al, Nat Commun. 2011;2:235. Authors of articles published by Nature Publishing Group do not need to seek permission to re-use of their material as long as the journal is credited with initial publication.*

**Figure 4. Genetic analysis of TSC2-null fibroblast-like cells.** *Reprinted from Li et al, Nat Commun. 2011;2:235. Authors of articles published by Nature Publishing Group do not need to seek permission to re-use of their material as long as the journal is credited with initial publication.*

**Figure 5. Xenograft model of TSC skin hamartomas.** *Reprinted from Li et al, Nat Commun. 2011;2:235. Authors of articles published by Nature Publishing Group do not need to seek permission to re-use of their material as long as the journal is credited with initial publication.*

**Figure 6. TSC angiofibroma (AF) cells induce human hair follicle formation in xenografts.** *Reprinted from Li et al, Nat Commun. 2011;2:235. Authors of articles published by Nature Publishing Group do not need to seek permission to re-use of their material as long as the journal is credited with initial publication.*

**Figure 8a. Tumor grafts replicate features of TSC skin tumors.** *Reprinted from Li et al, Nat Commun. 2011;2:235. Authors of articles published by Nature Publishing Group do not need to seek permission to re-use of their material as long as the journal is credited with initial publication.*

**Figure 8b. Effects of rapamycin on tumor and normal xenografts.** *Reprinted from Li et al, Nat Commun. 2011;2:235. Authors of articles published by Nature Publishing Group do not need to seek permission to re-use of their material as long as the journal is credited with initial publication.*